AEDC-TR-73-13

EXPERIMENTAL STUDY OF THE EFFECT OF SUBSONIC EXHAUST GAS DIFFUSERS ON THE TEST CELL WALL AND TF39 COLD-FLOW MODEL ENGINE EXHAUST NOZZLE PLUG AND CORE ENGINE COWL SURFACE PRESSURES

Delbert Taylor, Marvin Simmons, and Frank T. Lee

ARO, Inc.

April 1973

Approved for public release; distribution unlimited.

ENGINE TEST FACILITY
ARNOLD ENGINEERING DEVELOPMENT CENTER
AIR FORCE SYSTEMS COMMAND
ARNOLD AIR FORCE STATION, TENNESSEE

NOTICES

When U. S. Government drawings specifications, or other data are used for any purpose other than a definitely related Government procurement operation, the Government thereby incurs no responsibility nor any obligation whatsoever, and the fact that the Government may have formulated, furnished, or in any way supplied the said drawings, specifications, or other data, is not to be regarded by implication or otherwise, or in any manner licensing the holder or any other person or corporation, or conveying any rights or permission to manufacture, use, or sell any patented invention that may in any way be related thereto.

Qualified users may obtain copies of this report from the Defense Documentation Center.

References to named commercial products in this report are not to be considered in any sense as an endorsement of the product by the United States Air Force or the Government.

EXPERIMENTAL STUDY OF THE EFFECT OF SUBSONIC EXHAUST GAS DIFFUSERS ON THE TEST CELL WALL AND TF39 COLD-FLOW MODEL ENGINE EXHAUST NOZZLE PLUG AND CORE ENGINE COWL SURFACE PRESSURES

Delbert Taylor, Marvin Simmons, and Frank T. Lee
ARO, Inc.

FOREWORD

The work reported herein was conducted at and was sponsored by Arnold Engineering Development Center, Air Force Systems Command, Arnold Air Force Station, Tennessee, under Program Element 64719F.

The results presented were obtained by ARO, Inc. (a subsidiary of Sverdrup & Parcel and Associates, Inc.), contract operator of the Arnold Engineering Development Center (AEDC), Air Force Systems Command (AFSC), Arnold Air Force Station, Tennessee. The work was conducted in the Engine Test Facility (ETF) under ARO Project No. RW5224 from July 1971 to June 1972, and the manuscript was submitted for publication on August 11, 1972.

This technical report has been reviewed and is approved.

EDWARD W. HANSON
Captain, USAF
Requirements Planning Division
Directorate of Technology

ROBERT O. DIETZ
Director of Technology

ABSTRACT

An experimental investigation was conducted to determine the effects of exhaust gas collectors/subsonic diffusers on engine and test cell surface pressures during tests of high-bypass-ratio front-fan engines in ground test facilities. A one-tenth scale model of a TF39 turbofan engine installed in a one-tenth scale model of Propulsion Development Test Cell (J-1) was employed. Engine cowl and plug surface pressure data were recorded during model engine operation with cold air at five simulated power settings without exhaust collector, with exhaust collector, with exhaust collector equipped with a conventional subsonic diffuser, and with exhaust collector equipped with a segmented subsonic diffuser which separately diffused the fan and core engine exhaust jets. Stagnation pressure data were also recorded for the purpose of establishing the flow losses in the free-jet exhausts and in the diffusers. Data from all configurations were analyzed to determine the effect of exhaust jet collector/diffusers on engine and test cell surface pressures and to determine the efficiency of the diffusion process. Data from the full-scale TF39 engine in test cell J-1 of the ETF (Ref. 1), from the TF39 model test conducted in a scale model of test cell J-1 by Fluidyne (Ref. 2), and from this test compared favorably, thus indicating that the effect of the exhaust diffusers on test cell and engine surface pressures was negligibly small. "Splitting" and separately diffusing the fan and core exhaust streams did not affect test cell or engine surface static pressures. The diffusers produced static pressure rise ratios as high as 1.41 which corresponds to a decrease of approximately 28 percent in exhaust gas volume flow rate.

CONTENTS

APPENDIXES

I. ILLUSTRATIONS

Figure

NOMENCLATURE

A	Area, in.^{2}
B	Bias limit
$\mathbb{C}$	Centerline
C_{PR}	Pressure coefficients, $\frac{P_2 - P_1}{P_{t_1} - P_1} = \frac{P_e - P_i}{P_{t_1} - P_i}$
D	Diameter, in.
F	Impulse, lbf
L	Length, in.
P	Static pressure, psia
P_t	Total pressure, psia
R	Radius, in.
S	Precision error index
T_t	Total temperature, °F
t	Statistical distribution function
u	Uncertainty

SUBSCRIPTS

av	Average
C	Core
c	Test cell
co	Collector
d	Diffuser
e	Exit
ex	Exhaust
f	Fan
I	Air inlet
i	Inlet
j	Jet
n	Nozzle
r	Rake
w	Wall
1, 2, etc.	Station locations

SECTION I
INTRODUCTION

Large thrust high-bypass-ratio subsonic turbofans place stringent requirements on ground test facilities for two reasons:

1. The airflow which must be supplied to the engine inlet, and
2. The large volume flow of exhaust gases which must be removed from the test cell.

The very large airflow required by these turbofan engines exceeds the continuous air supply capability of existing ground test facilities when the engines are tested in the direct-connect mode. To alleviate this problem somewhat, it has been proposed that the fan and core engine exhaust jets be diffused separately. This facilitates redirecting the fan jet to the engine inlet. For a bypass ratio of 8:1, this would result in an approximate 80-percent reduction in the continuous airflow required of the test facility air supply system. At the same time, the core engine exhaust diffuser converts some of the exhaust jet kinetic energy to static pressure, thus reducing the volume flow which the facility exhausters must handle.

In a free-jet installation of a large thrust, high-bypass turbofan engine, separate diffusion is also needed, but for a somewhat different reason. Free-jet testing in a large wind tunnel requires that the core engine exhaust jet be scavenged so that the process air in the closed-loop wind tunnel does not become contaminated with exhaust products. Pressure recovery is needed not only to reduce the scavenge system exhauster capacity required but also to reduce the power requirements for the main wind tunnel compressors.

For either the direct-connect or the free-jet mode of testing at subsonic or transonic exhaust gas velocities, the proposed use of exhaust gas collectors/diffusers has raised questions concerning their influence on the test cell ambient and engine external surface pressures (cowling, boattails, etc.). Splitting the exhaust jets at the diffuser inlet may affect diffuser inlet flow to the extent that pressures on the engine and test cell surfaces are also affected; in which case extensive static pressure surveys would be required to permit one to analyze the effects on measured thrust.

An extensive literature search produced a limited amount of experimental performance data from tests of vaned or segmented diffusers of both the two-dimensional and axisymmetrical designs; none of the diffuser configurations reported were comparable with that required for separately diffusing the fan and core engine jets nor were the magnitudes of the diffuser inlet velocities and flow distortions.

Therefore, a study of concentric exhaust diffusers was initiated for the purpose of determining:

1. The magnitude of the effects of exhaust gas collectors/diffusers on test cell and engine surface pressures, and
2. The efficiency of the energy conversion which might be attained.

A one-tenth scale model of a TF39 turbofan engine was mounted in a one-tenth scale model of Propulsion Development Test Cell (J-1). The engine/test cell unit was installed in Propulsion Research Cell (R-2A-3) where the test program was conducted.

SECTION II
APPARATUS

2.1 TEST CELL SECTION

The test cell section was fabricated from two sections of nominal 20-in.-diam pipe (Fig. 1, Appendix I). The front section of the test cell was 39 in. long and was flanged to the aft section, which was 43.75 in. long giving an overall test cell length of 82.75 in., a scale model of AEDC test cell J-1. The upstream end was sealed by a flat plate which supported the 10-in.-diam air inlet connection to the engine fan section. The model TF39 was installed in the center of the aft section with the engine pylon secured to the test cell wall. The aft section contained two 6- by 15-in. rectangular observation windows and instrumentation access ports. The downstream end of the cell was connected to a 24-in.-diam exhaust duct, which links the test cell to the plant exhaust machines. Provisions were made at this point for installation of the diffuser configurations to be investigated.

2.2 ENGINE MODEL

Shown in Fig. 2 is a sectional view of the 1/10th-scale model of the TF39 engine. FluiDyne Engineering Corporation fabricated the model according to specifications supplied by Lockheed Aircraft Corporation and General Electric Corporation and conducted the static performance testing of the model engine. These results as well as detailed and assembly drawings of the model are presented in Ref. 2.

The model was installed inside and concentric with the aft test cell section. The 10-in.-diam air inlet duct was adapted to the engine fan nozzle inlet thus providing support for the model and direct connection to the plant air supply. The engine pylon was secured to the top of the test cell by a rectangular bracket that was utilized to align the model on the centerline of the test cell.

2.3 EXHAUST COLLECTOR

The exhaust collector (Fig. 3) is essentially a 1/10th-scale model of the exhaust collector with diffuser used in the full-scale test of the TF39 turbofan engine in the J-1 test cell. The collector was comprised of a truncated conical inlet section, 3.12 in. long, with a 30-deg converging angle and a 9.6-in.-diam cylindrical duct having a length-to-diameter ratio (L/D) of 0.5. Attached to the collector was the 14-in.-diam cylindrical section, which simulated the J-1 diffuser.

The exhaust collector (Fig. 4) was installed on, and concentric with, the centerline of the 24-in. exhaust duct. The collector inlet plane was positioned 5.5 in. downstream of the model exhaust plug.

2.4 CONVENTIONAL SUBSONIC DIFFUSER

The conventional subsonic diffuser (Fig. 5) was comprised of the 1/10th-scale model of the J-1 exhaust collector equipped with a truncated conical diffuser having an exit-to-entrance area ratio of 4 and a cone angle of 10 deg. Installation of the diffuser (Fig. 6) was similar to that of the exhaust collector with the spacing between the model exhaust plug and the diffuser inlet plane maintained at 5.5 in.

2.5 SEGMENTED DIFFUSER

The segmented diffuser (Fig. 7a) consisted of two truncated conical diffusers: the core jet diffuser and the fan jet annular segmented diffuser.

The core jet diffuser was designed to capture and diffuse the high energy flow of the core engine exhaust. The entrance section was cylindrical with a diameter of 3.5 in. and a length-to-diameter ratio (L/D) of 2.75. The diverging section had a 10-deg cone angle with an area ratio of 4.0.

The fan jet annular segmented diffuser, designed to separately diffuse the fan exhaust gas, was installed concentric with the core jet diffuser and positioned so that the diffusers terminated in the same plane. The diverging conical section had a cone angle of 25 deg with an annular entrance area of 62.86 $in.^2$. The inlet to the fan jet diffuser was geometrically similar to the exhaust collector; however, the capture duct diameter was increased 0.2 in. to compensate for the area loss caused by the capture duct of the core jet diffuser.

Ten radial splitter plates were installed in the annular passage to divide it into 10 diffusers of equal dimensions having effective conical diffusion angles of approximately 8 deg and area ratios of 4. The splitter plates were 0.25-in.-thick steel plates, 19.9 in. long and were welded to the outside surface of the core jet diffuser. The assembly (Fig. 7b) fits inside the collector-fan diffuser. The plates were installed in the annular passage with the leading edge 2.2 in. downstream of the junction of the collector and the fan diffuser to compensate for the flow area blockage by the plates. The total flow area at the entrance of the plates was 70.20 $in.^2$.

Installation of the segmented diffuser (Fig. 8) was identical to the installation of the J-1 exhaust collector-conventional subsonic diffuser with the inlet 5.5 in. downstream of the model TF39 exhaust plug.

To compensate for the low energy wake in the fan jet which resulted from the pylon blockage and boundary layer, a high energy air jet was installed (Fig. 9a) at the inlet to the segmented fan diffuser section behind the pylon to accelerate this flow; then the air jet was removed, and a streamlined plug (Fig. 9b) was inserted in this diffuser section. The plug sealed the inlet to this diffuser segment and extended forward to guide the low energy flow into the adjacent segments.

To improve the performance of the diffuser, the leading edges of the 1/4-in.-thick splitter plates were modified by adding wedges which were 2 in. in axial length and had sharp leading edges (Fig. 9c).

The segmented diffuser was further modified to improve the performance by removing four of the splitter plates, forming six segments (Fig. 9d), and by removing all the splitter plates except the two on the horizontal centerline (Fig. 9e).

2.6 INSTRUMENTATION

2.6.1 Data Conditioning and Recording

All pressure and temperature data obtained during this test were recorded on a computer-controlled digital acquisition system. This system has the capability of obtaining 100 high speed channels of data at a scan rate of 14, 500 channels/sec and an additional 448 channels of data at a scan rate of 200 channels/sec and of automatically controlling the stepping of 30 scanner valves of that 360 channels of pressure data can be obtained with 30 transducers. The computer automatically controlled and recorded millivolt calibrations of all temperature channels, resistance calibration of all pressure channels, and in-place calibration of pertinent pressure channels.

Operation was conducted in an on-line mode; the ETF computer was used to record all the data and to provide in real time selected parameters for use in evaluating the validity of the test conditions.

The computer in all cases was utilized during testing to obtain important test parameters for a display on a cathode-ray tube. Data displayed in this manner was updated every 2 sec permitting monitoring of up to 20 parameters of data during operation.

2.6.2 Instrument Calibration

Calibrations of all instrument parameters before and after each test period were conducted as required. These included millivolt calibrations of all temperature parameters and resistance calibrations of all pressure parameters. The results of these calibrations were reviewed and discrepancies corrected before each test.

2.6.3 Test Data Measurement Uncertainty

For simplicity and comparison of data, uncertainty is used to express a reasonable limit for error. Uncertainty is calculated as follows (Ref. 3):

$$U = \pm(B + t_{0.95}\, S)$$

where

B is the bias limit

S is the precision error index

t is the 95th percentile point for the two tailed student "t" distribution (The t value is a function of the number of degrees of freedom used in calculating S. The t is arbitrarily selected to equal 2 for samples sized from 30 to infinity.)

Although uncertainty is not a statistical confidence interval, it is an arbitrary subsitute which is probably best interpreted as the largest error we might expect. Under any reasonable assumption for the distribution of bias, the coverage of U is greater than 95 percent (Ref. 3).

In these data, the uncertainty for an average of four measurements of pressure is

$$U = \pm(B + tS) = 0.020 \text{ psi}$$

where

B = 0.0116 psi

tS = 0.0084 psi

t = 2

Range of pressure data = 3 to 15 psia

This level of uncertainty reflects the characteristics of the transducers, electrical systems, data recording systems, and data processing systems. It does not consider the physical condition of the taps or the flow conditions existing in the region of the taps.

2.6.4 Pressure Sensing Locations

The model exhaust plug and nacelle surface static pressure probe locations are shown in Figs. 10 and 11, respectively. The fan nozzle

exit, core engine air supply venturi, and core engine nozzle pitot tube locations are shown in Fig. 2.

Axial stations and circumferential locations of test cell static pressure probes are shown in Fig. 12.

Four pitot tubes positioned on equal areas were installed in the 10-in. air supply duct at station 5 for measuring air inlet total pressure (Fig. 12). Inlet air temperature was sensed by a copper-constantan thermocouple installed at station 5.

Station 20 was at the plane of the inlet of the collector-diffuser configurations (5.5 in. from the engine exhaust plug). During testing without a diffuser (test cell only), pitot tubes were installed for measuring the total pressure profile at the collector-diffuser inlet plane (Figs. 13a and b).

A pressure survey rake (Fig. 14) containing 39 pitot tubes for documenting the pressure profile of the model TF39 fan jet was used at station 20 (diffuser inlet plane) and at a position 6.65 in. downstream of the fan nozzle exit.

Stations 26 and 30 represent the location conventional and the segmented diffuser exits, respectively. Diffuser exit pitot tube arrangements are shown in Figs. 15, 16a, and 16b.

A rake was installed behind the pylon of the model TF39 to measure the total pressure profile across (horizontally) the wake of the pylon. The rake contained seven pitot tubes and was centered on the vertical centerline 3.8 in. downstream of the model exhaust plug exit and at 3.45 in. above the centerline of the model (Fig. 17).

Six pitot tubes, three at the 90-deg and three at the 180-deg circumferential locations looking downstream, were installed between the test cell wall and the subsonic diffuser inlet (Fig. 18) to document impact pressures in this area.

A laser doppler velocimeter was used on four tests for determining the gas velocity at the plane of the collector inlet to avoid perturbating the flow with standard pressure measuring instrumentation. The principle of operation of the velocimeter is explained in Refs. 4 and 5.

SECTION III
PROCEDURE

The test cell exhaust plant isolation valves were opened, and the plant exhausters were employed to evacuate the test installation. The desired test cell ambient pressure was established, and an altitude instrumentation check was taken. The air supply plant isolation valves were opened to initiate airflow to the model engine. Steady-state conditions were established, and test data were recorded.

The five test conditions at which each configuration was evaluated are presented in the following:

$\frac{P_{t_{f_e}}}{P_{c_{av}}}$	P_c, psia	P_{t_i}, psia	T_{t_i}, °F
2.34	3.28	7.85	100 to 110
2.02	3.28	6.85	↓
1.62	3.28	5.50	
1.48	3.28	4.98	
2.20	6.30	14.13	

SECTION IV
RESULTS AND DISCUSSION

4.1 EFFECT OF EXHAUST COLLECTOR-DIFFUSER ON TEST CELL PRESSURE

The effect of the exhaust configurations tested on test cell pressure is shown in Figs. 19a through d. These graphs depict the averages of a number of pressures located circumferentially at each of several stations divided by the average of all the test cell pressures measured. Individual values of test cell pressure are tabulated in Table I (Appendix II). The trends of the nondimensionalized average test cell pressures are similar and compare with those presented in Fig. 38 of Refs. 1 and 2. The exhaust collector apparently caused a slight depression in the curve at the downstream end of the test cell; however, the addition of diffusers caused little if any additional change except at the fan

nozzle pressure ratio of 1.57 where the conventional subsonic diffuser apparently caused a random variation in pressure which is of questionable validity since it produced no effect at the other fan nozzle pressure ratios.

The test cell wall pressure tap located at station 20 (Fig. 19) which is at the inlet plane of the exhaust collector consistently recorded the largest value of test cell pressure except at the fan nozzle pressure ratio of 1.57. The large value of pressure is probably the result of the tap being located in the impact zone of the test cell vortex, indicated in Fig. 8.

4.2 EFFECT OF EXHAUST COLLECTOR DIFFUSERS ON ENGINE SURFACE PRESSURES

Engine surface pressures, nondimensionalized by the average test cell pressure, are presented in Figs. 20a through e for all configurations tested. These graphs also present results from the full-scale test in J-1 test cell and/or from the scale model study reported in Refs. 1 and 2. The method of connecting the test points was taken from Ref. 2 so that the trends could be compared directly. The variations in fan and core engine nozzle pressure ratios among runs caused the variation in the axial location of the curve peaks; however, there is no apparent effect of the exhaust collector-diffusers on engine surface pressures. The full-scale engine core nozzle pressure ratio was varied during developmental testing in J-1, and the effect of this variation is noticeable in these comparison curves of tail-pipe plug surface pressures (see Figs. 20a through e).

4.3 ENGINE EXHAUST FLOW FIELD SURVEYS

During tests of the full-scale engine in J-1 test cell, a total pressure rake was installed on the vertical centerline of the exhaust jet at the plane of the inlet to the exhaust collector. The rake extended from the test cell floor to a point a short distance above the engine centerline. The results of the pressure survey conducted during full-scale engine test without the exhaust collector and during these model studies are presented in Figs. 21b and 21a and c, respectively. The peak pressure in the flow field of the full-scale engine occurred at a radius of 3.0 ft which shows that the high energy core of the fan jet followed the surface of the core engine cowl as expected. The wake behind the core engine nozzle plug is located above the engine centerline and has a

discrete velocity decrement. The model engine plug wake was also located above the engine centerline. The effect of the fan jet converging on the core jet is discussed in Ref. 2. Test results (Ref. 2) taken with the core jet only and with both the core jet and fan jet flowing showed that the core nozzle plug surface pressures are larger when both jets are flowing. This was attributed to the convergence of the fan jet on the core jet, which can also explain the plug wake position: the very large engine mounting pylon that bisects the fan jet from a plane inside the fan nozzle to the core nozzle exit plane generates a very large wake plus boundary layers on both sides of the pylon. Thus, there is an arc of some 30 to 45 deg on each side of the vertical centerline of the engine at the core nozzle exit plane which is essentially the pylon wake flow and is, therefore, at a low level of kinetic energy (Fig. 22). The remaining fan flow field exerts a larger force as it converges on the core jet than does the pylon wake, and therefore, a radial force imbalance exists in the combined jet flow field downstream of the core nozzle which results in moving the core jet toward the pylon.

Pressure and velocity surveys were conducted in the exhaust jet at the plane of the collector inlet prior to its installation. The results are presented in Figs. 23a through e. Velocity profiles determined from pressure measurements are along the vertical centerline below the center of the jet; those determined by the velocimeter are along the horizontal centerline from beyond the center toward the left when viewing the engine from the jet collector. The calculated velocities were derived from the measured stagnation pressures and temperatures and the average test cell static pressure and thus are of questionable accuracy; however, the velocity profiles determined by the two methods compare favorably as do the profiles determined by the velocimeter during tests of different exhaust hardware configurations at comparable values of fan nozzle pressure ratios, thus indicating that the exhaust collector-diffusers tested exerted a negligible influence on the velocity of the exhaust jet near the collector inlet.

The laser velocimeter was used to indicate the exhaust gas velocity along the horizontal centerline of the jet near the plane of the collector inlet during tests with the various collector-diffusers installed in order to get an immediate indication of any appreciable level of disturbance caused by these configurations without additional disturbances caused by conventional instrumentation hardware in the stream.

The pressure surveys recorded from tests with the circular rake (Figs. 24a through f) show the radial and circumferential gradients in the fan flow field at the plane of the collector inlet and at a plane approximately midway between the exit planes of the fan and core nozzles. The pressure surveys recorded during tests with the rake located in the pylon wake at a station 3.45 in. above the engine centerline and 3.8 in. aft of the core engine plug (Fig. 22) indicate the extent and the energy level of the wake at the inlet to the collector-diffusers.

4.4 COLLECTOR-DIFFUSER PERFORMANCE

The static pressure rise ratio of the exhaust collector and the exhaust collector-conventional diffuser are presented in Fig. 25 as a function of the fan nozzle pressure ratio. In order to determine the pressure coefficient $\left(C_{PR} = \frac{P_e - P_{c_{av}}}{P_{t_{d_{i_{av}}}} - P_{c_{av}}}\right)$ of the collector-diffuser, the average value of the ratio of stagnation-to-static pressures upstream of the collector was determined from a one-dimensional application of the conservation analysis as follows.

The average values of $P_{t_{d_{i_{av}}}} / P_{c_{av}}$ at the diffuser inlet was calculated by a one-dimensional application of the momentum analysis, the assumption of an ideal fluid, and the assumption that the static pressure at the diffuser inlet equals the average value of the test cell pressure.

$$F_{co_i} = P_{c_{av}} \left[A_{co_i} - (A_{f_j} + A_{C_j})\right] + F_{f_n} + F_{C_n}$$

where

$$A_{f_j} = A_{f_n} \left(\frac{A_{f_j}}{A_{f_n}}\right) \text{ for } \frac{P_{c_{av}}}{P_{t_{f_n}}} < 0.528$$

and

$$A_{C_j} = A_{C_n} \left(\frac{A_{c_j}}{A_{C_n}}\right) \text{ for } \frac{P_{c_{av}}}{P_{t_{C_n}}} < 0.528$$

The results of these evaluations were used to estimate the ideal value of the pressure coefficient (C_{PR} = 1.0) which is also presented in Fig. 25. Test results indicate that the pressure coefficient of the collector-conventional diffuser exceeds 0.62 which is quite satisfactory for this configuration with the relatively large value of average inlet velocity and the extremely poor velocity distributions. It is probable that the minimum area of the diffuser system should be made more nearly equal to the sum of the engine nozzle areas in order to prevent the distribution of the kinetic energy in the exhaust jets over such a large area. Obviously, the length of the minimum area section is much too short to effect a uniform velocity profile at the diffuser inlet. Total pressure surveys at the diffuser exit (Fig. 26) show that there remains only a small average velocity head to recover, which also indicates that the diffuser area is too large. Note also that the total pressure profile measured by the vertical rake reflects only a very slight depression at the top of the diffuser where the effect of the pylon wake, were it not thoroughly mixed, should be quite noticeable.

The segmented diffuser which split the fan and core flows did not affect the upstream flow field; however, it performed so poorly (Fig. 27) that a number of modifications were incorporated in an effort to effect a reasonably acceptable pressure recovery. The poor performance was attributed to the concentric ducts which limit the amount of mixing and thus momentum transfer through the constant area annulus. The pressure surveys conducted at the exit of the diffuser (Figs. 28a through e) show that the top segment limited pressure recovery. Therefore, an air jet with an impulse of 12 to 16 lbf was installed in the annulus behind the pylon to impart energy to the flow. The results of a test of this configuration indicated that a large quantity of air would be required to effect the level of performance desired. Therefore, this method was abandoned, and the top segment was plugged at the inlet by a streamlined wooden plug designed to guide the flow from this area into adjacent segments. Pressure survey rakes were installed at the exit of each segment (Figs. 29a through e). The diffuser performance with the segment plugged approached that of the diffuser with the air jet augmentation.

The diffuser splitter plates were equipped with sharp leading edges which further improved its performance (Figs. 30a through e). The performance of the diffuser with four of the splitter plates removed showed slight improvement (Figs. 31a through e); therefore, the plug and all the splitter plates except those located on the horizontal centerline were removed resulting in slightly improved performance at the

larger values of fan nozzle pressure ratios (Figs. 32a through e). All diffuser exit pressure surveys show a circumferential variation of stagnation pressure; therefore, an additional length of cylindrical ducts upstream of the concentric diffusers could be expected to produce further improvements in the diffuser performance by providing for further smoothing of the velocity profile at the inlet to the diffuser segments.

The circumferential variation in the wall static pressure near the exit plane of the 9.8-in.-diam cylindrical duct (Fig. 33) permits a determination of the maximum static pressure rise through some individual diffuser segments. The segment at 30 deg produced a static pressure rise ratio of 1.152, whereas those at 180 and 210 deg produced ratios of 1.502 and 1.495, respectively. The area-weighted pressure ratio ($P_{t_{av}}/P_{c_{av}}$) on the 180-deg radial line at the inlet to the annular fan collector was 1.78 for this test point. The flow was assumed to attain some circumferential velocity, as it moved through the constant area annulus to the inlets of the diffuser segments, due to the circumferential variation in total pressure in the exhaust jet. Therefore, the total pressure and thus the pressure ratio ($P_{t_{av}}/P_{c_{av}}$) at the inlet to the 180-deg diffuser segment may have been somewhat smaller in value than the 1.78 measured at the collector inlet. At the engine operating point corresponding to a fan nozzle pressure ratio of $P_{t_{fn}}/P_{c_{av}} = 2.34$, the wall static pressure ratio $P_w/P_{c_{av}}$ at 180 deg was 0.876. Since subsonic flow in a constant area channel cannot accelerate beyond the velocity of sound, it can be assumed that the maximum pressure ratio at the station of this wall static pressure tap is $P_{t_{av}}/P_w = 1.89$; thus the minimum value of the total pressure decrease in the constant area annulus between the collector inlet and the static pressure tap location (1/4 in. upstream of the junction between the cylindrical duct and the truncated diffuser) is

$$\Delta P_t\Big]_{co}^{di} = \frac{1.78 - 1.89\,(0.876)}{1.78} = \frac{1.78 - 1.656}{1.78} = 0.0697$$

or approximately 7 percent. The decrease in total pressure may have been greater which would have made the flow subsonic at the plane of the static tap; however, if the flow was sonic, then the maximum recovery in the 180-deg diffuser segment could be determined only by measuring the wall static pressure at the inlet to the truncated section just downstream of the junction of the cylindrical duct and the truncated diffuser duct. This analysis leads to the belief that the slight increase

in rise ratio resulting from the removal of splitter plates was the effect of mixing of the low energy pylon wake and adjacent higher energy air in the diffuser.

SECTION V
SUMMARY OF RESULTS

The results of this study of exhaust gas collectors-diffusers may be summarized as follows:

1. The diffusers tested caused no discernible effect on flow parameters in the test cell except for one configuration at one specific test point.
2. The collector-conventional subsonic diffuser produced a maximum rise ratio (test cell to exhaust duct) of 1.4 which corresponds to a decrease in exhaust gas volume flow $\geq$ 28 percent.
3. The collector-segmented diffuser produced a maximum rise ratio of 1.3.
4. The performance of individual diffuser passages in the segmented diffuser indicates that the diffuser design was adequate ($C_{PR_{minimum}} = 0.64$), since the minimum energy conversion exceeded that normally used in performance designs of systems with highly nonuniform velocity profiles, and that lengthening the cylindrical duct inlet to the diffuser would improve its overall efficiency.
5. This experiment should be extended to document, in detail, the experimental performance of diffuser configurations having a smaller cylindrical duct diameter and utilizing long, shallow angle converging sections upstream of the cylindrical duct.

REFERENCES

1. Kimzey, W. F. and Rakowski, W. J. "Preparatory Studies for for Qualification Testing of the TF39 Turbofan Engine in the Propulsion Engine Test Cell (J-1)." AEDC-TR-69-85 (AD855621L), July 1969.

2. Aircraft Engine Group. "Aerodynamic Model Test Report (Engine), 1/10-Scale Model Exhaust System Static Performance, TF39 Engine for C-5A Aircraft." GE No. 6DT006A03, February 14, 1968.

3. Abernethy, R. B., Colbert, D. L., and Powell, B. D. "ICRPG Handbook for Estimating the Uncertainty in Measurements Made with Liquid-Propellant Rocket Engine Systems." Performance Standardization Group, CPIA No. 180, April 30, 1969.

4. Shipp, J. I., Hines, R. H., and Dunnill, N. A. "Development of a Laser Velocimeter System." AEDC-TR-67-175 (AD821534), October 1967.

5. Lennert, A. E., Brayton, D. B., Crosswy, F. L., et al. "Summary Report of the Development of a Laser Velocimeter to be used in AEDC Wind Tunnels." AEDC-TR-70-101 (AD871321), July 1970.

APPENDIXES

I. ILLUSTRATIONS

II. TABLE

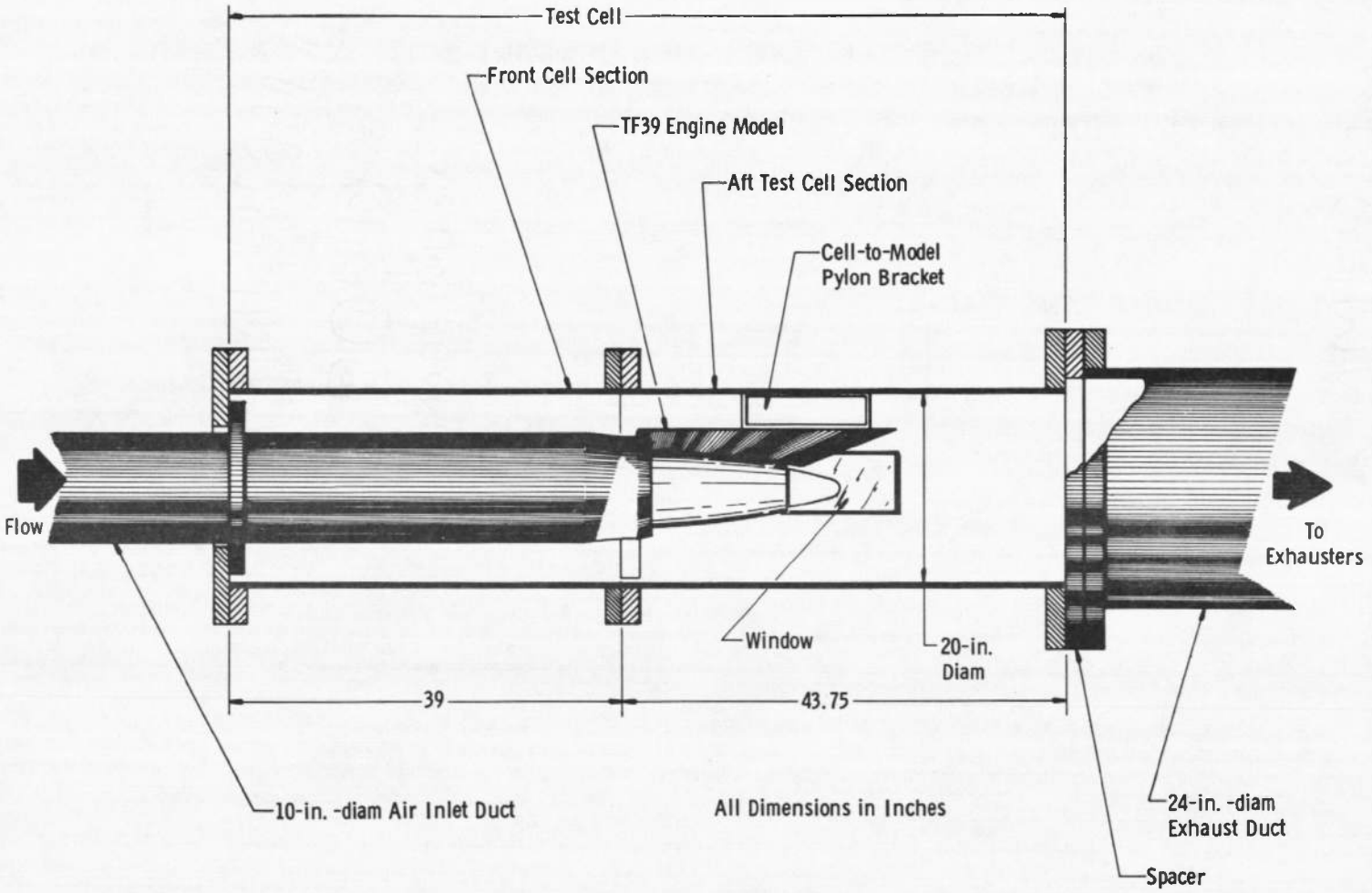

Fig. 1 Test Cell Installation

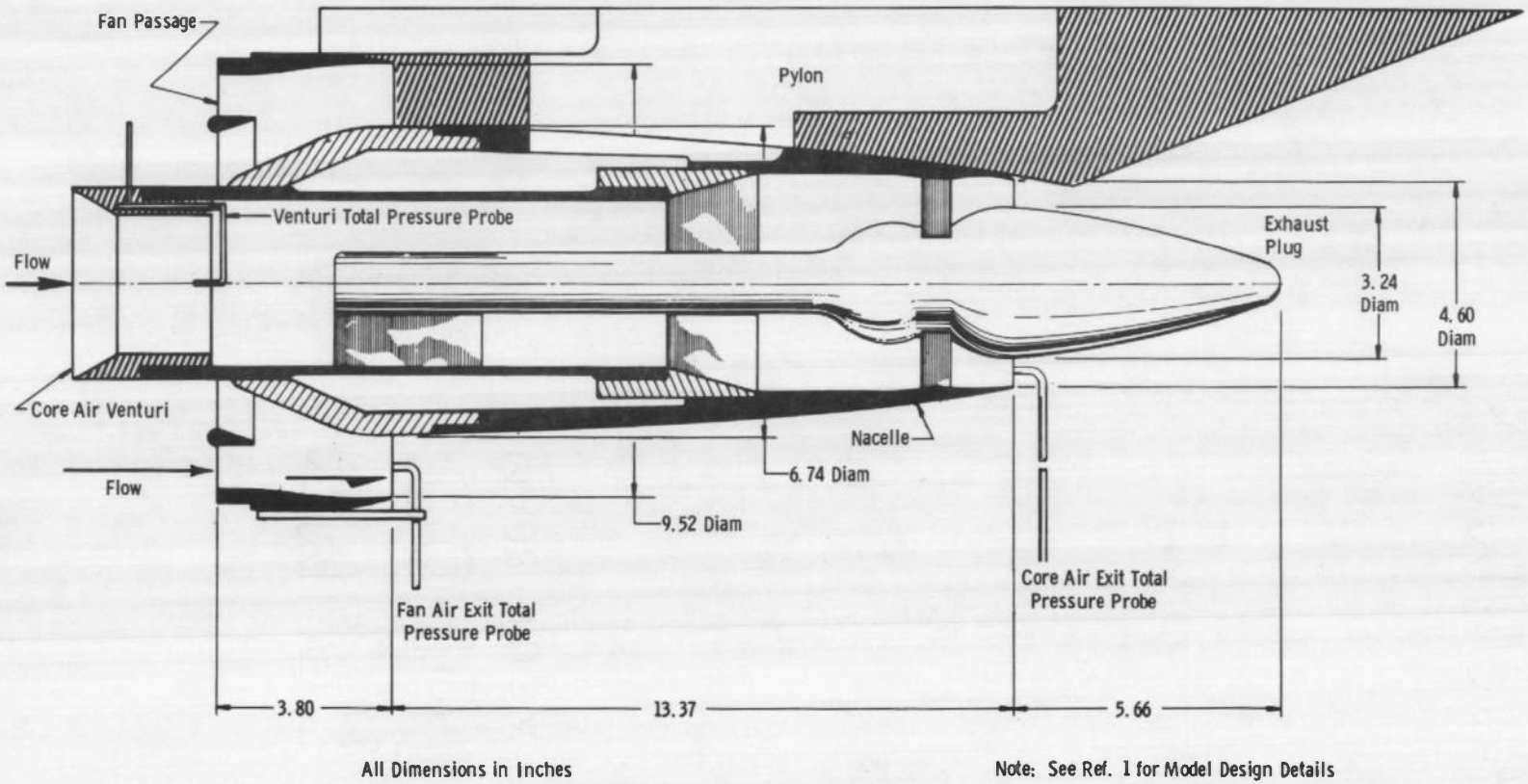

Fig. 2 1/10th-Scale Model of the TF39 Engine

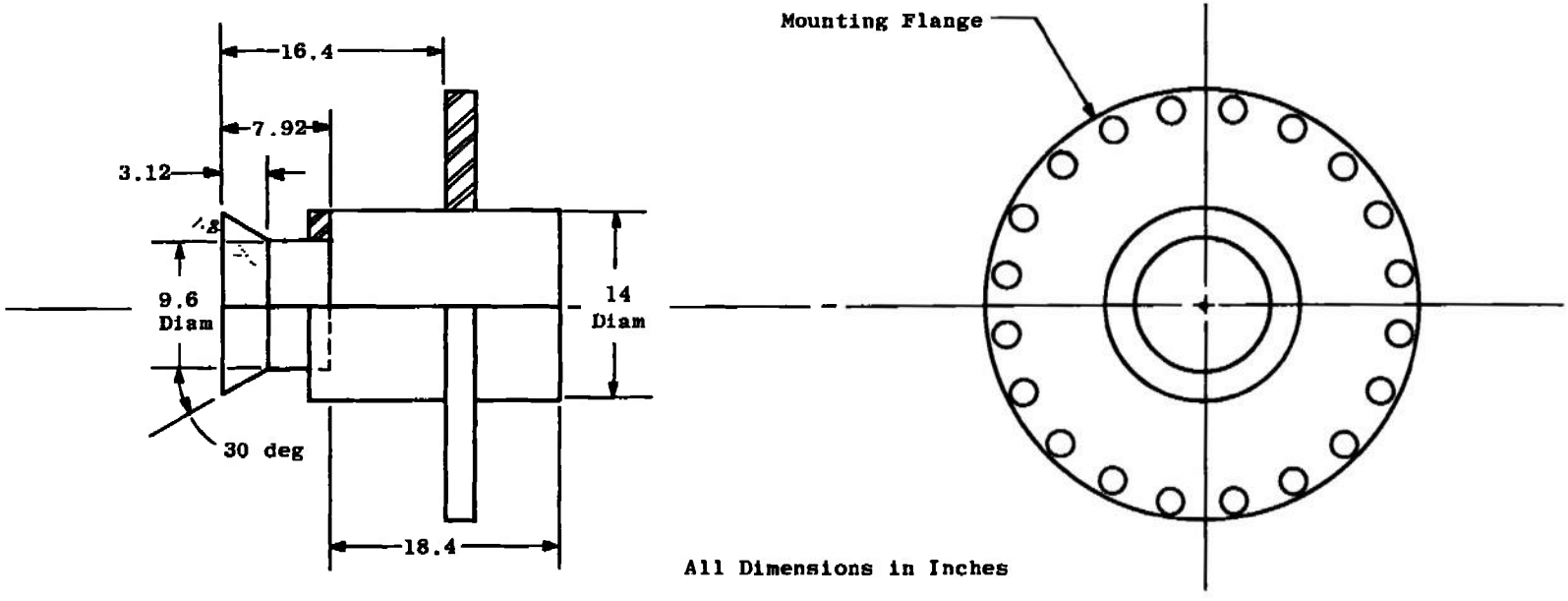

Fig. 3 Simulated J-1 Exhaust Collector Details

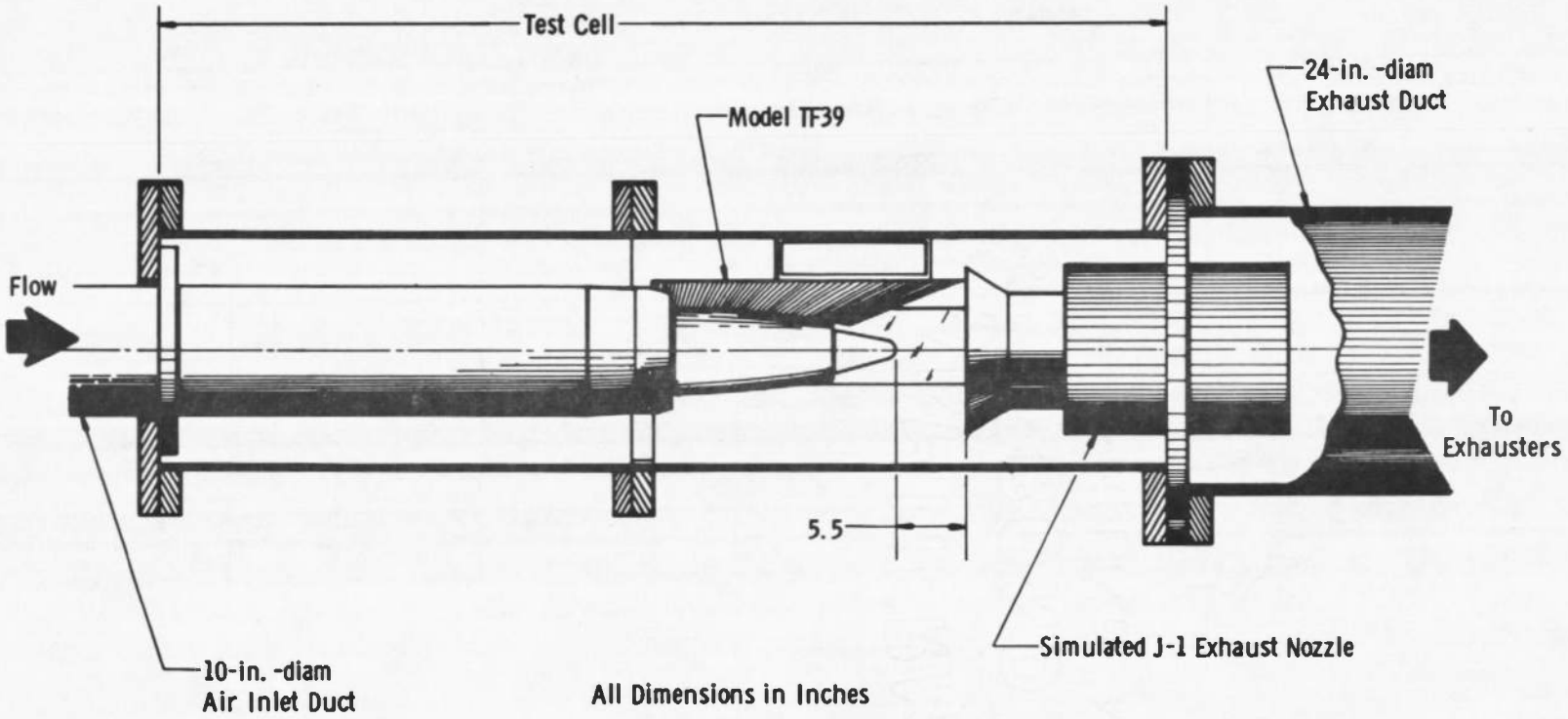

Fig. 4 Test Section with Simulated J-1 Exhaust Collector Installed

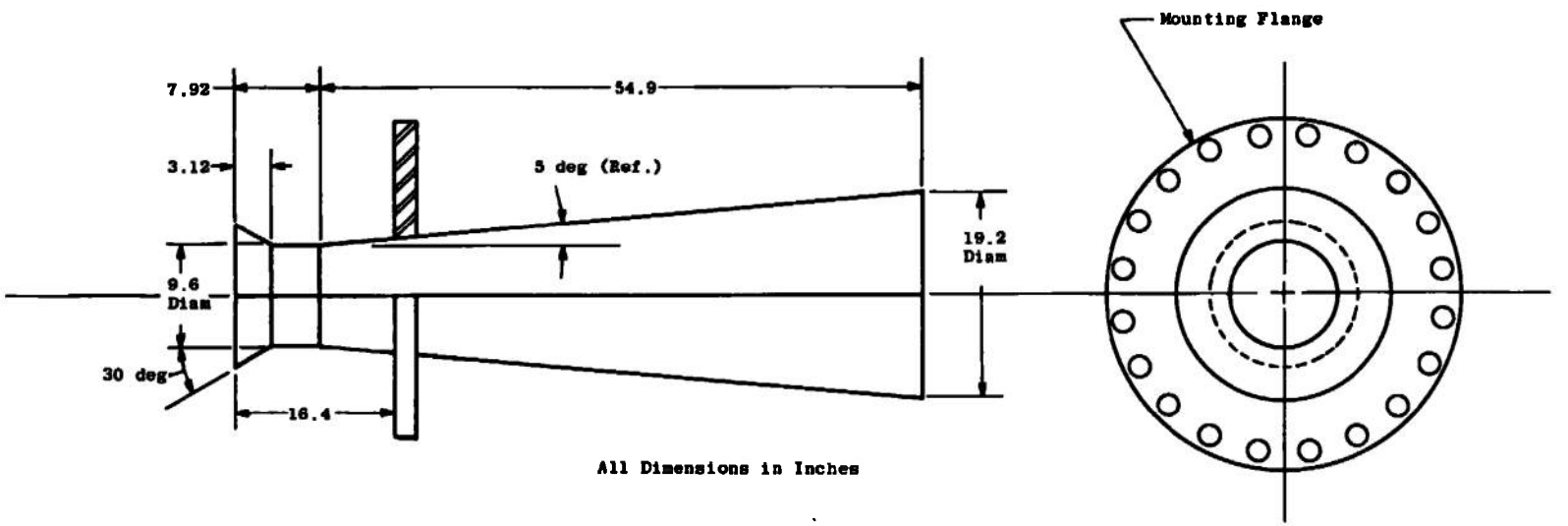

Fig. 5 Conventional Subsonic Diffuser Details

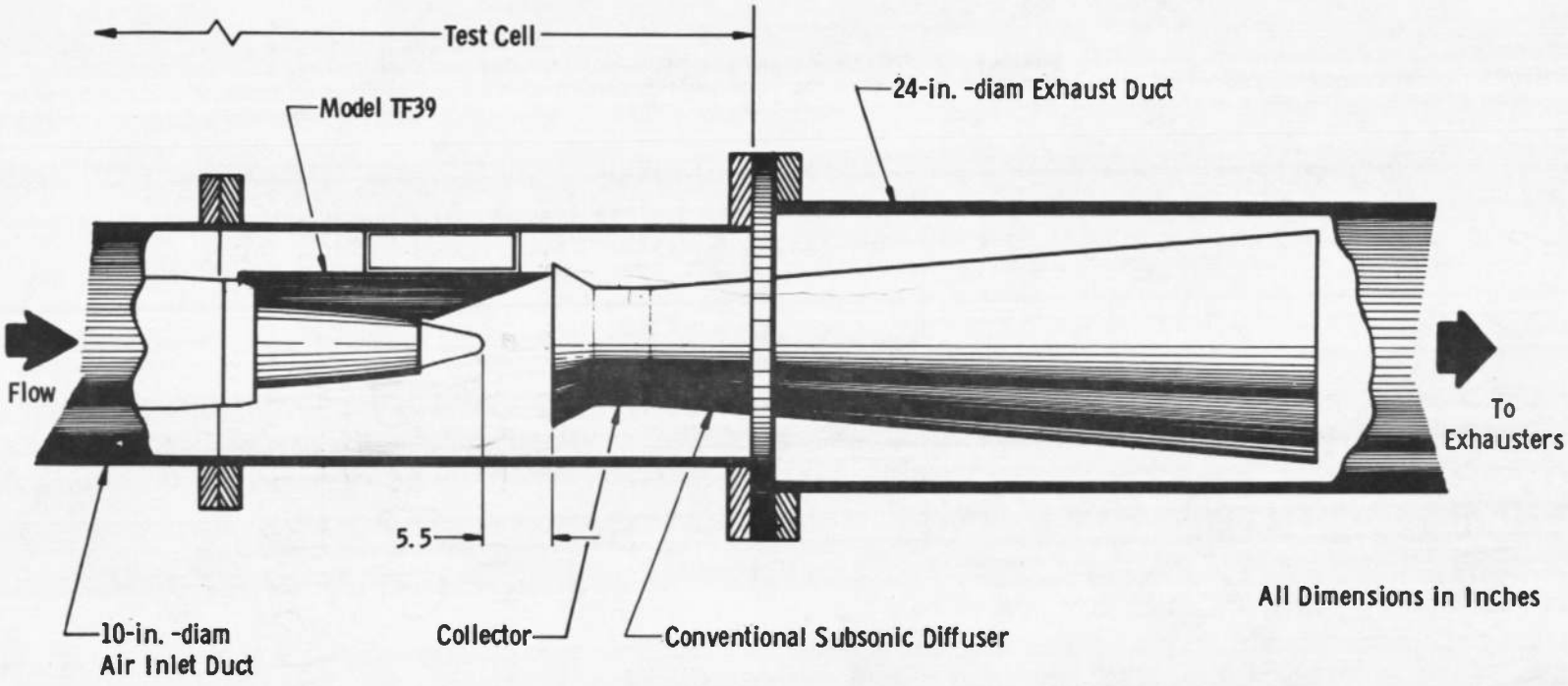

Fig. 6 Test Section with Conventional Subsonic Diffuser Installed

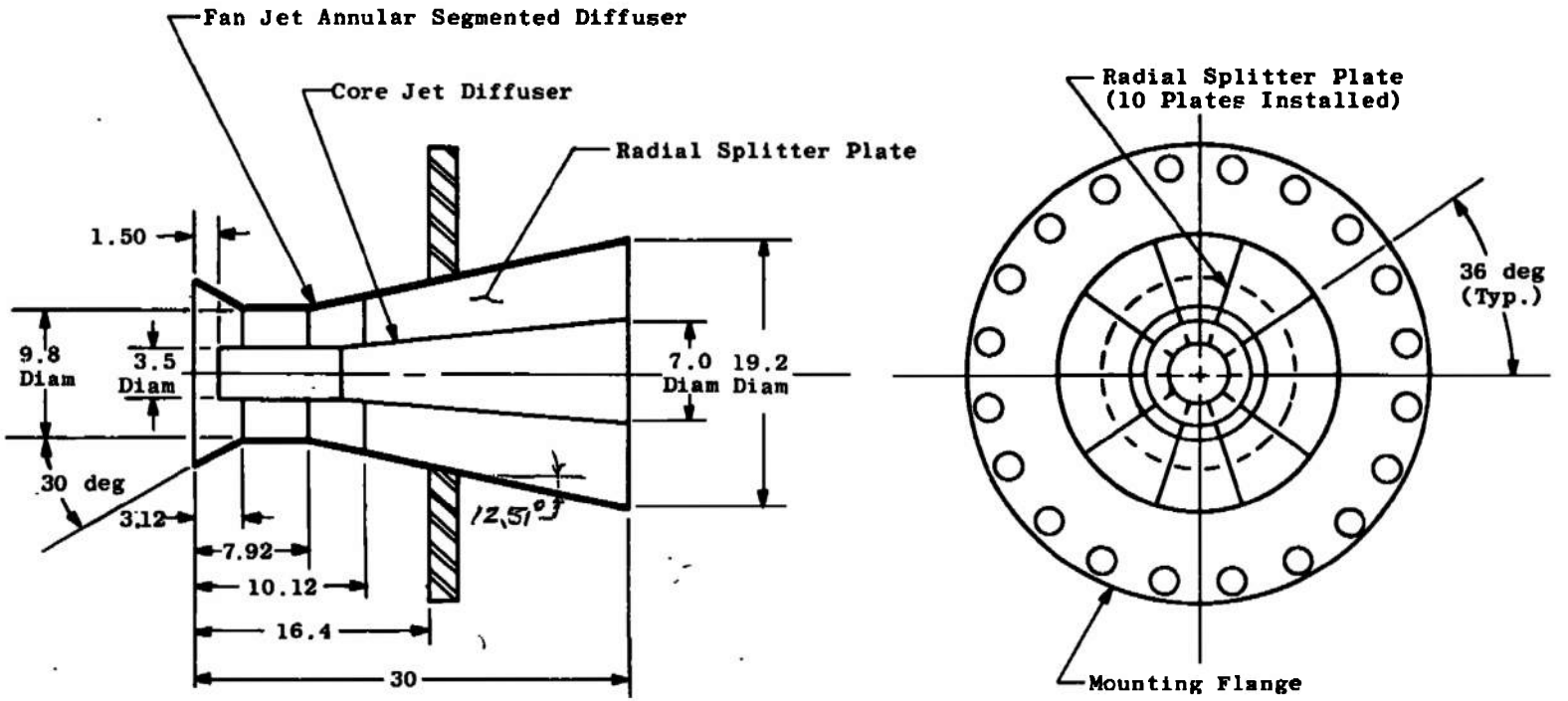

All Dimensions in Inches

a. Design Details

Fig. 7 Segmented Diffuser

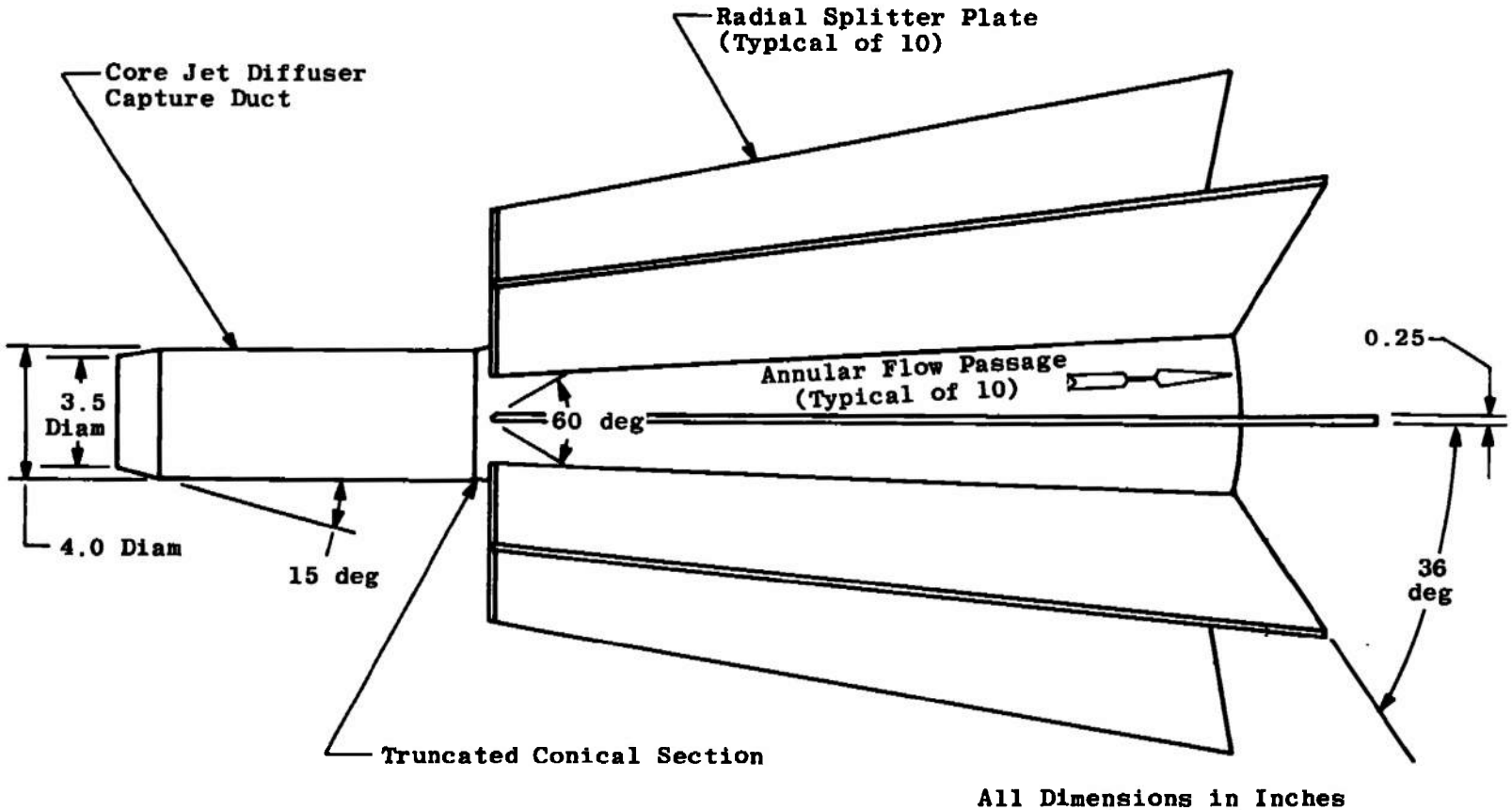

b. View of Core Jet Diffuser with Radial Splitter Plates Installed
Fig. 7 Concluded

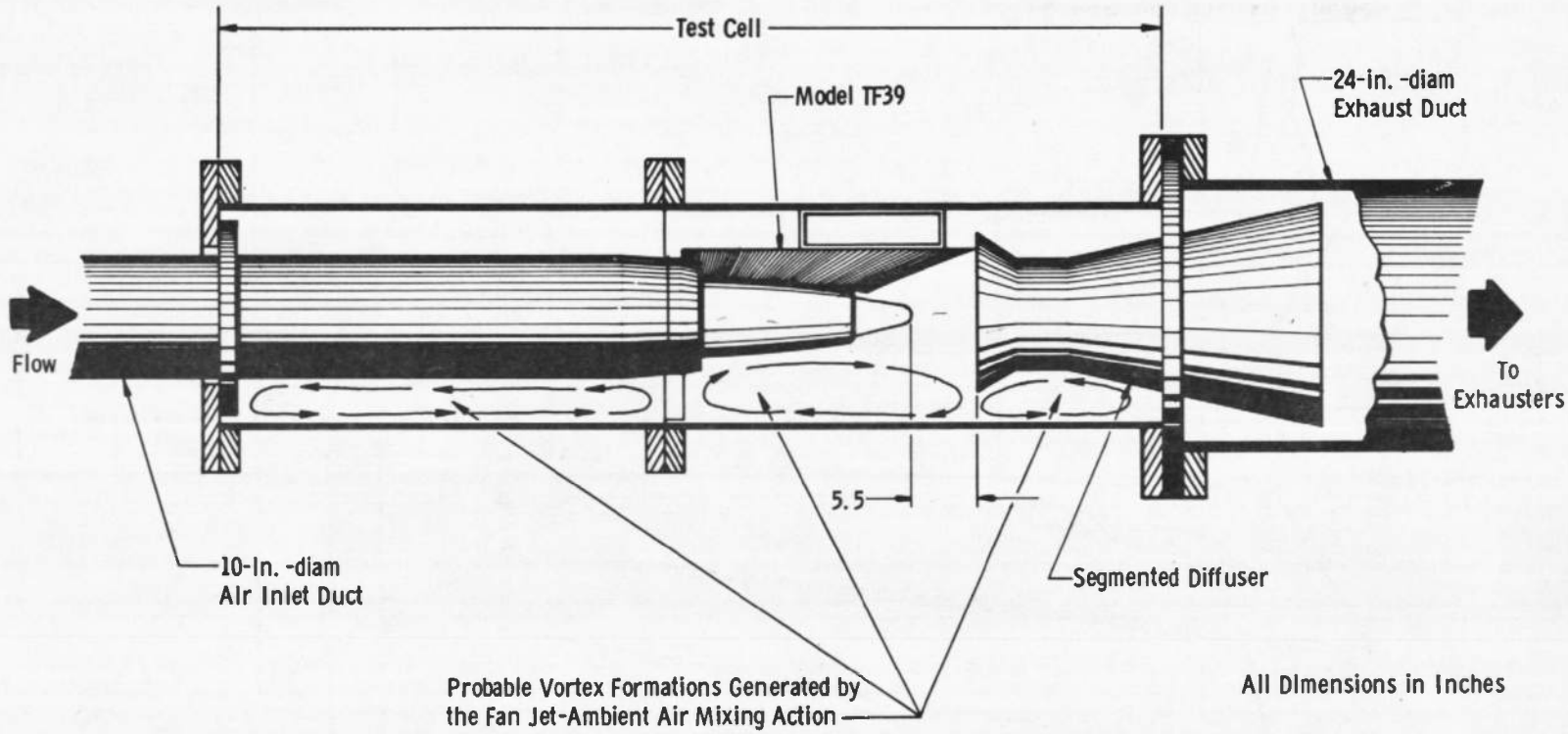

Fig. 8 Test Section with Segmented Diffuser Installed

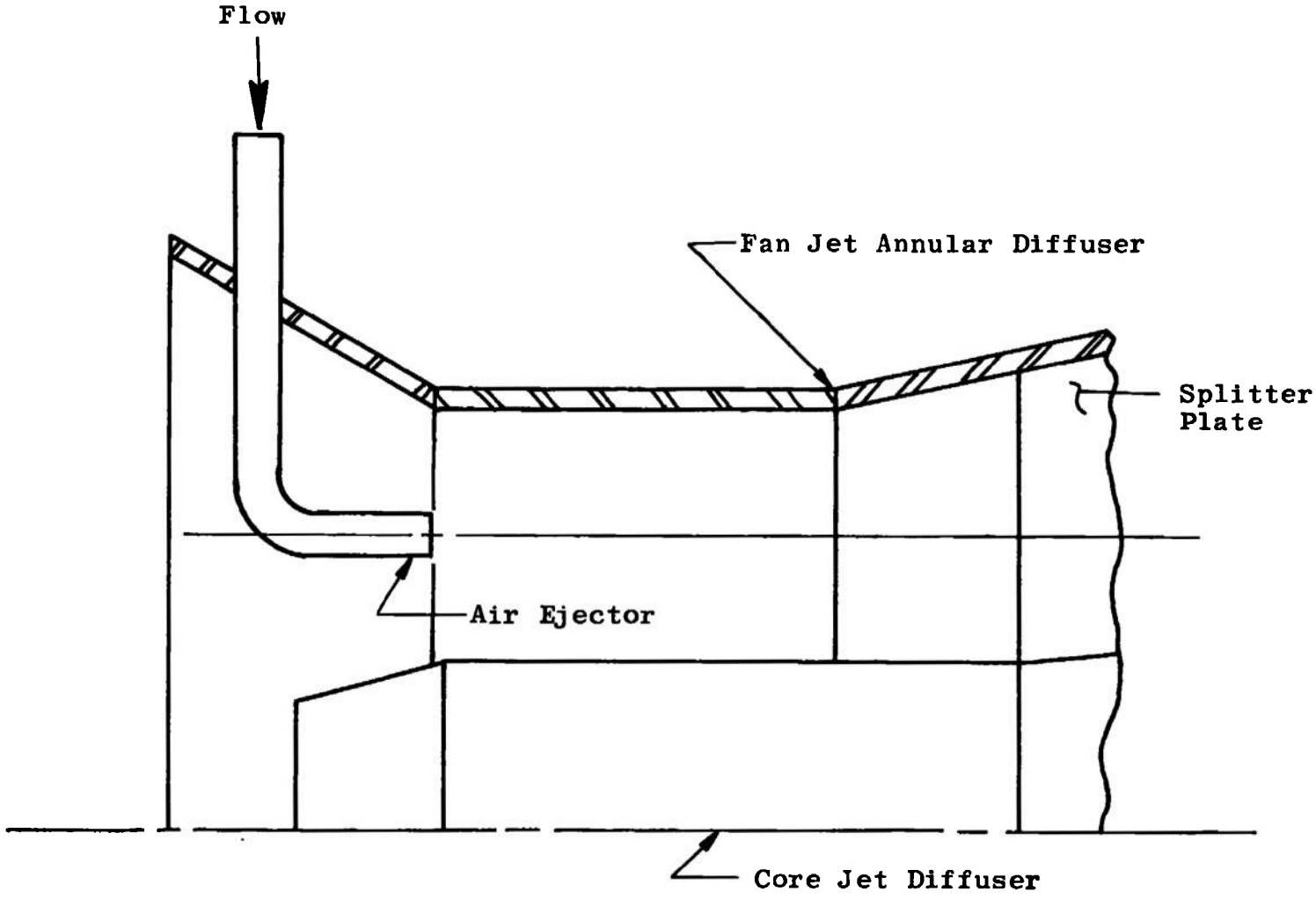

a. Sketch of Air Ejector in the Annular Diffuser

Fig. 9 Modifications Made to the Segmented Diffuser for Improving Diffuser Performance

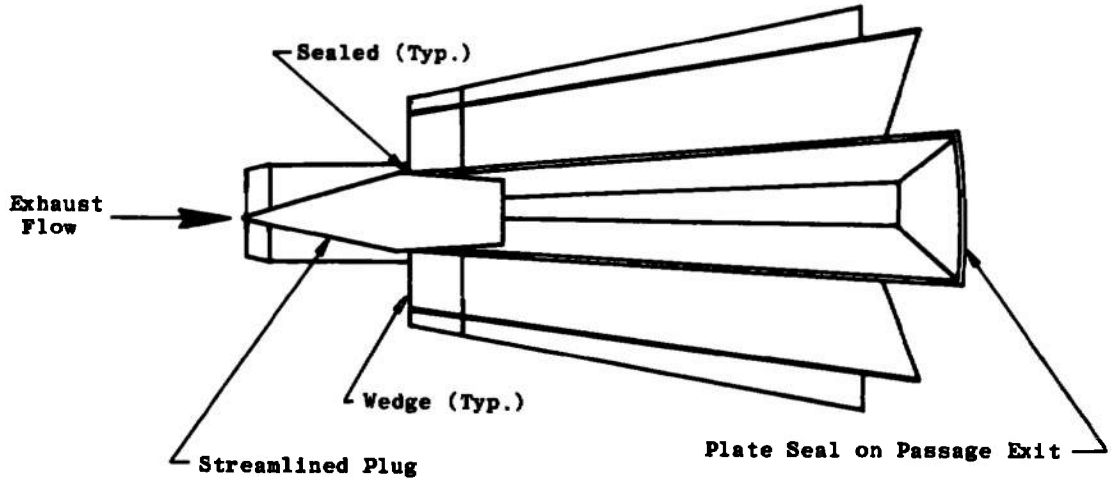

b. Top Annular Passage Sealed with Streamlined Plug

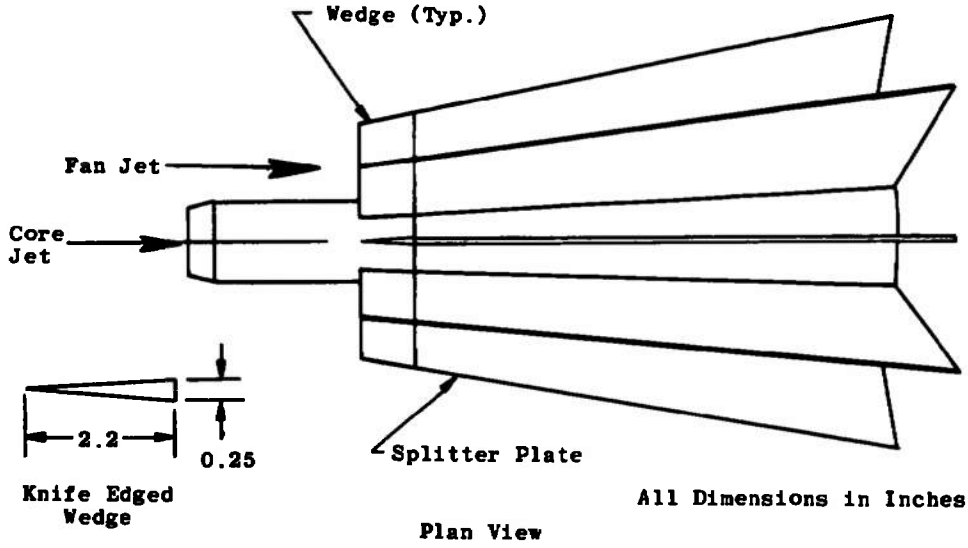

c. Splitter Plates with Knife-Edged Wedges

Fig. 9 Continued

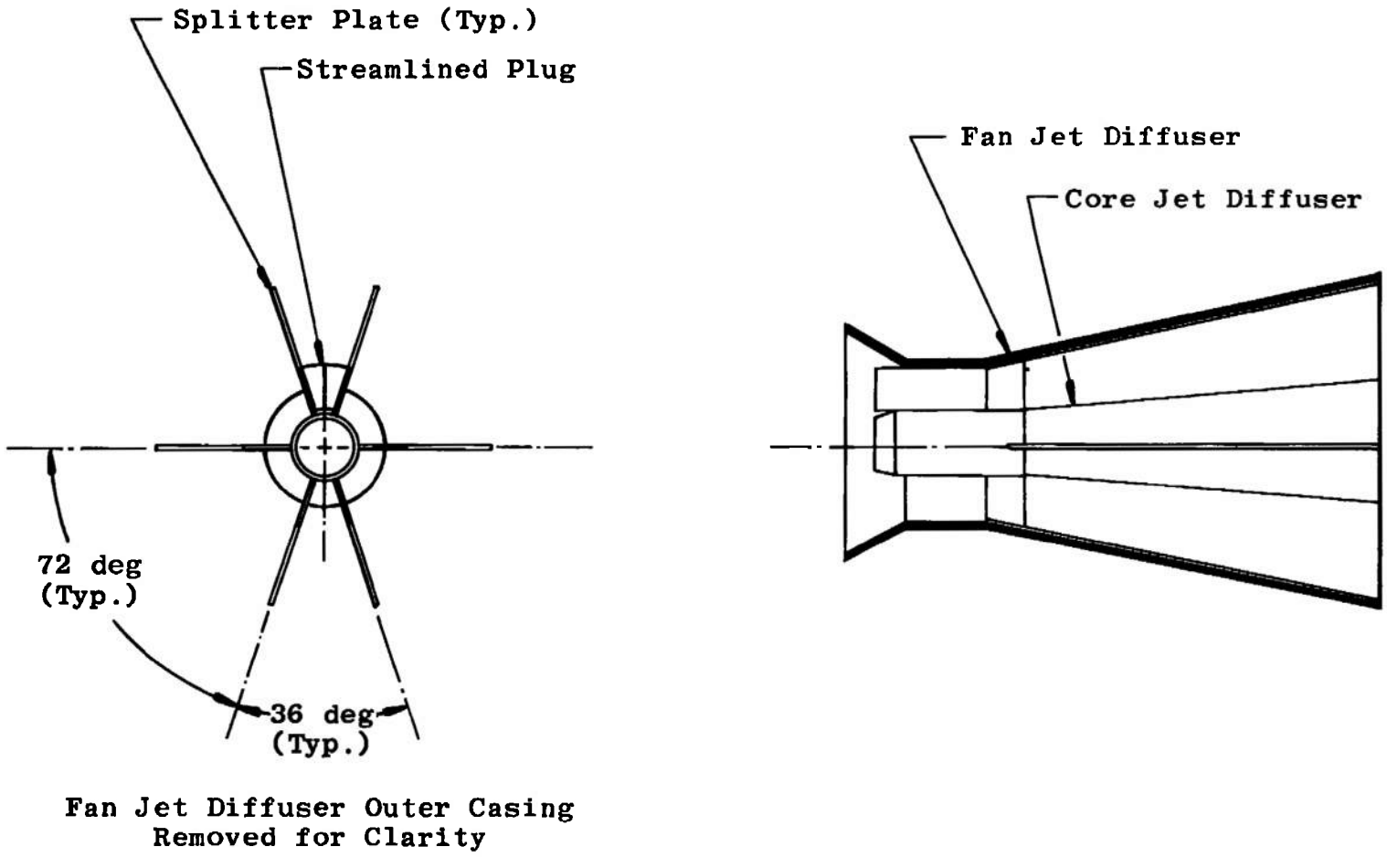

d. Segmented Diffuser with Four Splitter Plates Removed

Fig. 9 Continued

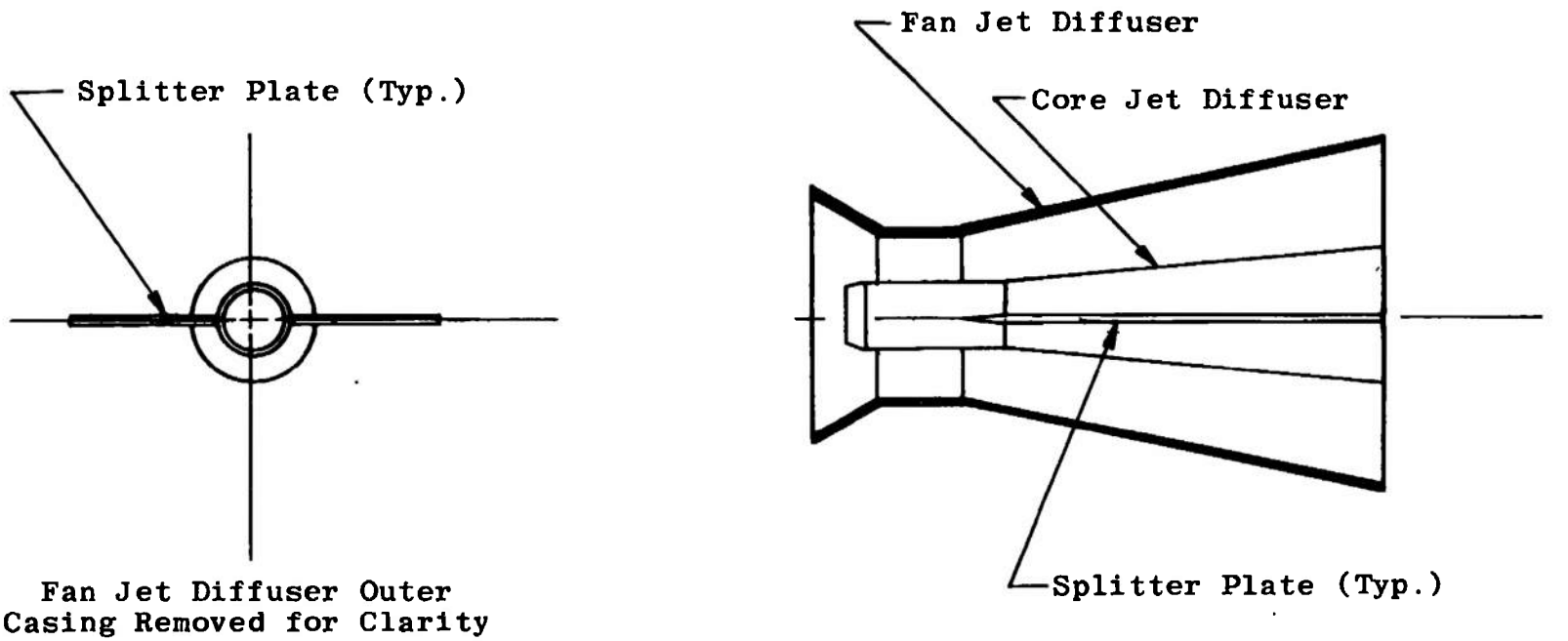

e. Segmented Diffuser with Only the Two Horizontal Splitter Plates Installed
Fig. 9 Concluded

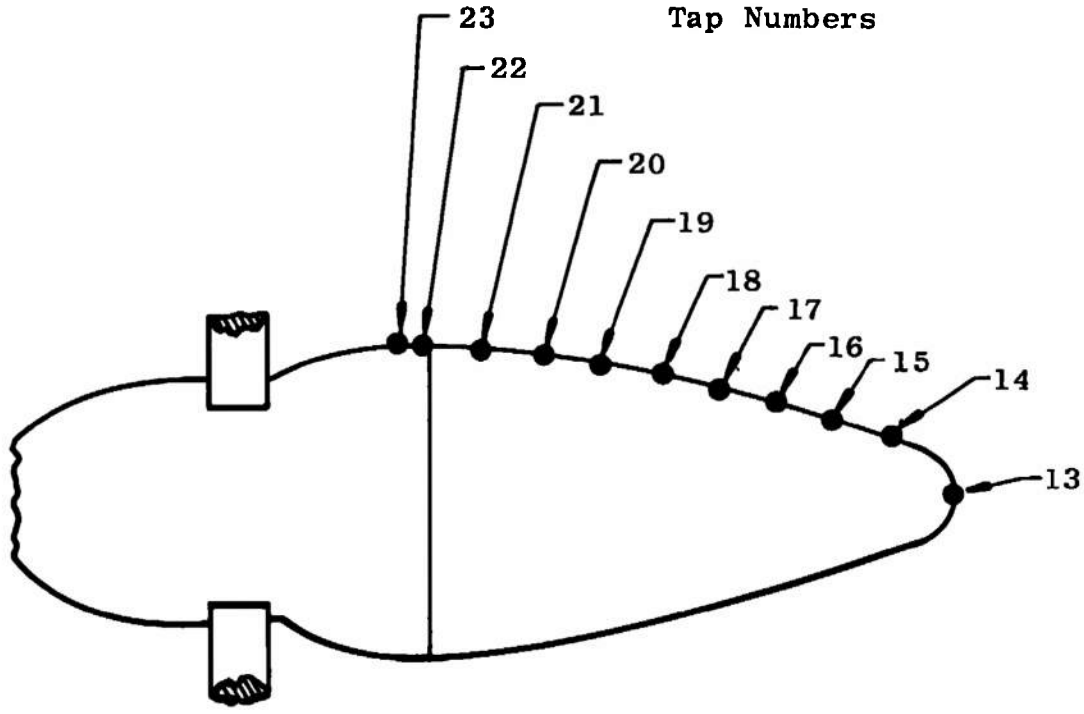

Taps Rotated for Clarity
Radial Location of Taps 330 deg

Tap No.	Engine Station
13	30.15
14	29.55
15	29.05
16	28.45
17	27.80
18	27.05
19	26.35
20	25.55
21	25.05
22	24.70
23	24.60

Static Pressure Tap Location on Engine Nacelle

Fig. 10 Model TF39 Exhaust Plug Static Pressure Tap Location

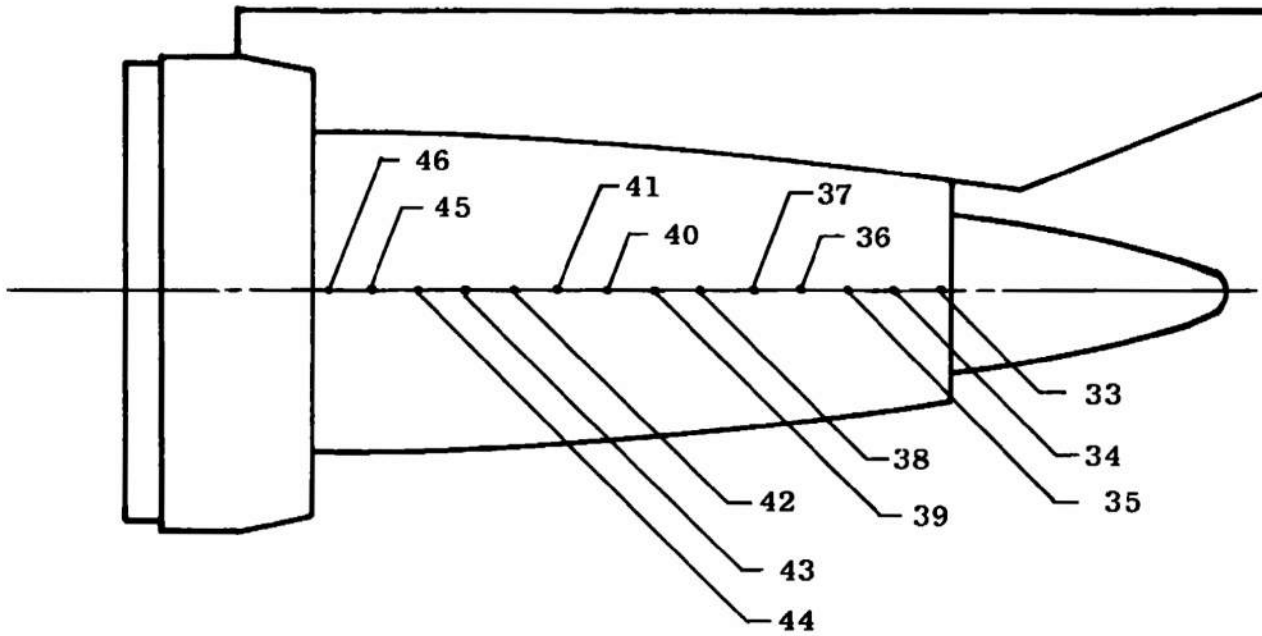

Pressure Taps Rotated 180 deg for Clarity

Tap No.	Engine Station
33	23.85
34	22.85
35	21.85
36	20.95
37	20.05
38	19.15
39	18.00
40	17.30
41	16.25
42	15.30
43	14.40
44	13.55
45	13.05
46	12.50

Static Pressure Tap Locations on Engine Nacelle

Fig. 11 Model TF39 Nacelle Static Pressure Tap Location

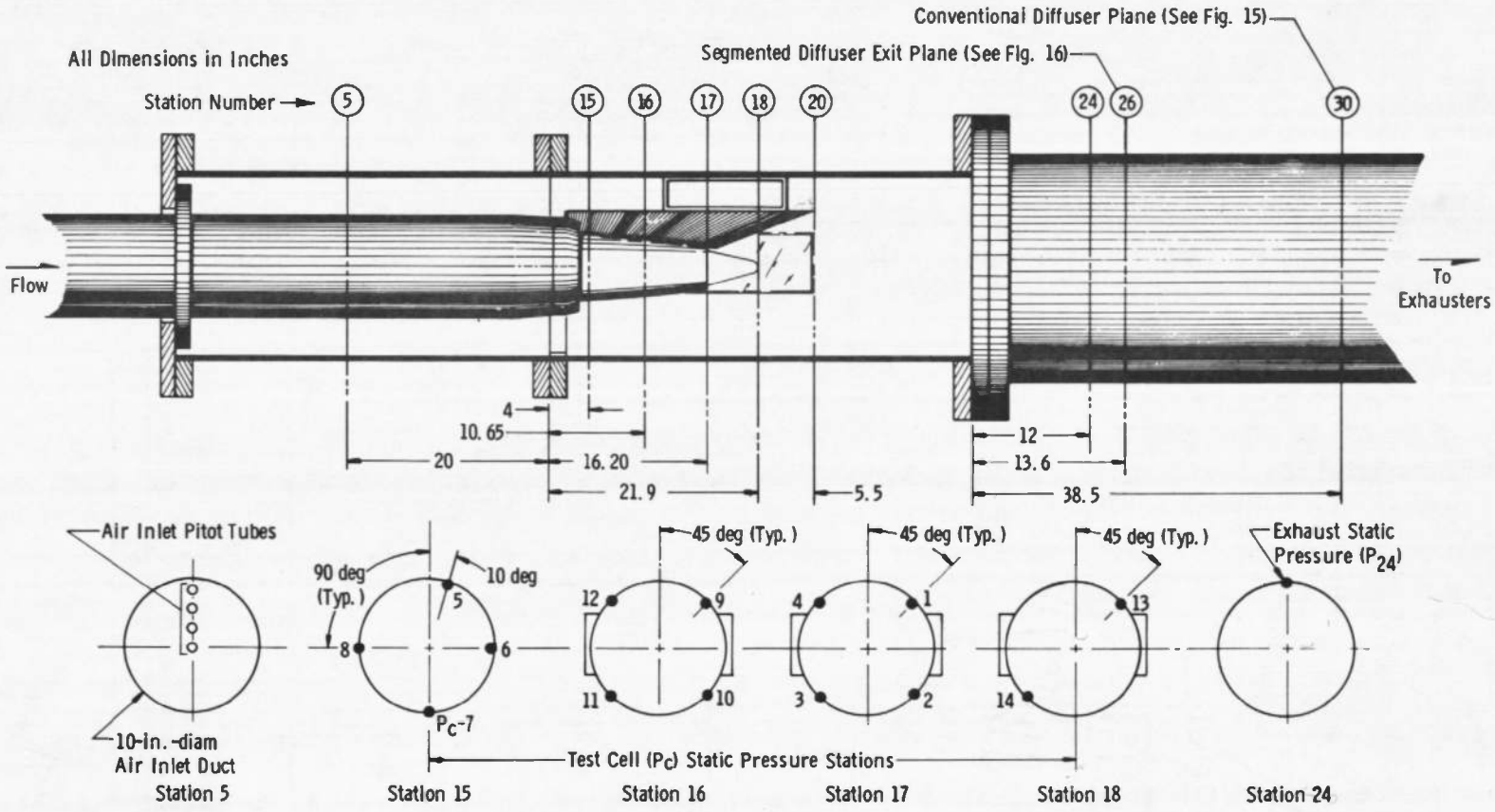

Fig. 12 Test Section Instrumentation Stations

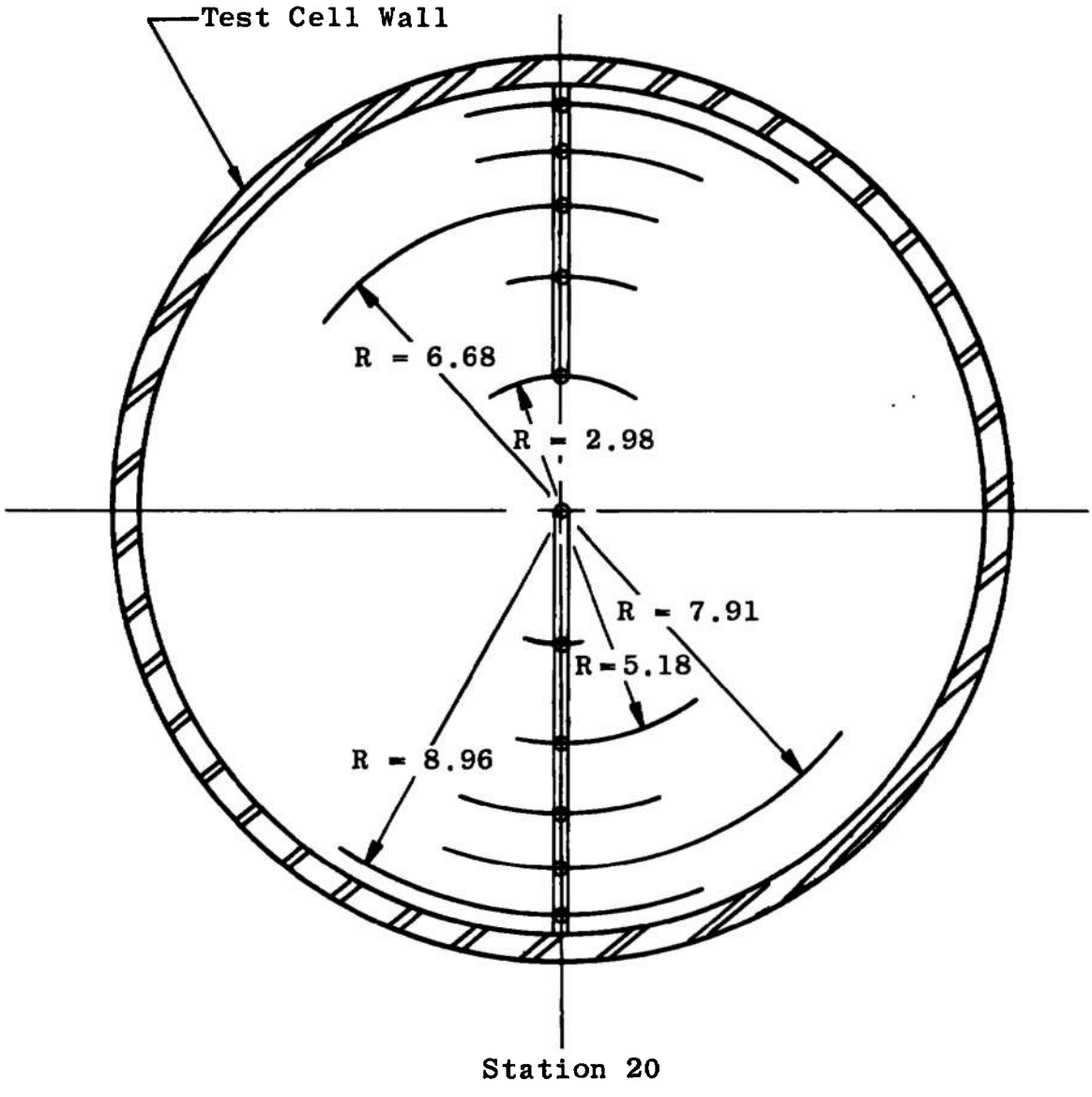

a. Total Pressure Probe Arrangement, 10 Probes on Equal Areas with One on Centerline

Fig. 13 Pitot Tube Arrangement at Collector Inlet Plane

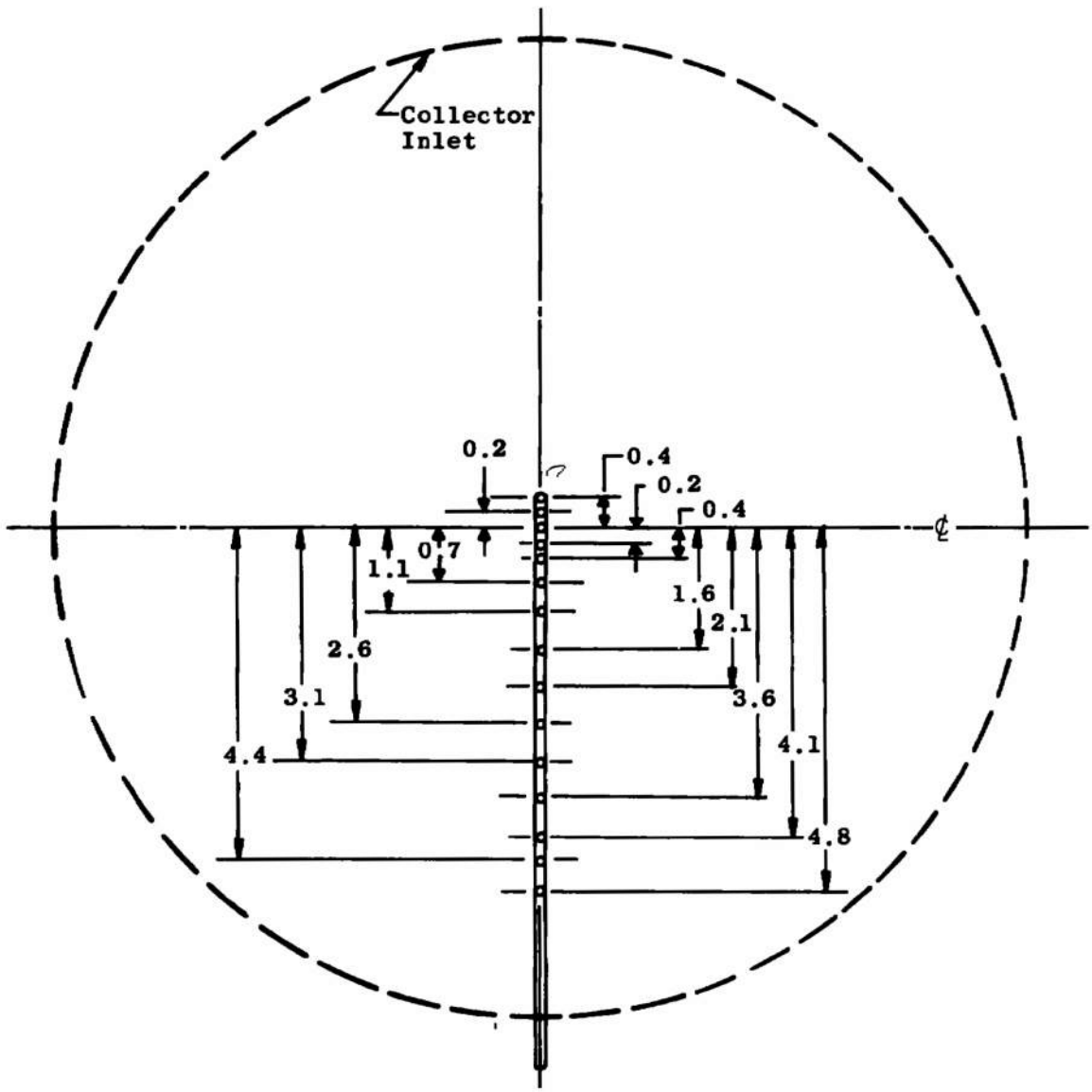

Station 20

b. 15 Total Pressure Probe Arrangement
Fig. 13 Concluded

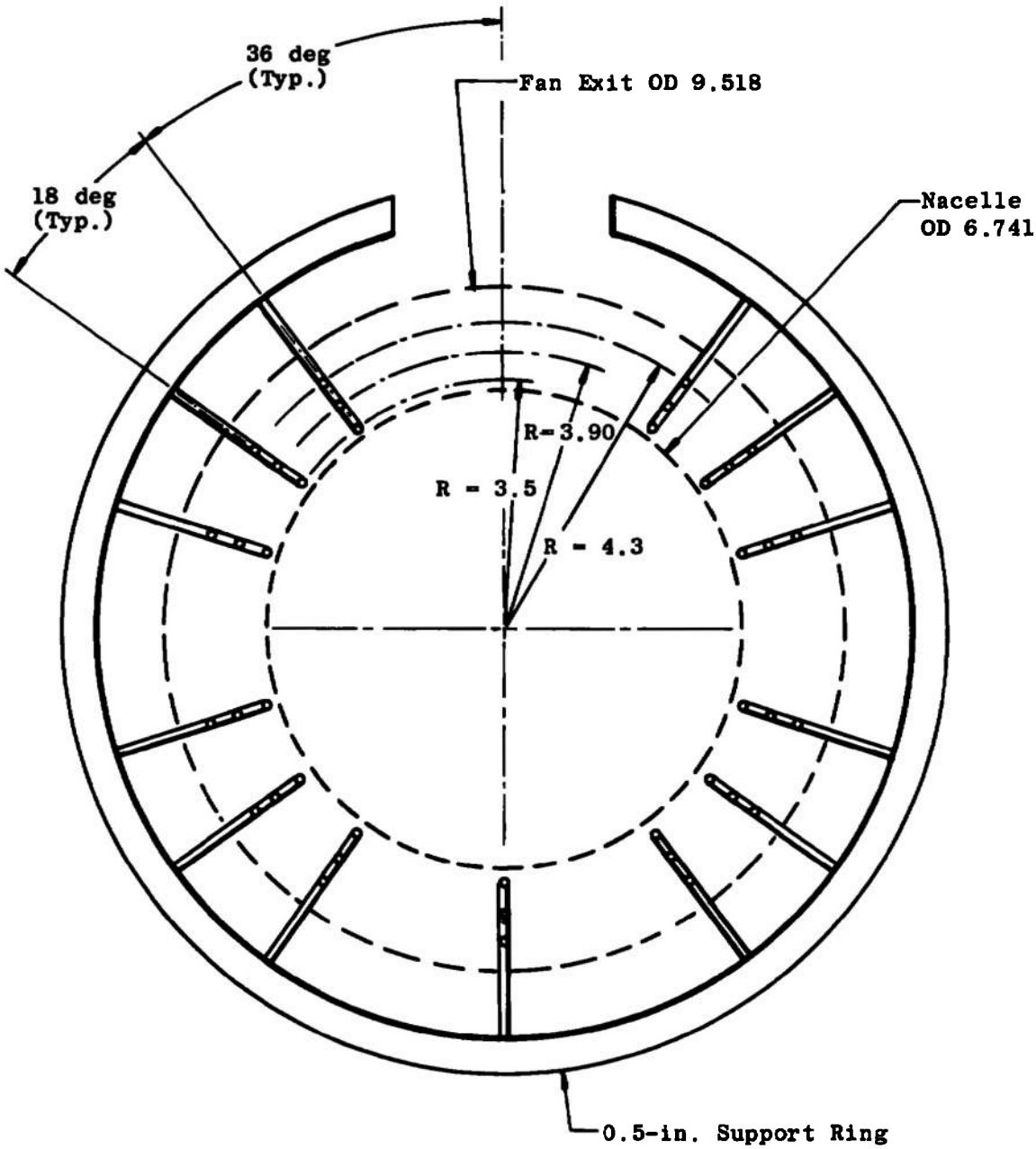

Fig. 14 Total Pressure Survey Rake Showing Probe Location

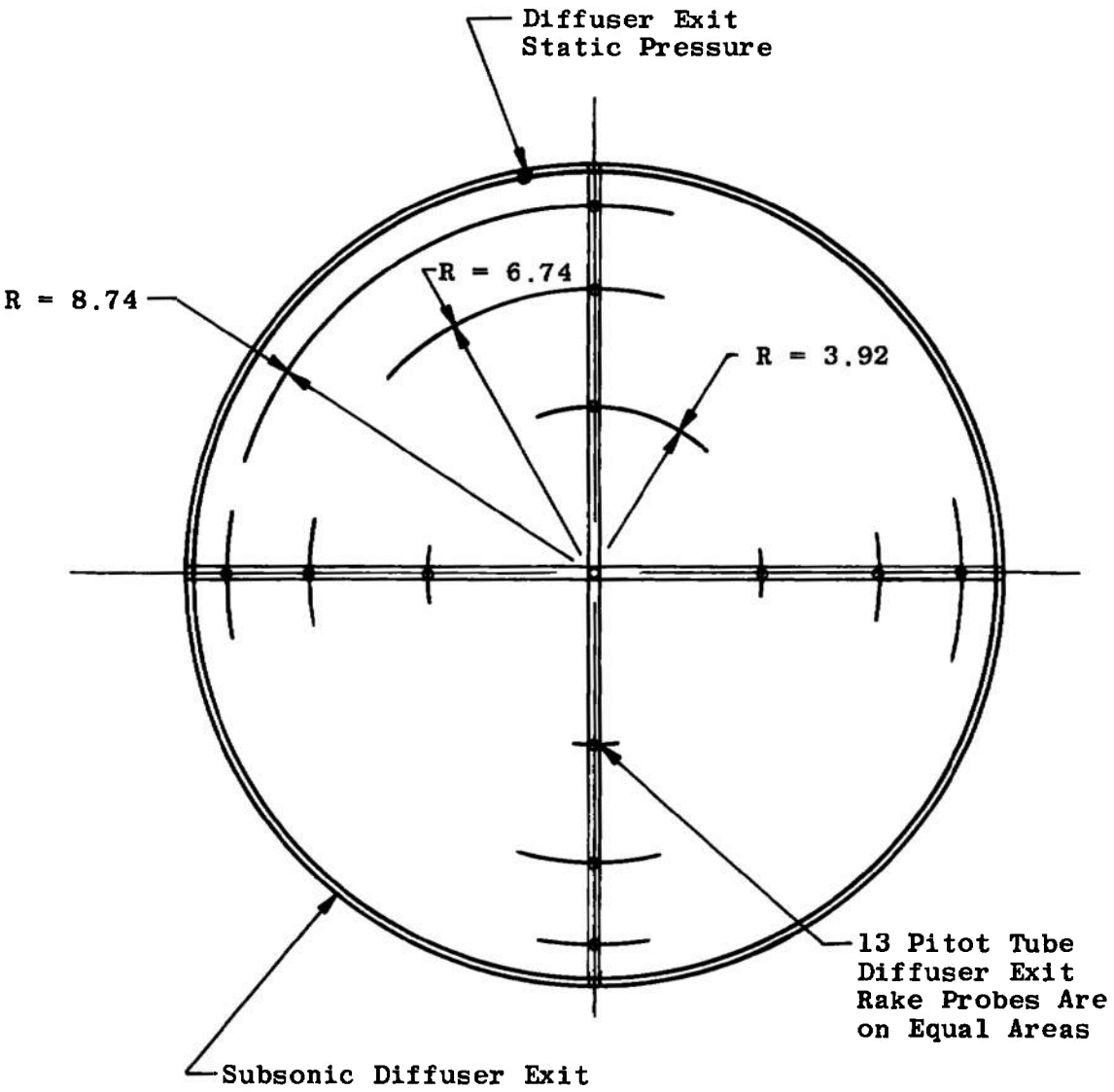

Fig. 15 Subsonic Diffuser Exit Pitot Tube Arrangement

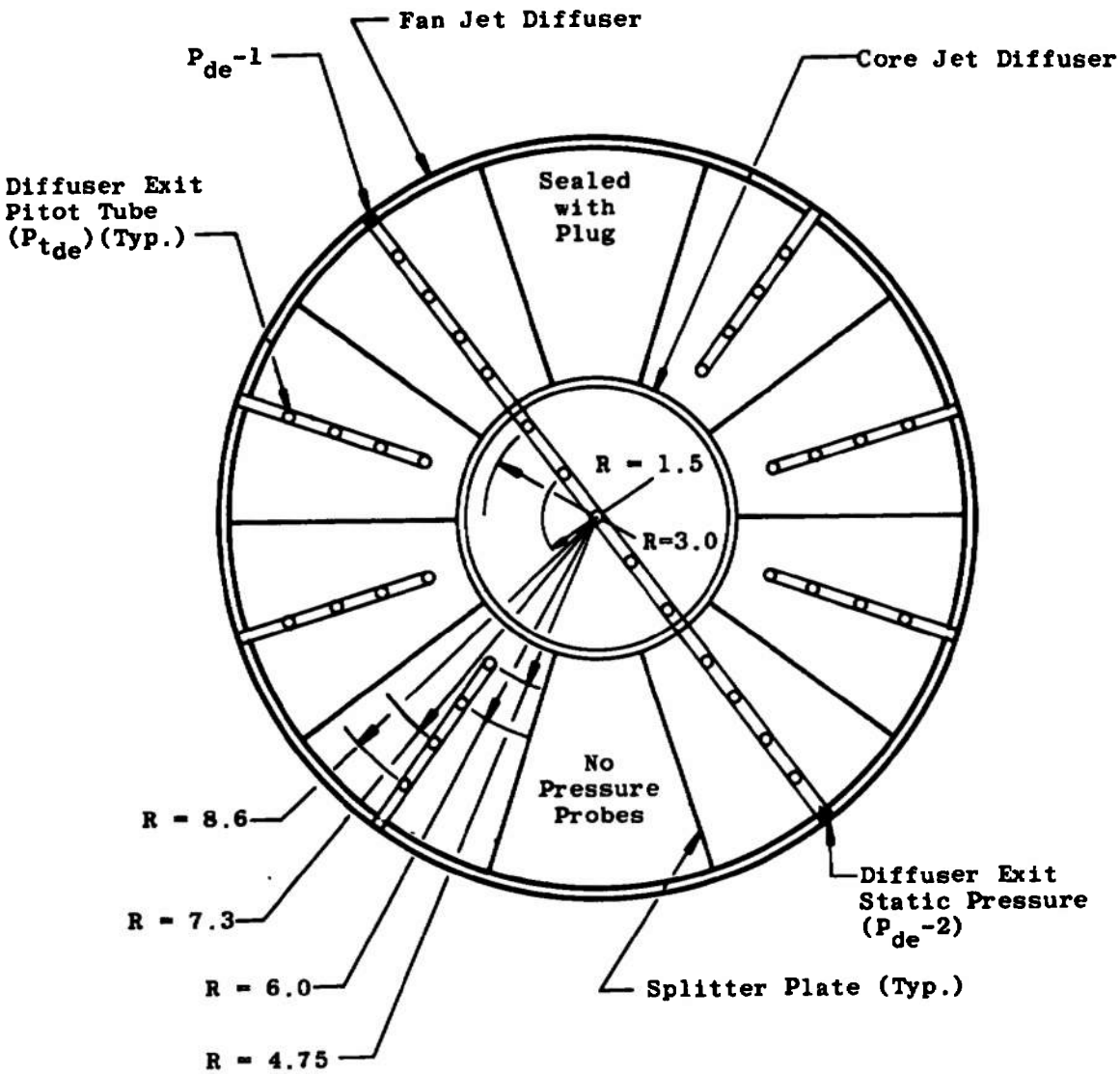

a. Diffuser with Pitot Tubes in the Exit of Each Passage

Fig. 16 Segmented Diffuser Exit Pitot Tube Arrangement

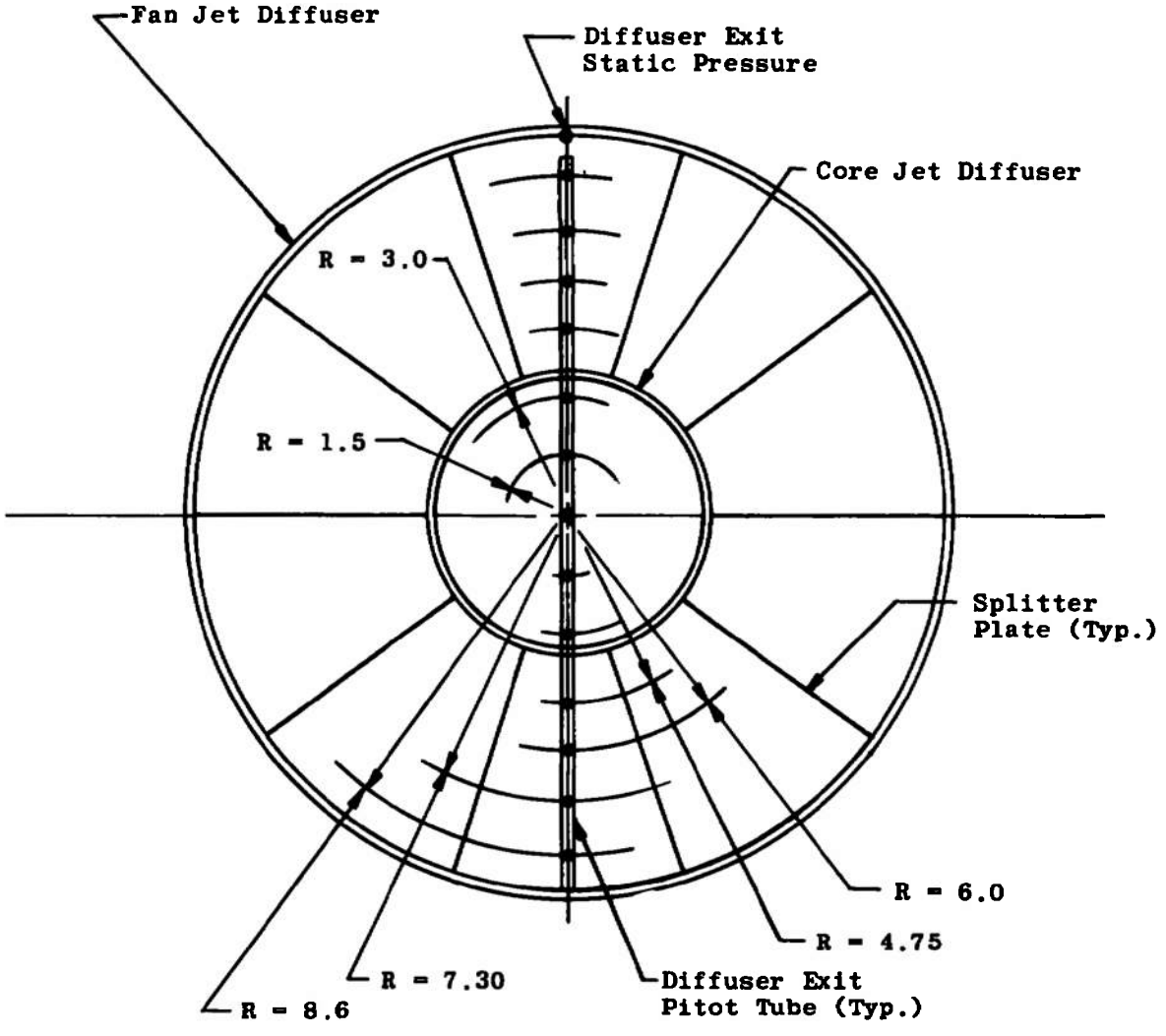

b. 13-Pitot Tube Rake Installed Vertically, Top Passage Open
Fig. 16 Concluded

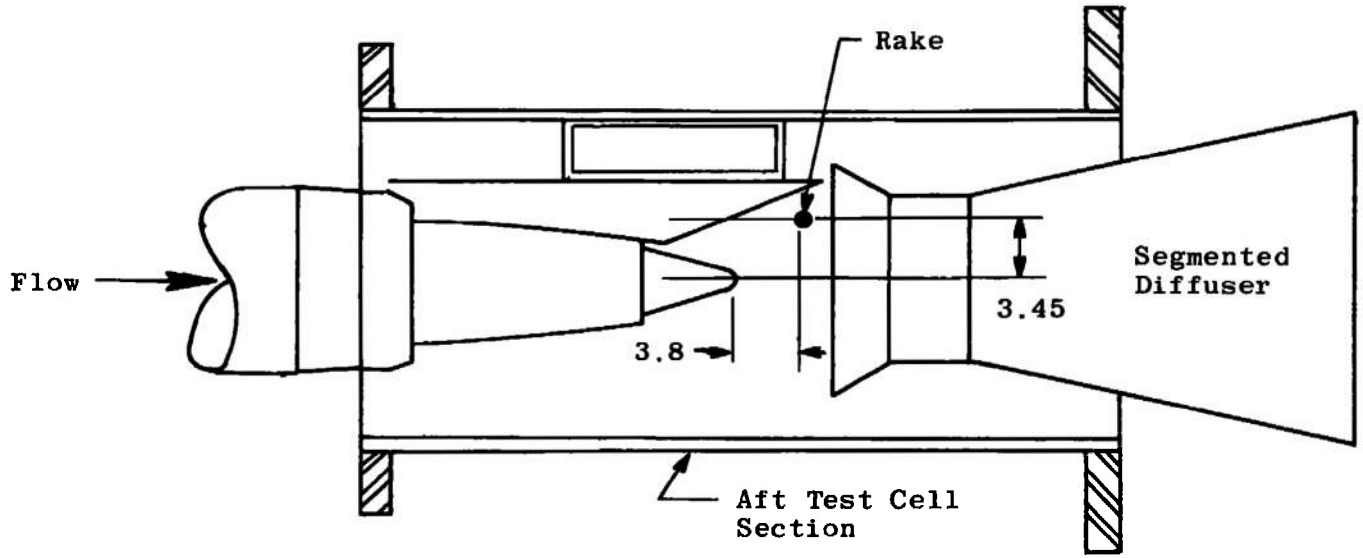

All Dimensions in Inches

Rake Location

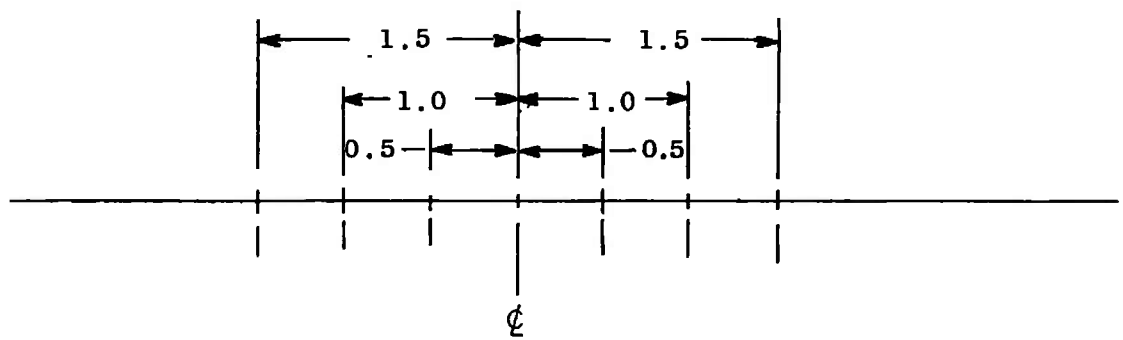

Pitot Tube Arrangement

Fig. 17 Total Pressure Rake Arrangement and Location for Measuring the Pylon Wake

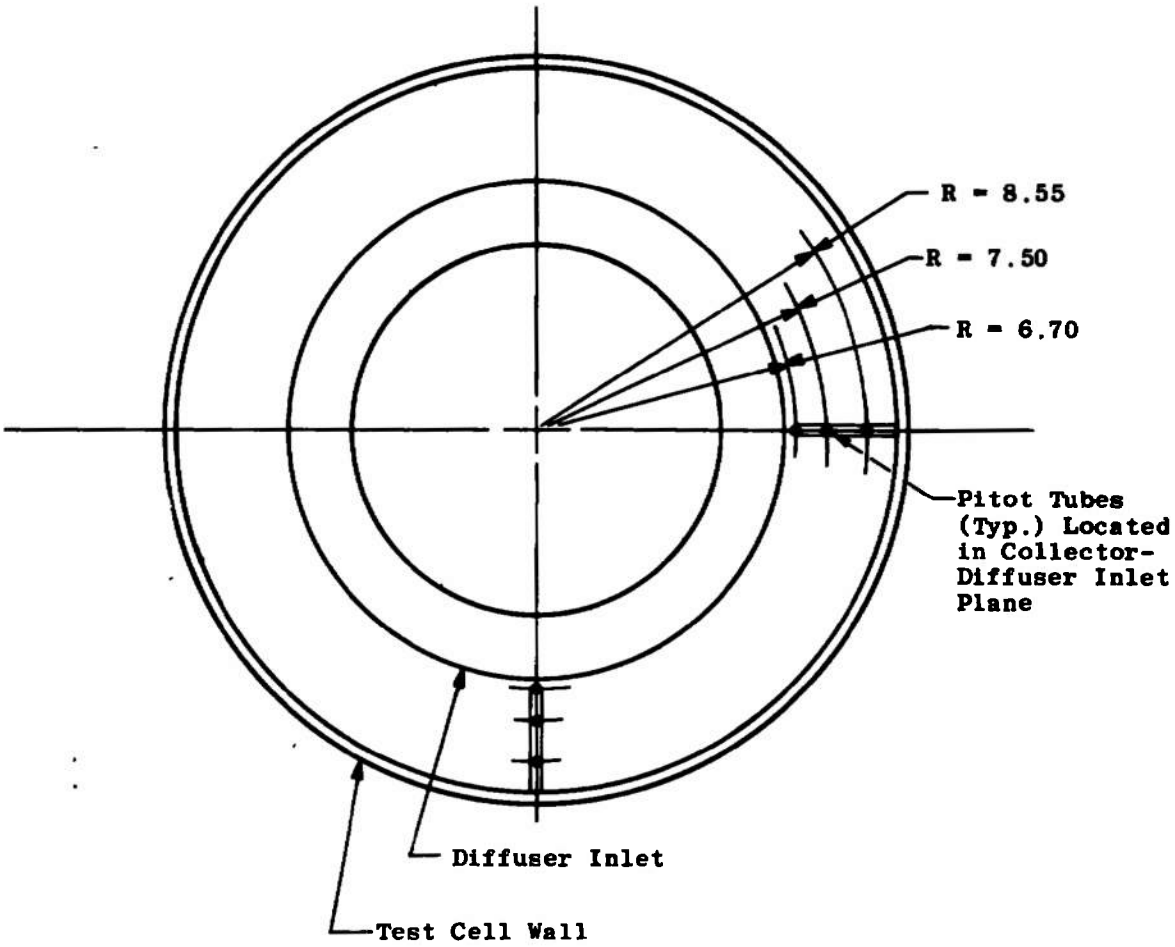

Fig. 18 Location of Pitot Tubes for Flow Check Outside Diffuser Inlet

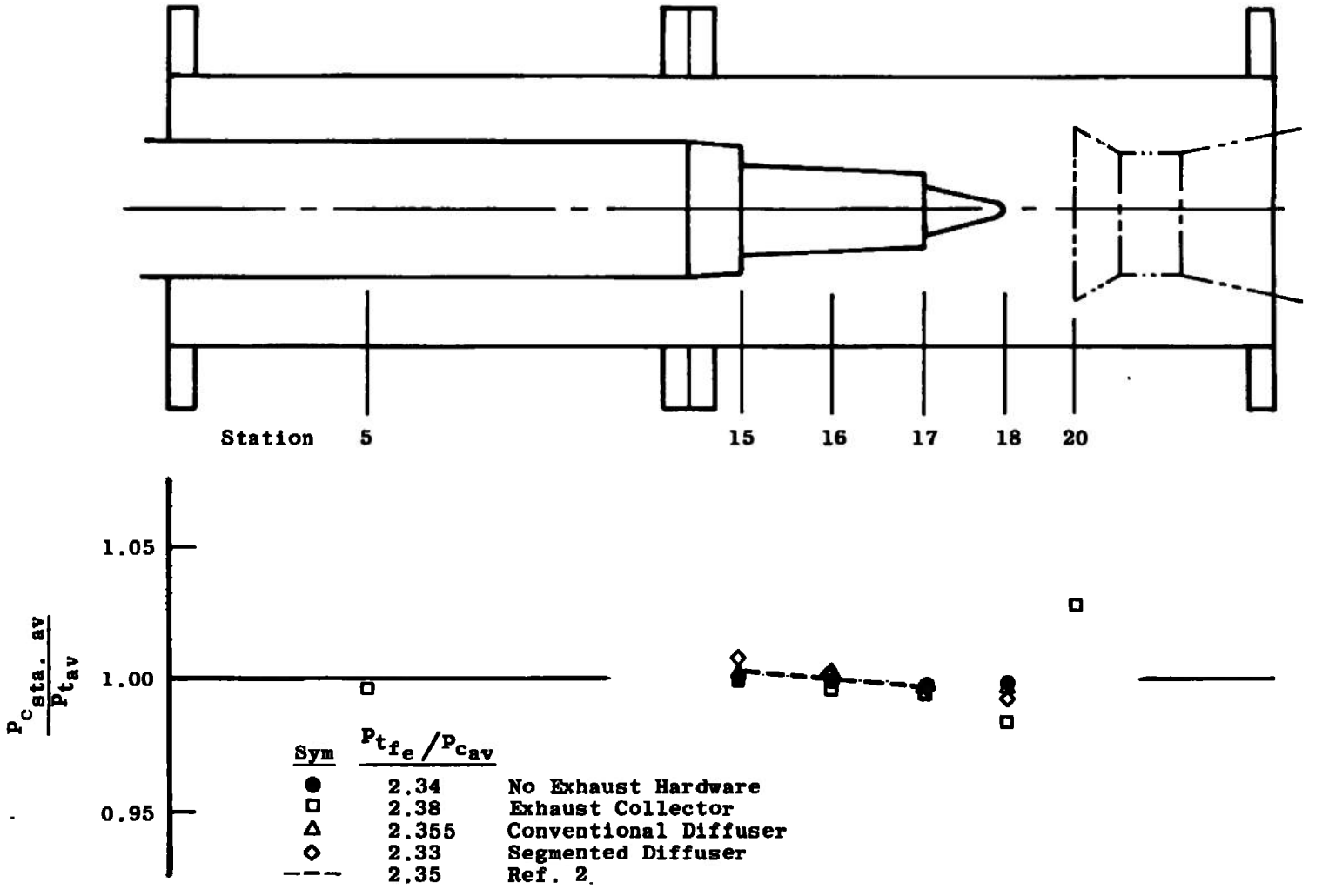

a. For $P_{t_{f_e}}/P_{c_{av}}$ Ratio of 2.34

Fig. 19 Test Cell Surface Pressures

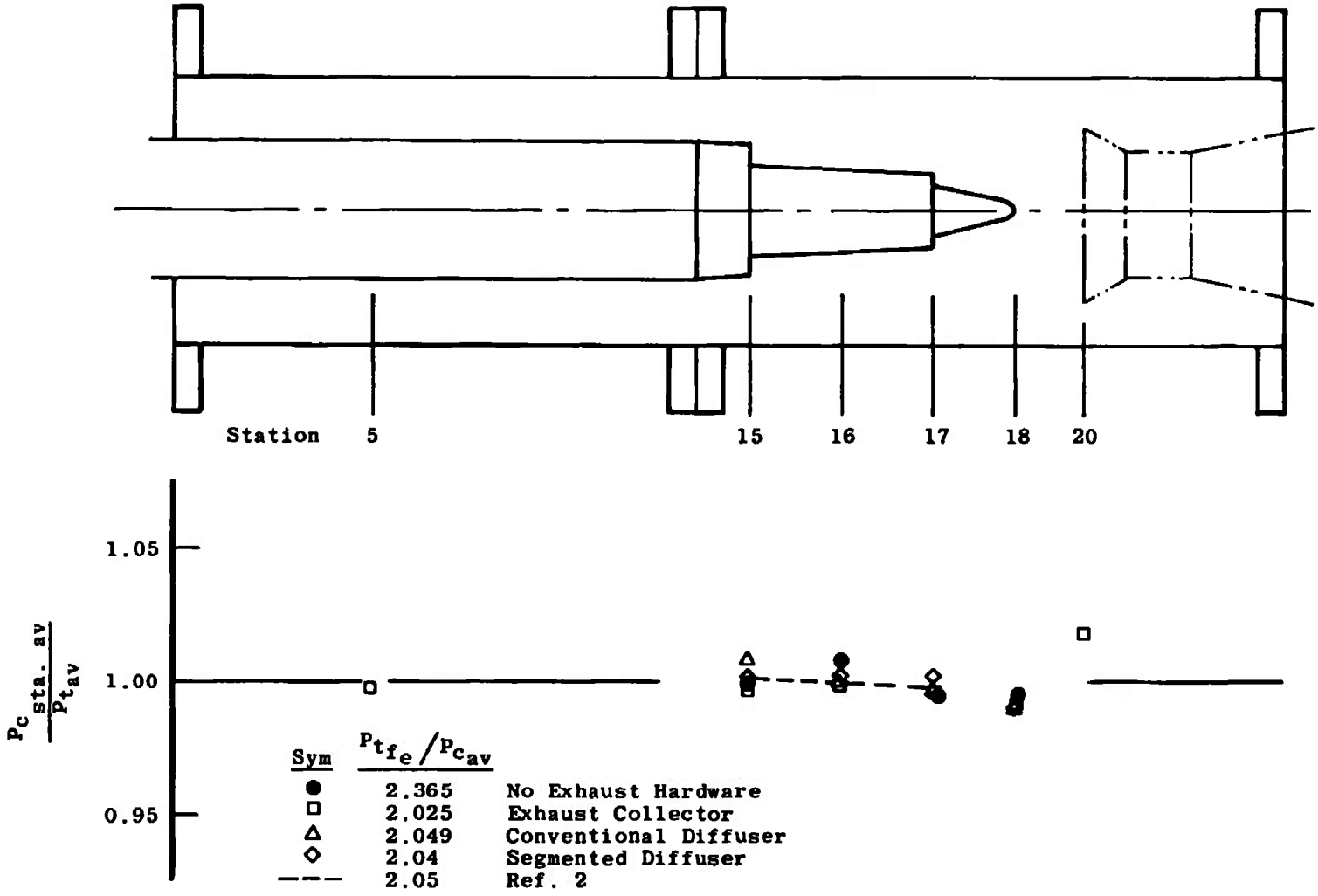

b. For $P_{t_{f_e}}/P_{c_{av}}$ Ratio of 2.04

Fig. 19 Continued

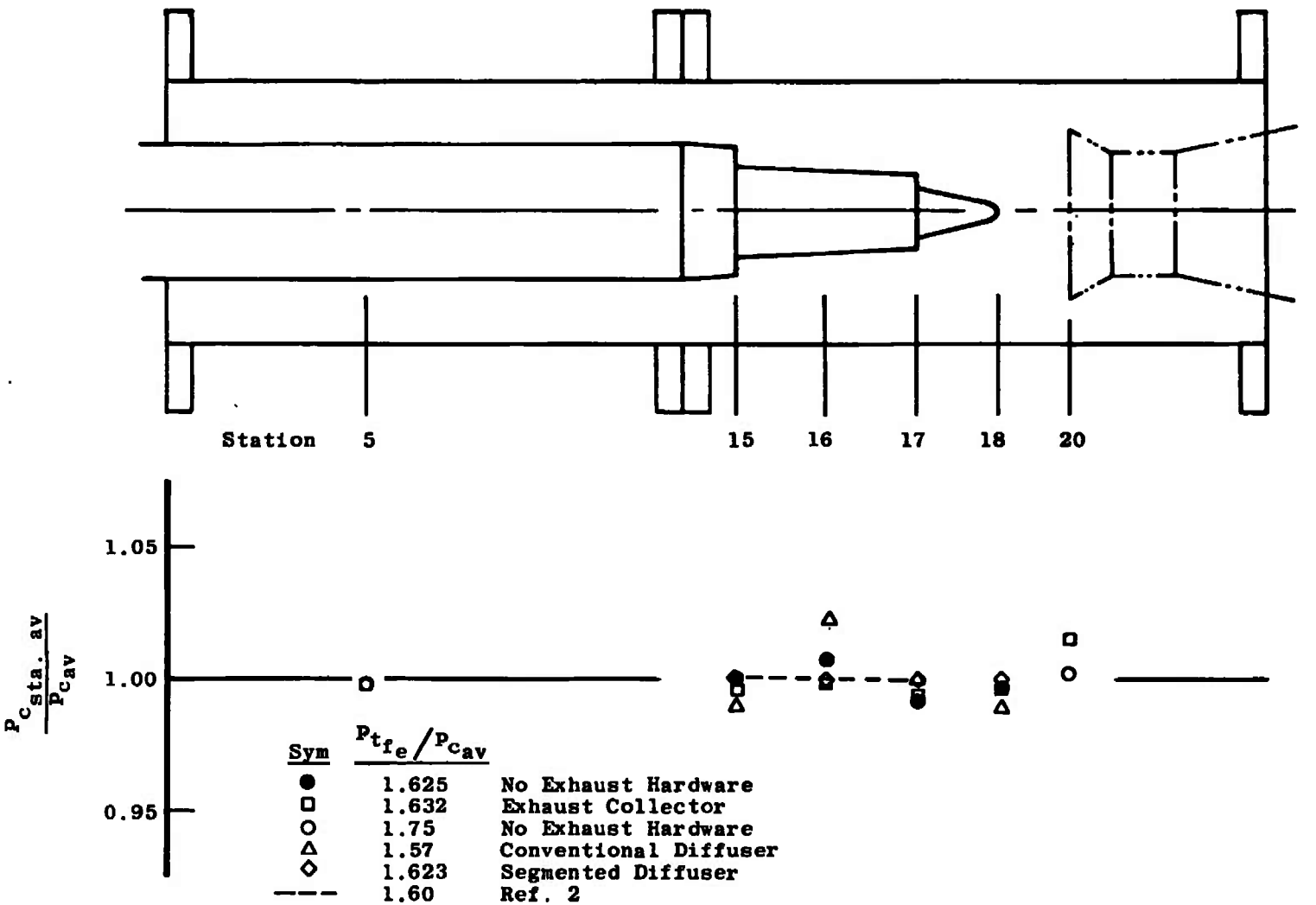

c. For $P_{t_{f_e}}/P_{c_{av}}$ Ratio of 1.60

Fig. 19 Continued

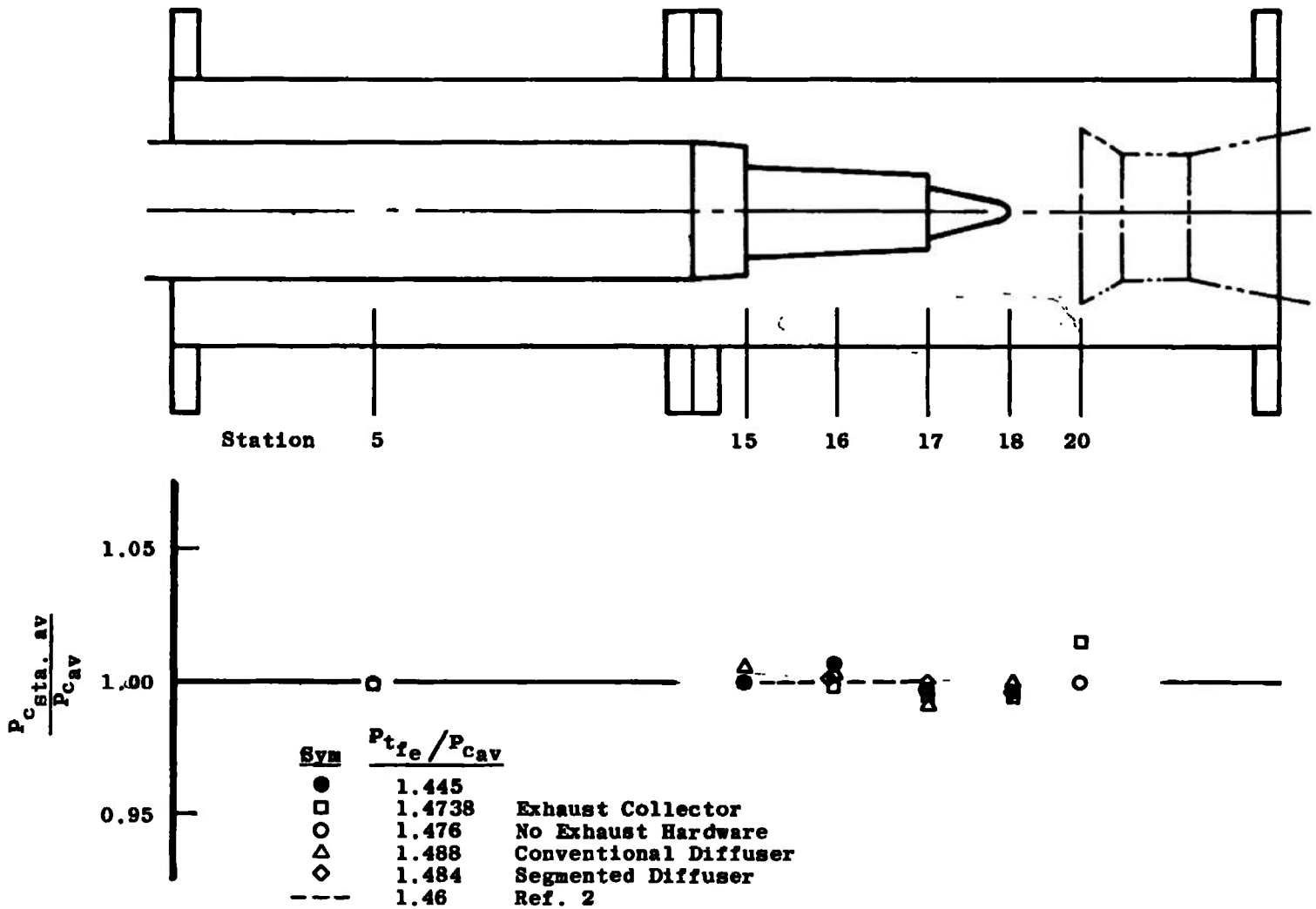

d. For $P_{t_{f_e}}/P_{c_{av}}$ Ratio of 1.47

Fig. 19 Concluded

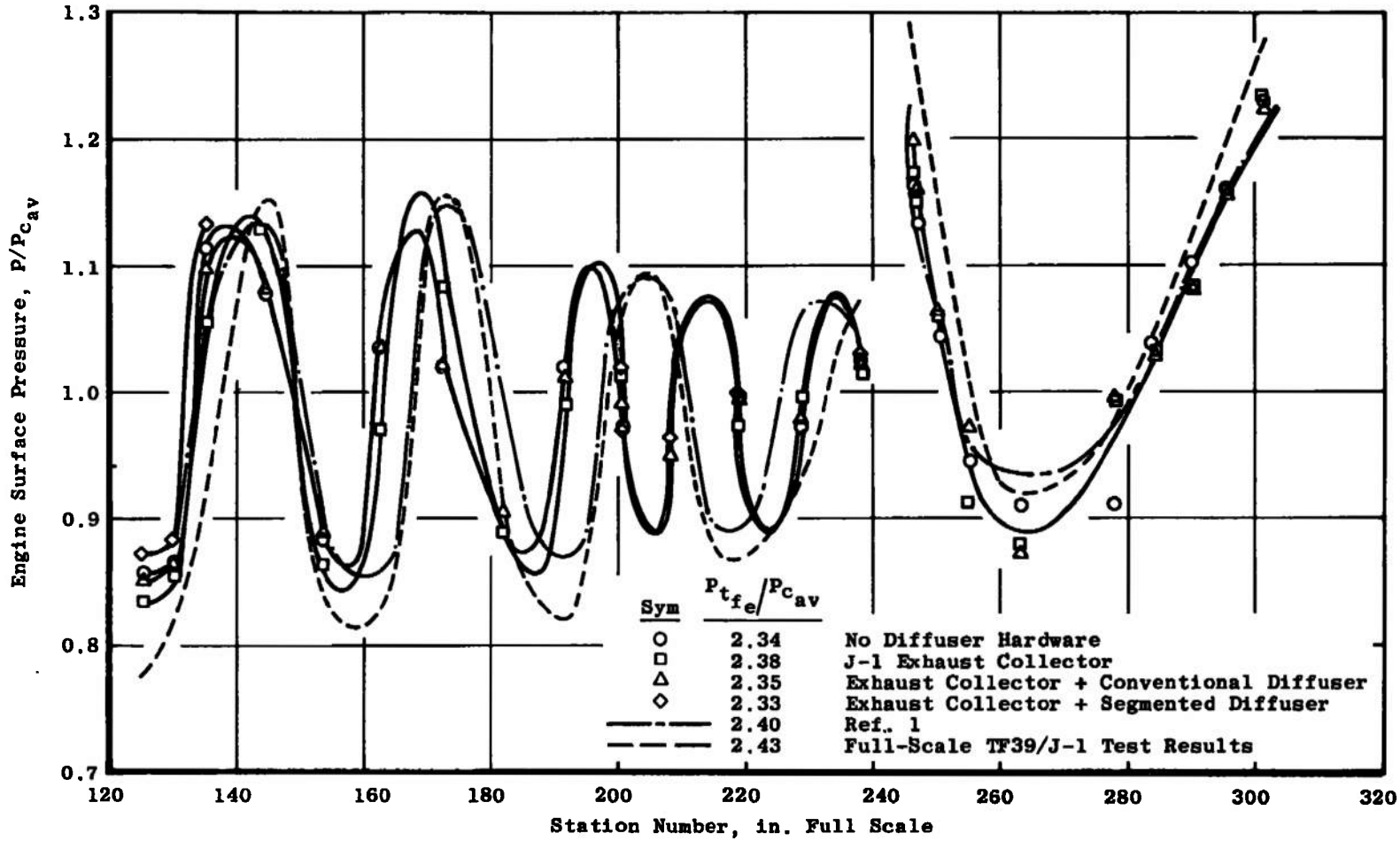

a. For $P_{t_{f_e}}/P_{c_{av}}$ Ratio of 2.34

Fig. 20 Turbofan Engine Surface Pressures

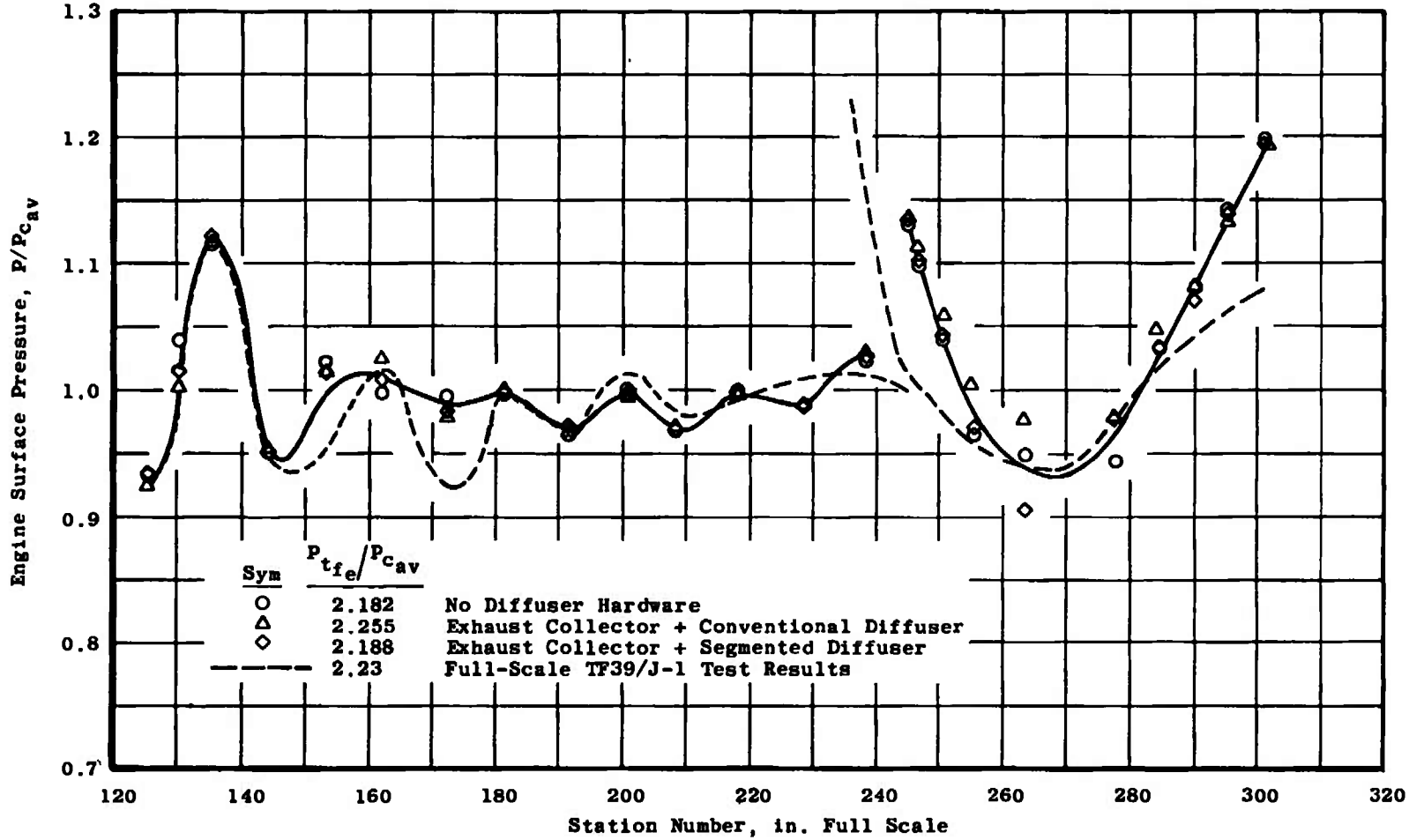

b. For $P_{t_{f_e}}/P_{c_{av}}$ Ratio of 2.20

Fig. 20 Continued

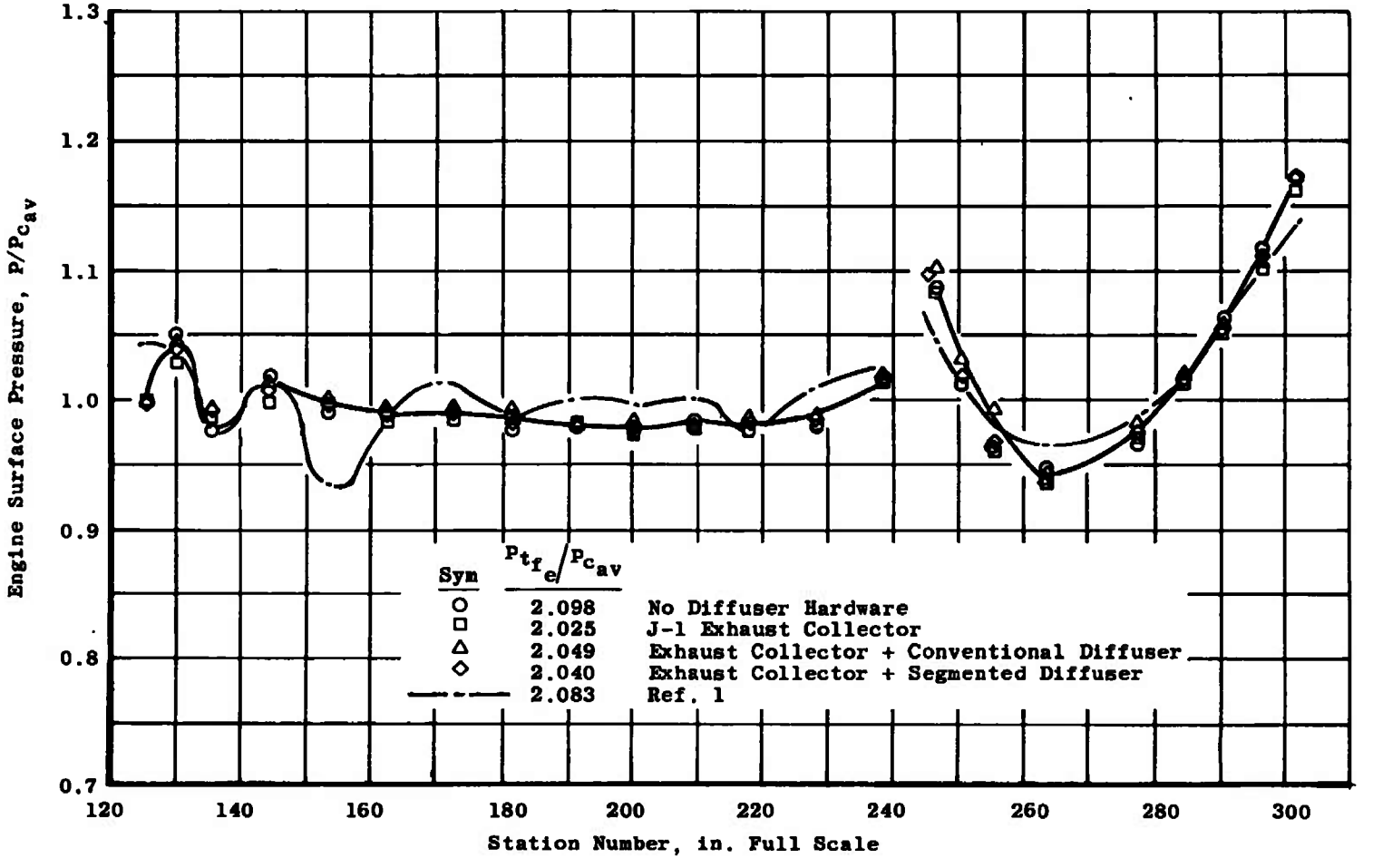

c. For $P_{t_{f_e}}/P_{c_{av}}$ Ratio of 2.04

Fig. 20 Continued

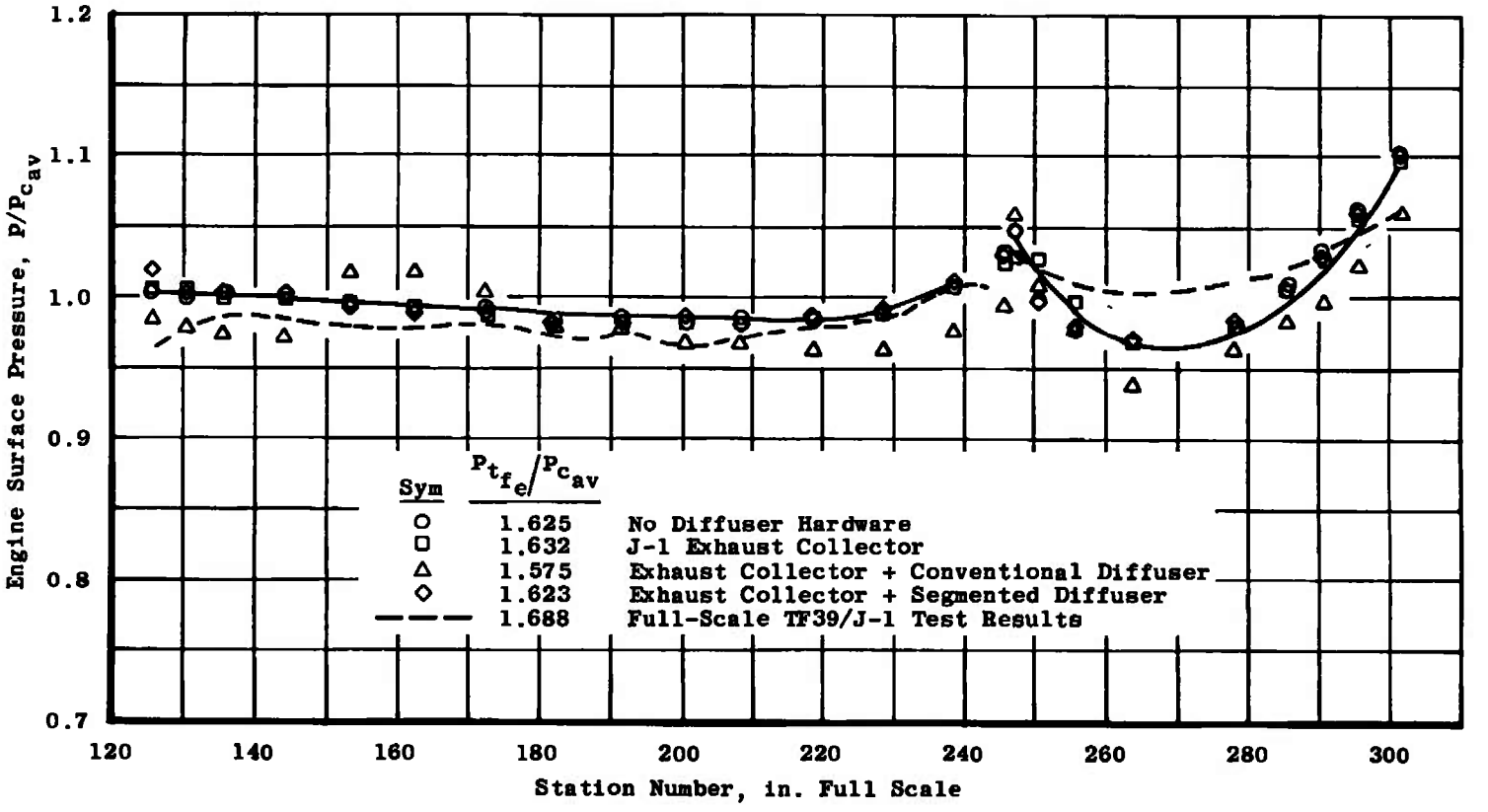

d. For $P_{t_{f_e}}/P_{c_{av}}$ Ratio of 1.60

Fig. 20 Continued

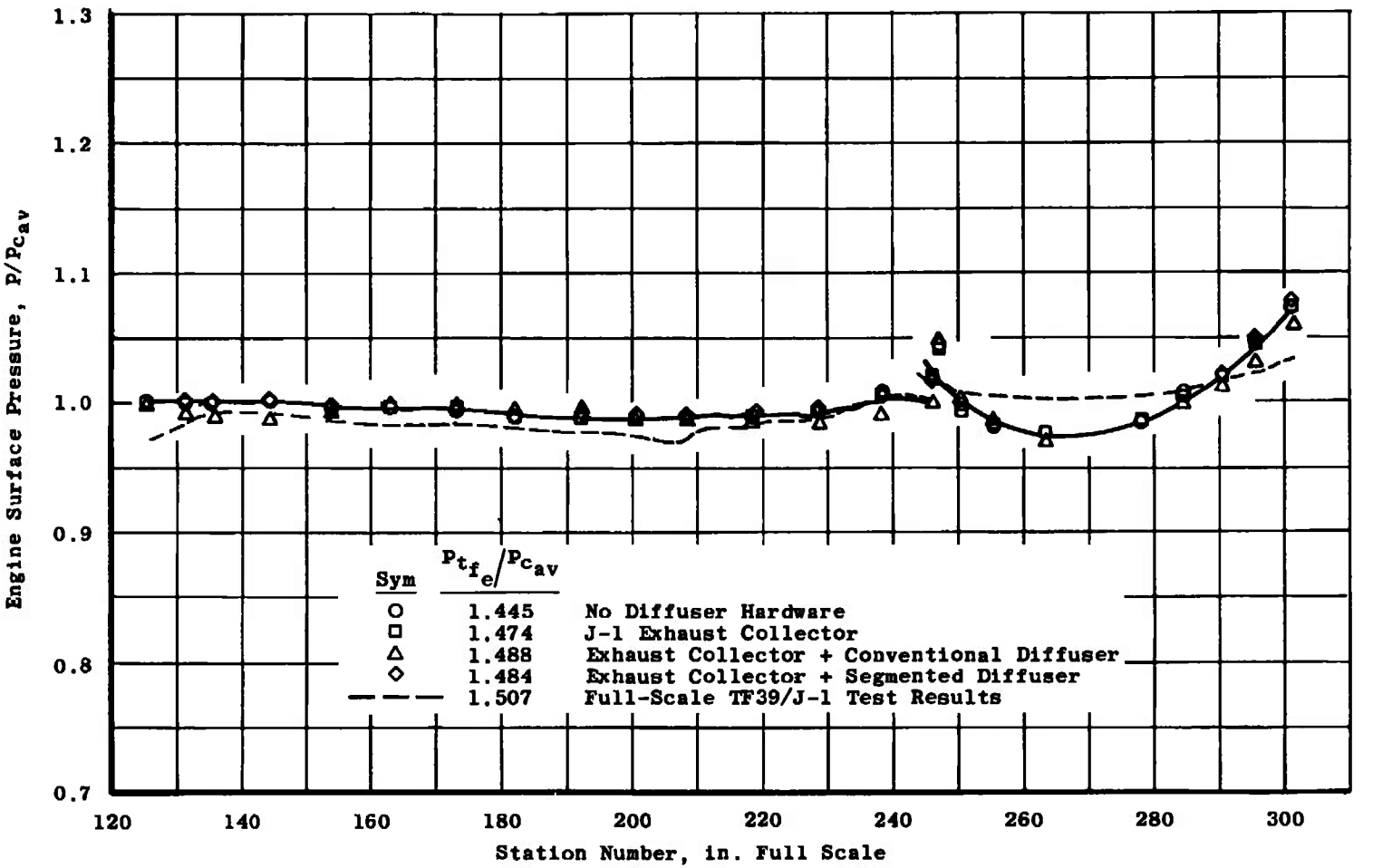

e. For $P_{t_{f_e}}/P_{c_{av}}$ Ratio of 1.47

Fig. 20 Concluded

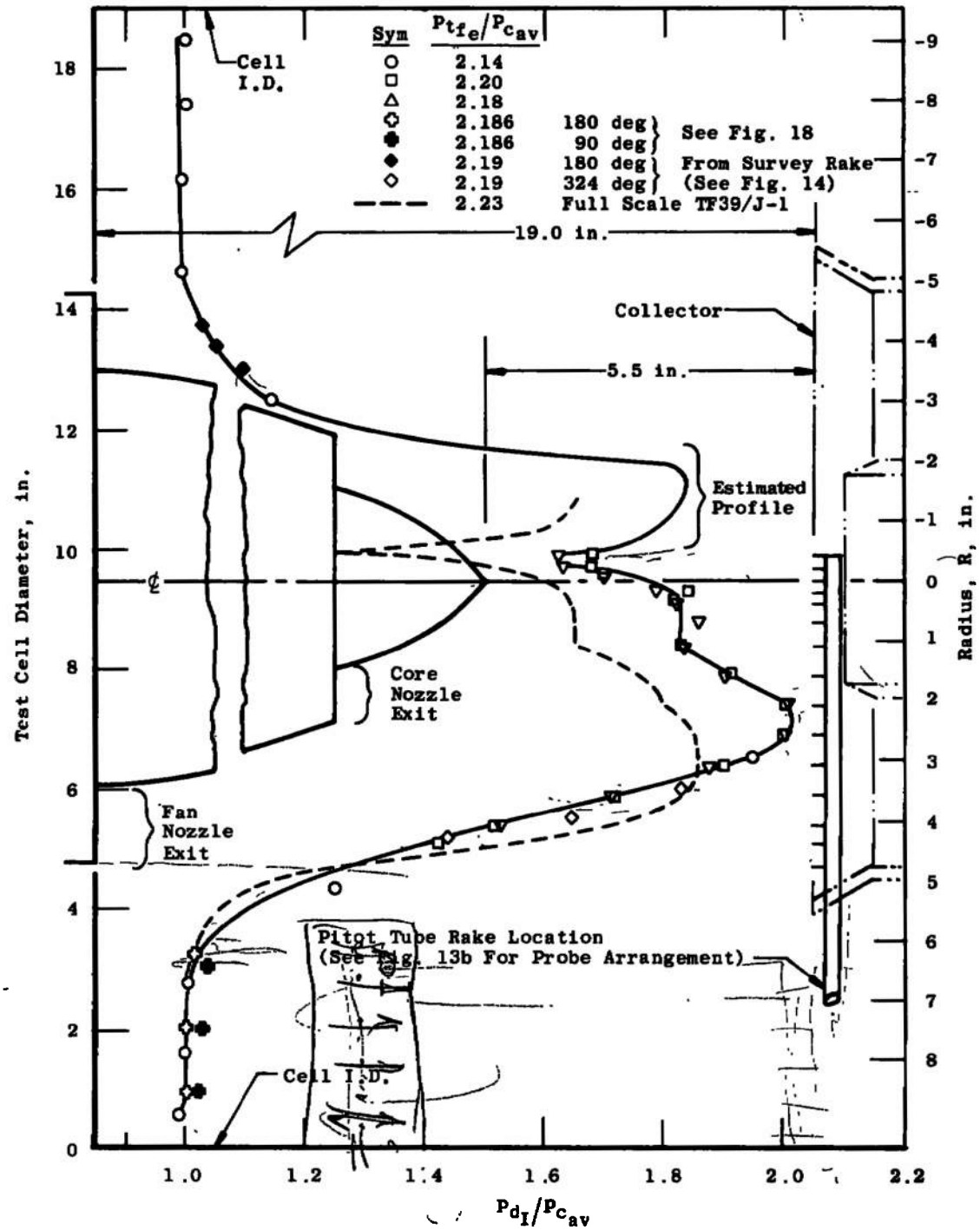

a. For $P_{tf_e}/P_{c_{av}}$ Ratio of 2.20

Fig. 21 Exhaust Jet Pressure Survey at Collector Inlet Plane

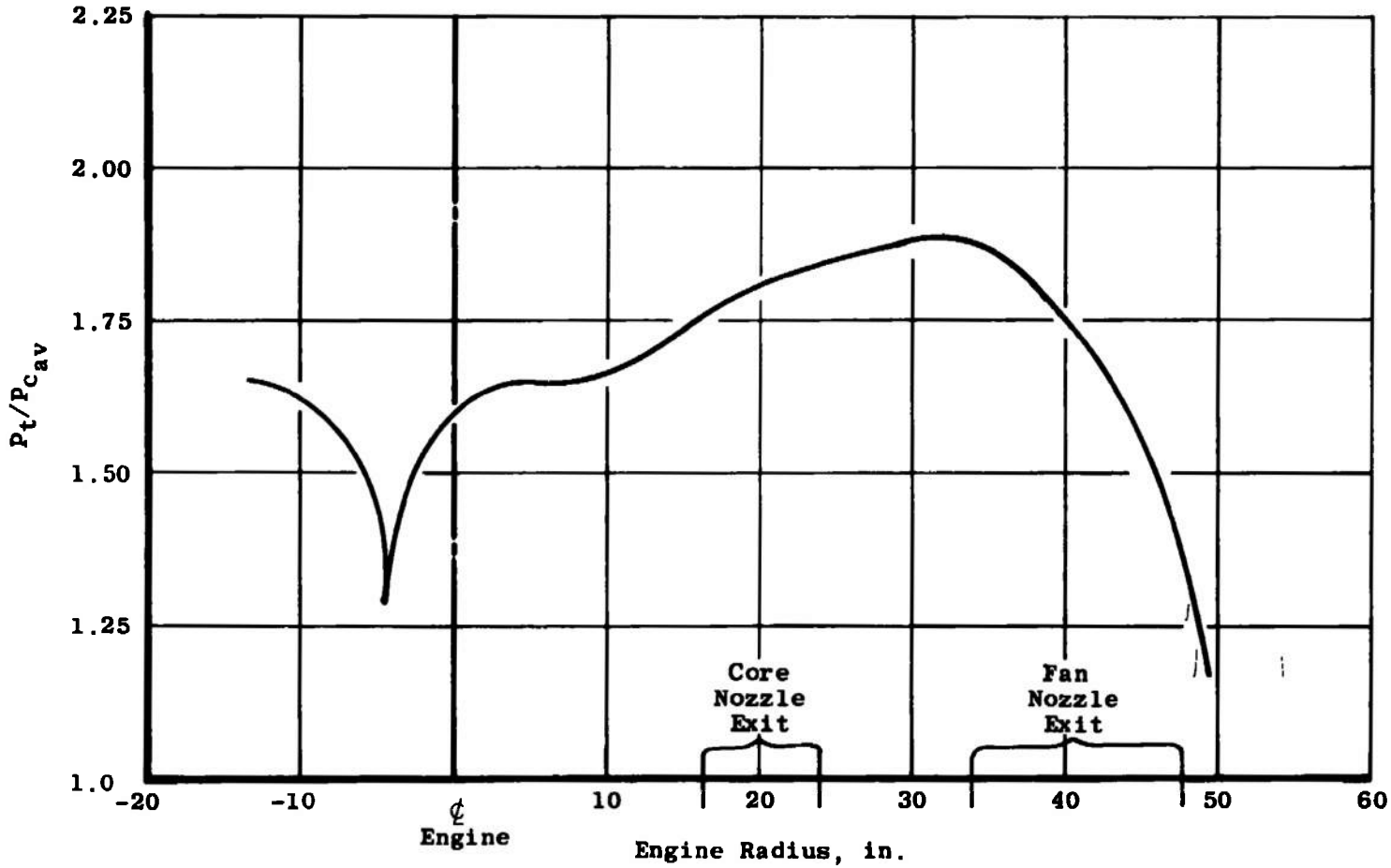

b. Results from Full-Scale TF39 Test in Test Cell J-1 for $P_{t_{f_e}}/P_{c_{av}}$ Ratio of 2.23

Fig. 21 Continued

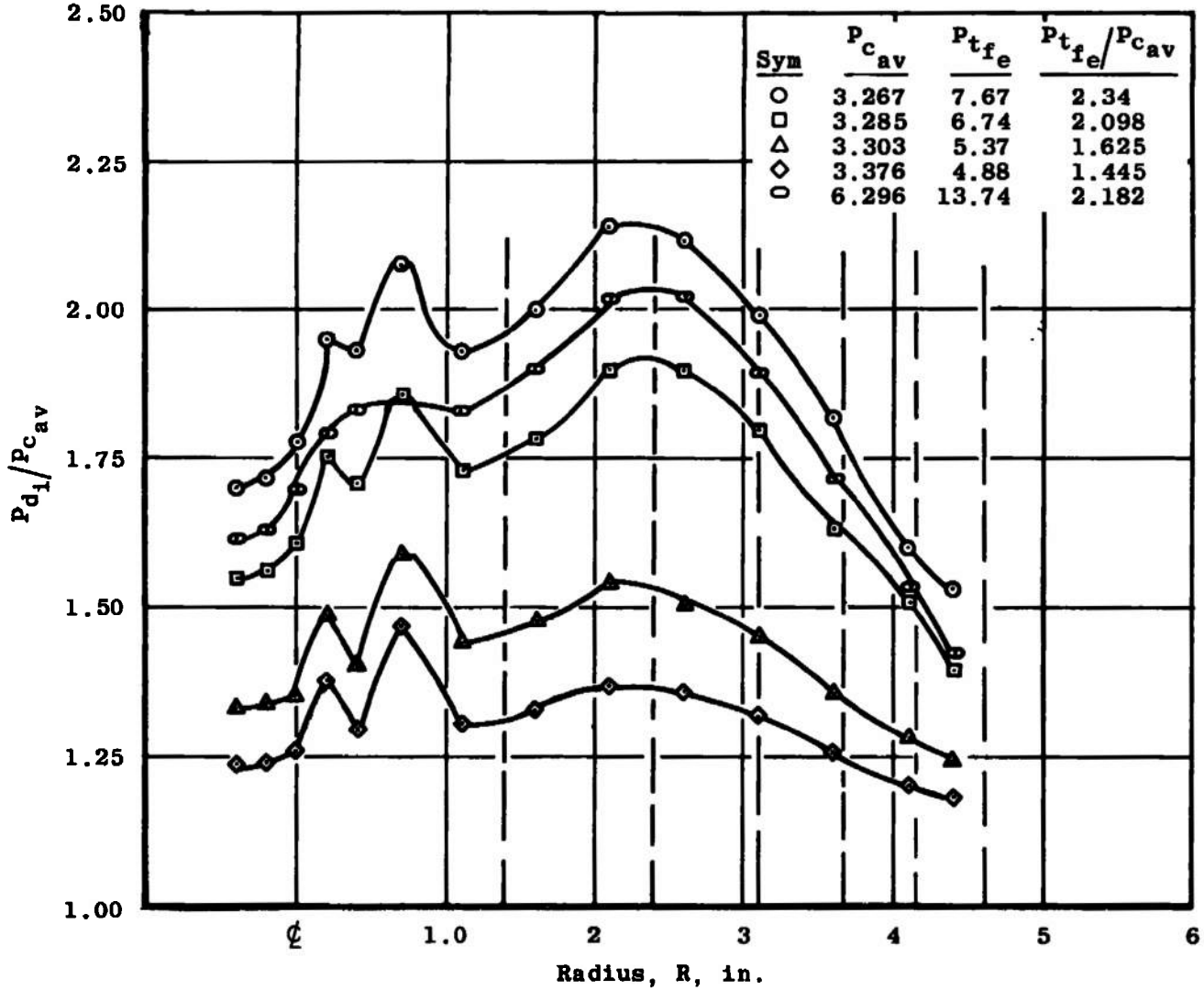

c. Model Study Results for Each Fan Nozzle Pressure Ratio Tested

Fig. 21 Concluded

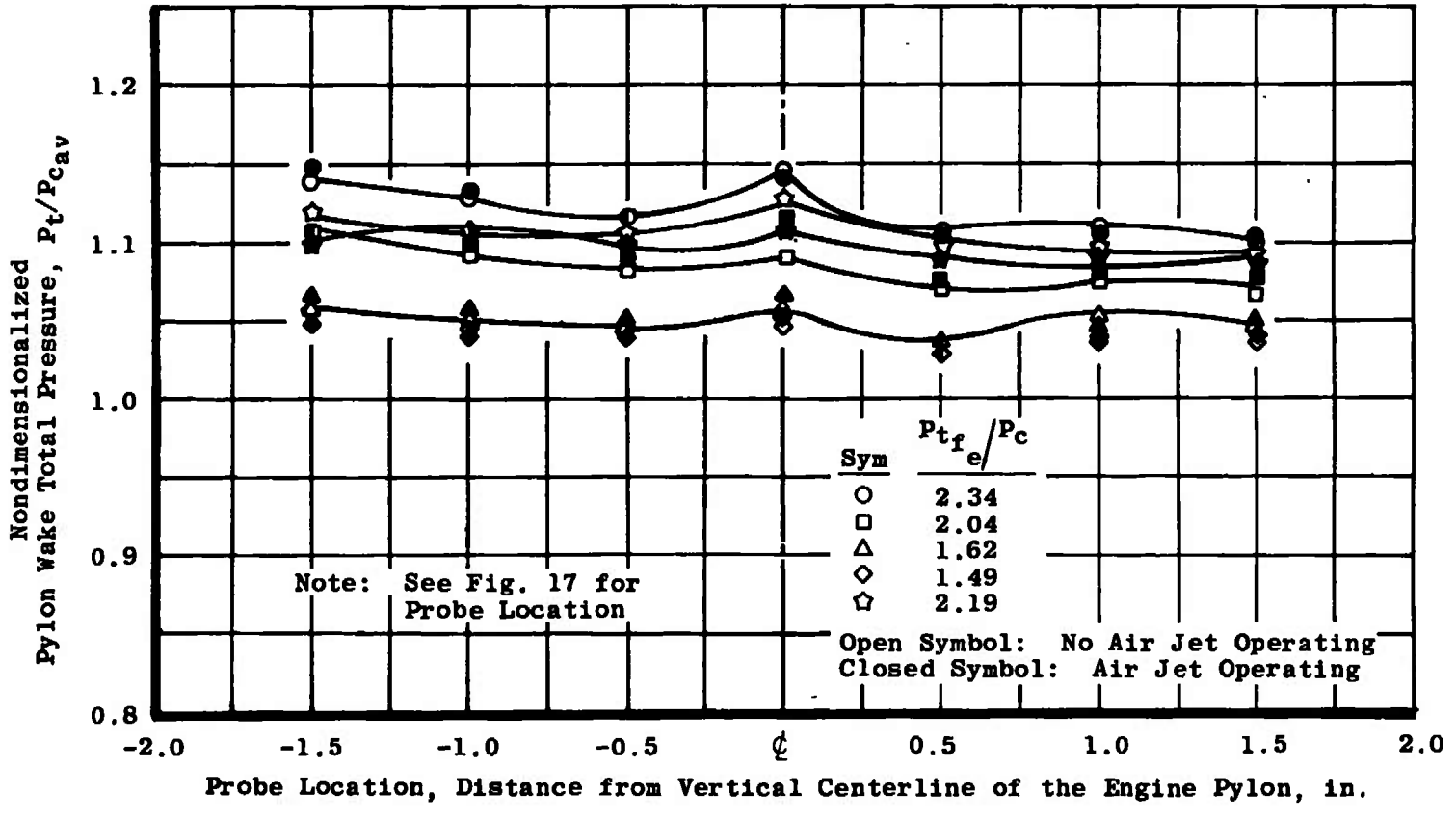

Fig. 22 Total Pressure Survey in Pylon Wake, Collector Inlet Plane

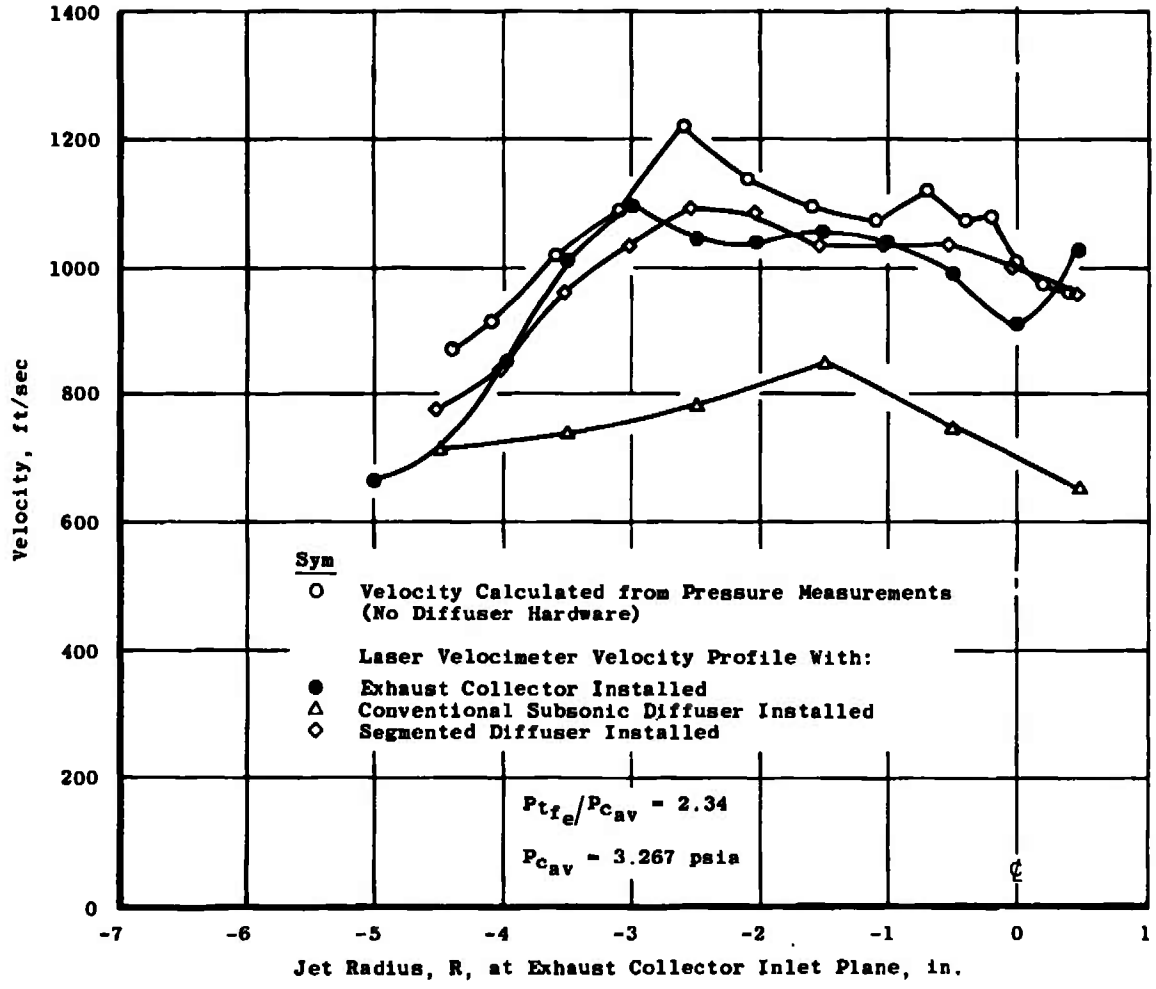

a. For $P_{t_{f_e}}/P_{c_{av}}$ Ratio of 2.34

Fig. 23 Comparison of Collector Inlet Velocity Profile between Laser Velocimeter and Calculated Values

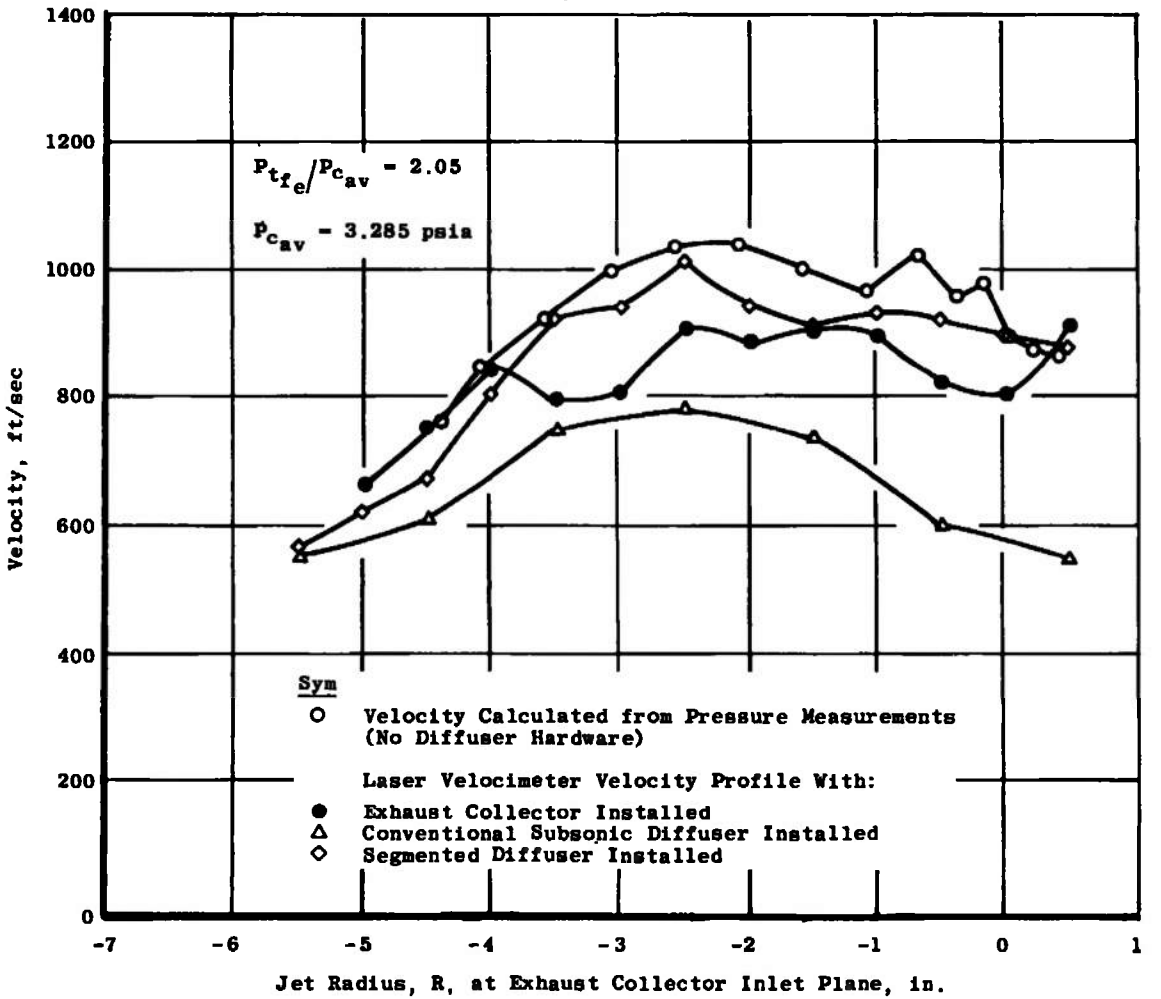

b. For $P_{t_{f_e}}/P_{c_{av}}$ Ratio of 2.05

Fig. 23 Continued

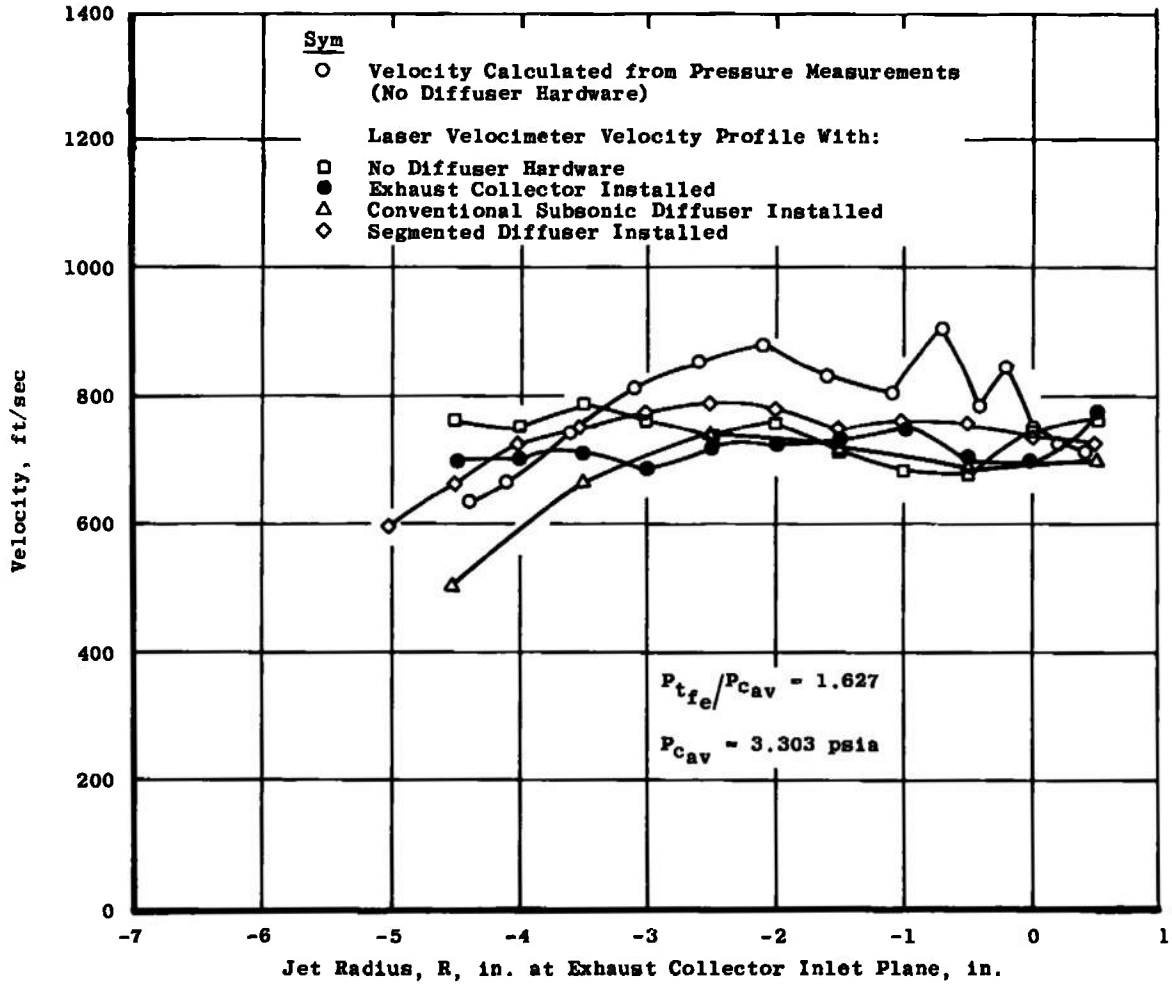

c. For $P_{t_{f_e}}/P_{c_{av}}$ Ratio of 1.63

Fig. 23 Continued

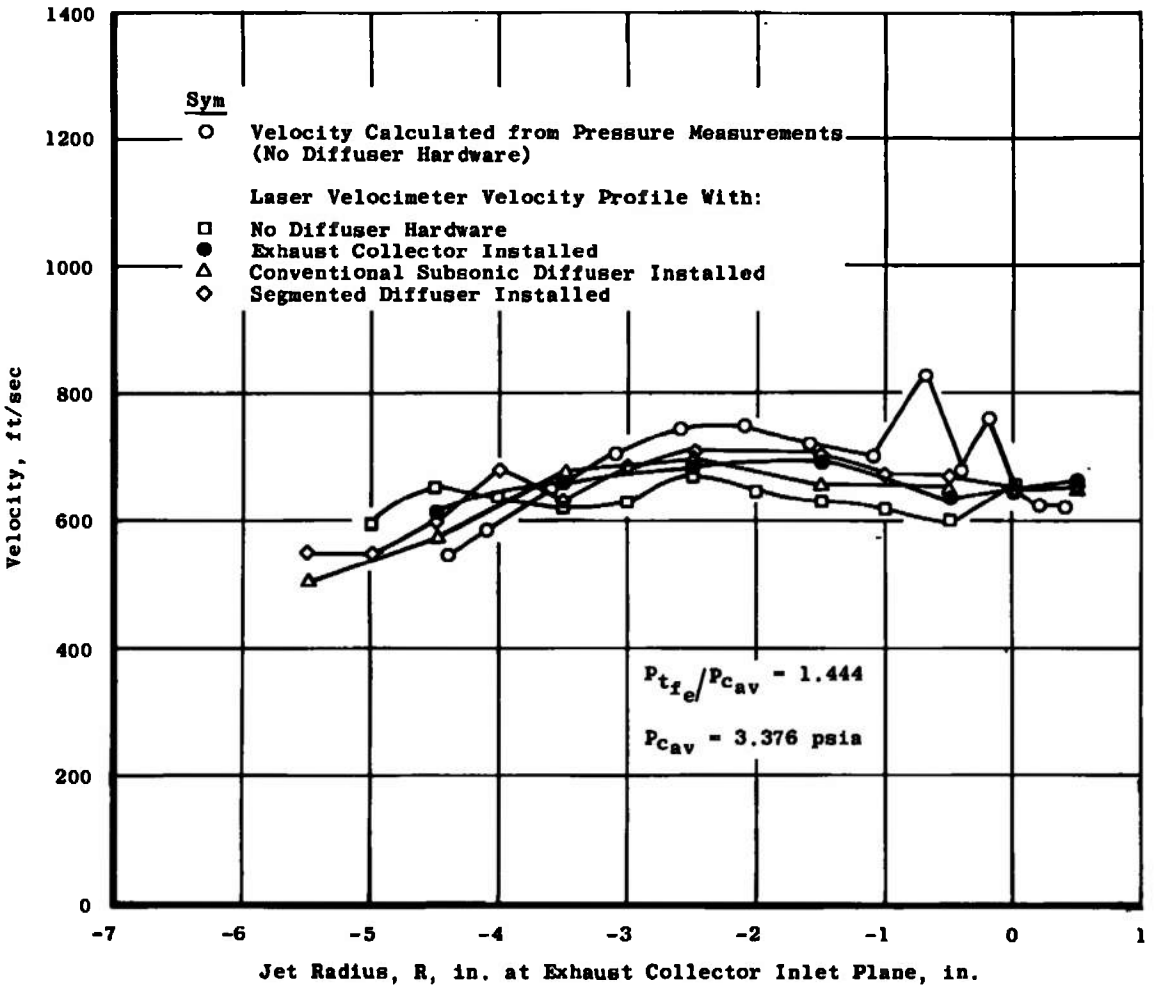

d. For $P_{t_{f_e}}/P_{c_{av}}$ Ratio of 1.44
Fig. 23 Continued

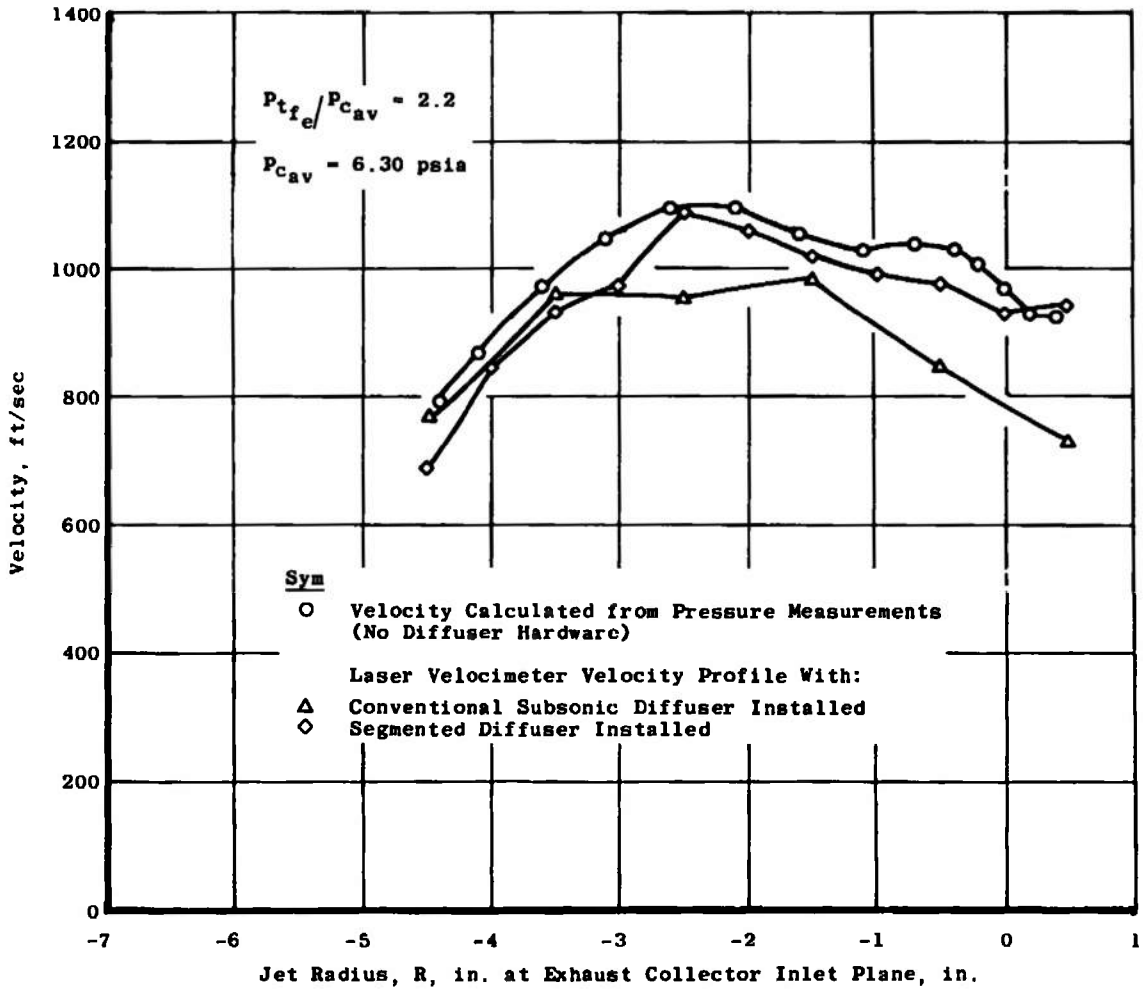

e. For $P_{t_{f_e}}/P_{c_{av}}$ Ratio of 2.18

Fig. 23 Concluded

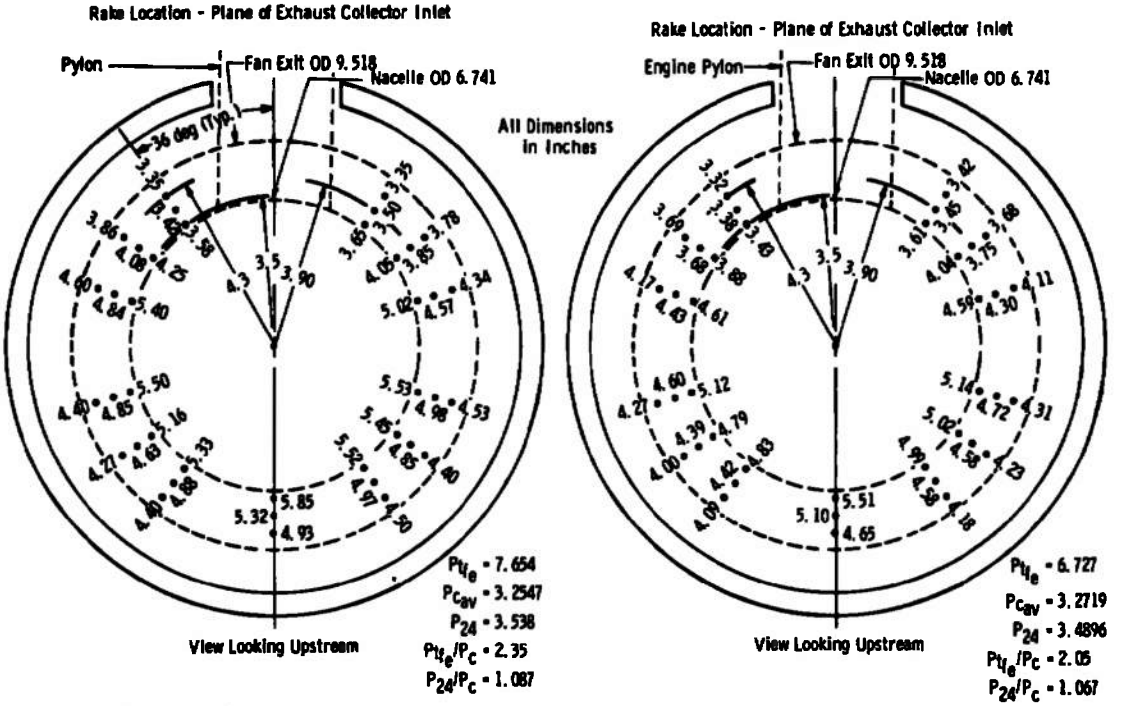

a. For $P_{t_{f_e}}/P_{c_{av}}$ Ratio of 2.35

b. For $P_{t_{f_e}}/P_{c_{av}}$ Ratio of 2.05

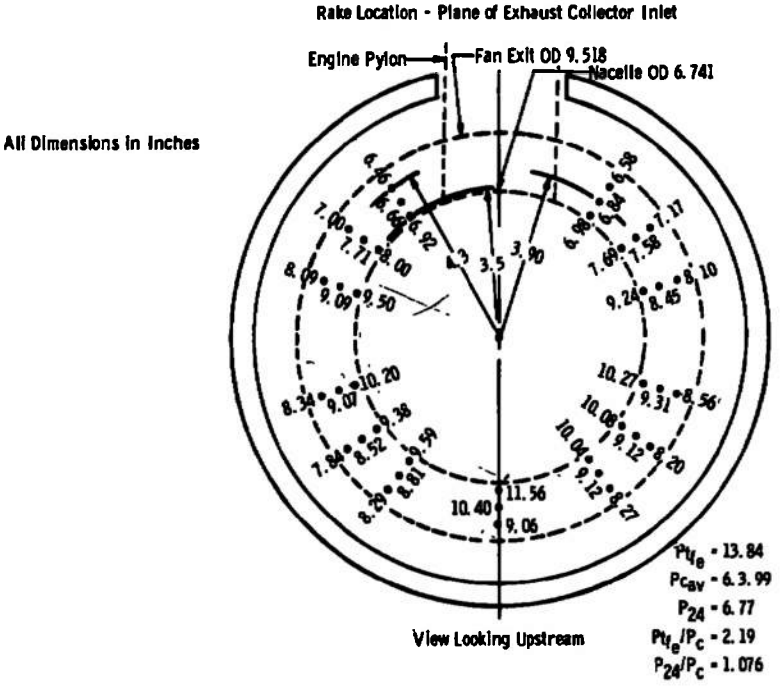

c. For $P_{t_{f_e}}/P_{c_{av}}$ Ratio of 2.20

Fig. 24 Total Pressure Survey Rake Showing Pitot Tube Locations and Measured Pressures

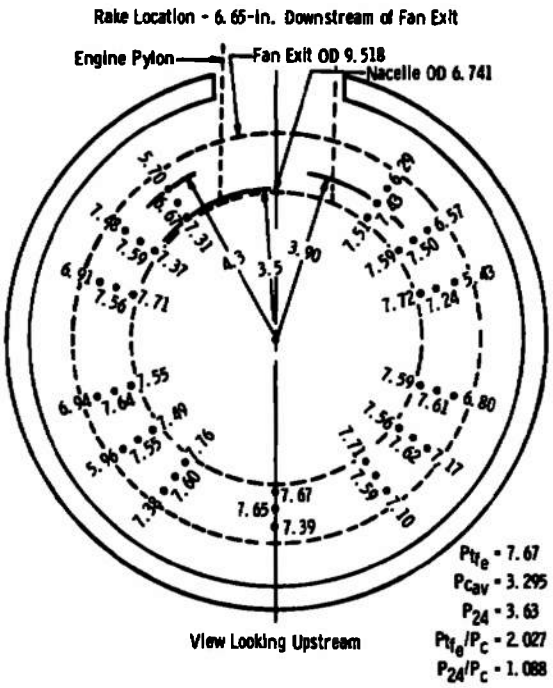

d. For $P_{t_{f_e}}/P_{c_{av}}$ Ratio of 2.27

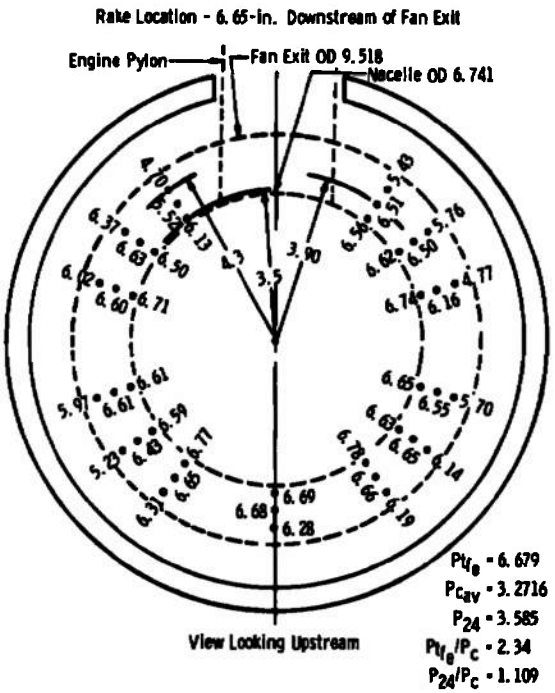

e. For $P_{t_{f_e}}/P_{c_{av}}$ Ratio of 2.34

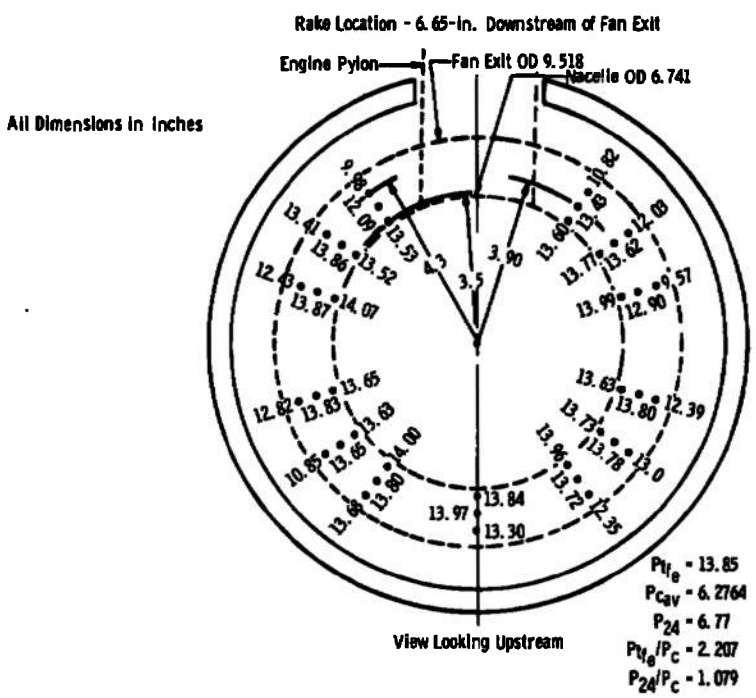

f. For $P_{t_{f_e}}/P_{c_{av}}$ Ratio of 2.20

Fig. 24 Concluded

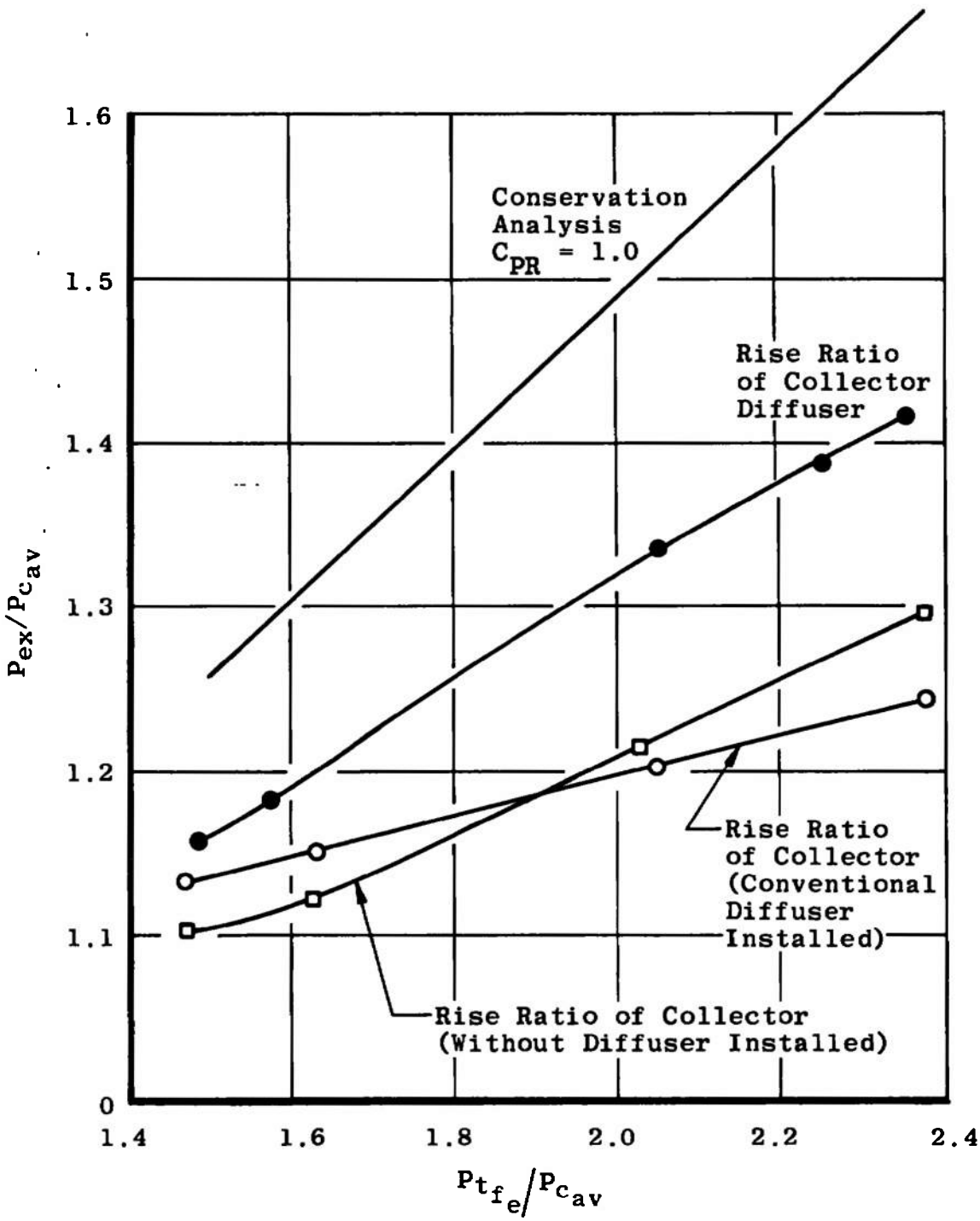

Fig. 25 Collector-Conventional Diffuser Performance

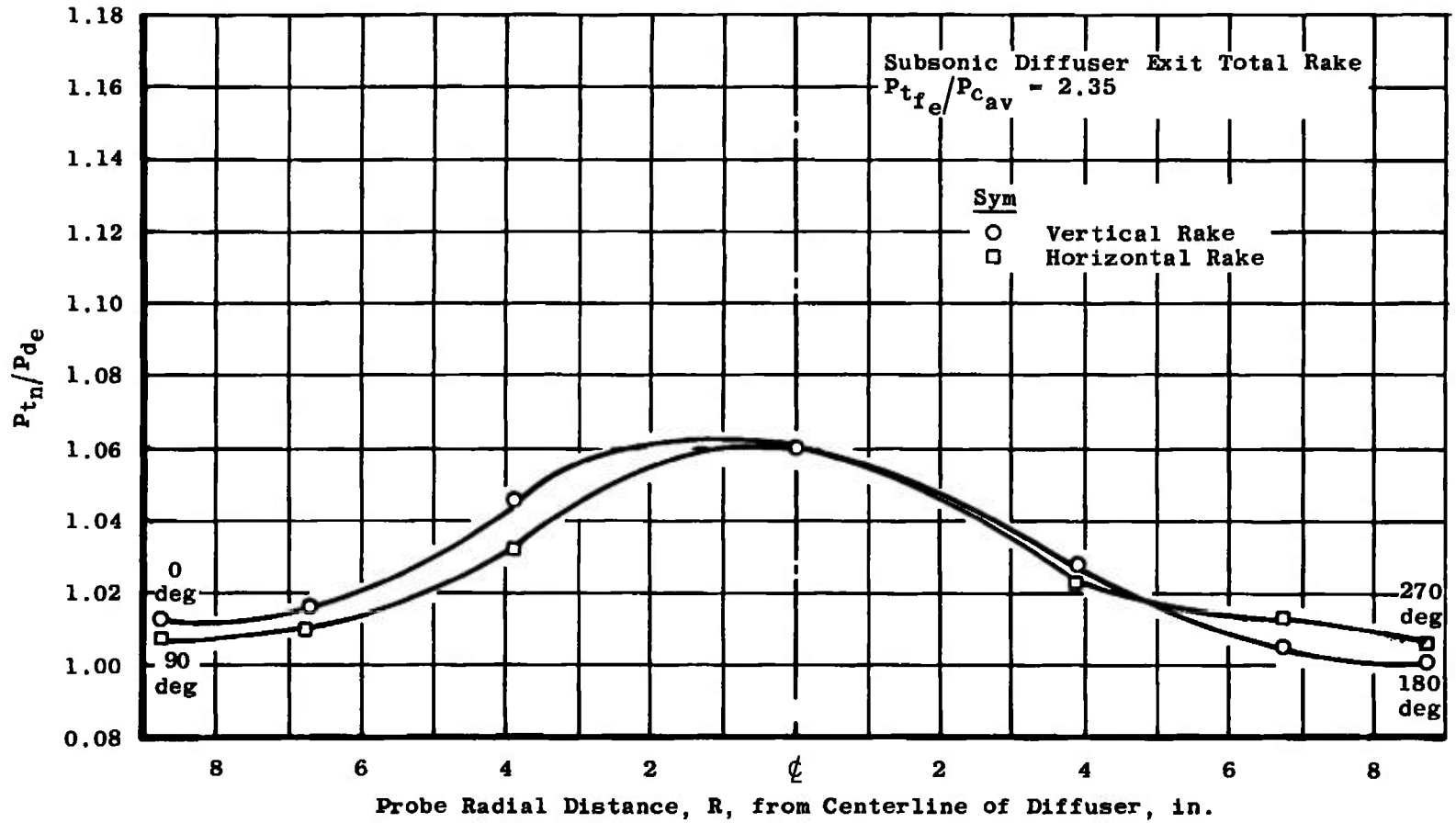

Fig. 26 Conventional Diffuser Exit Total Pressure Survey

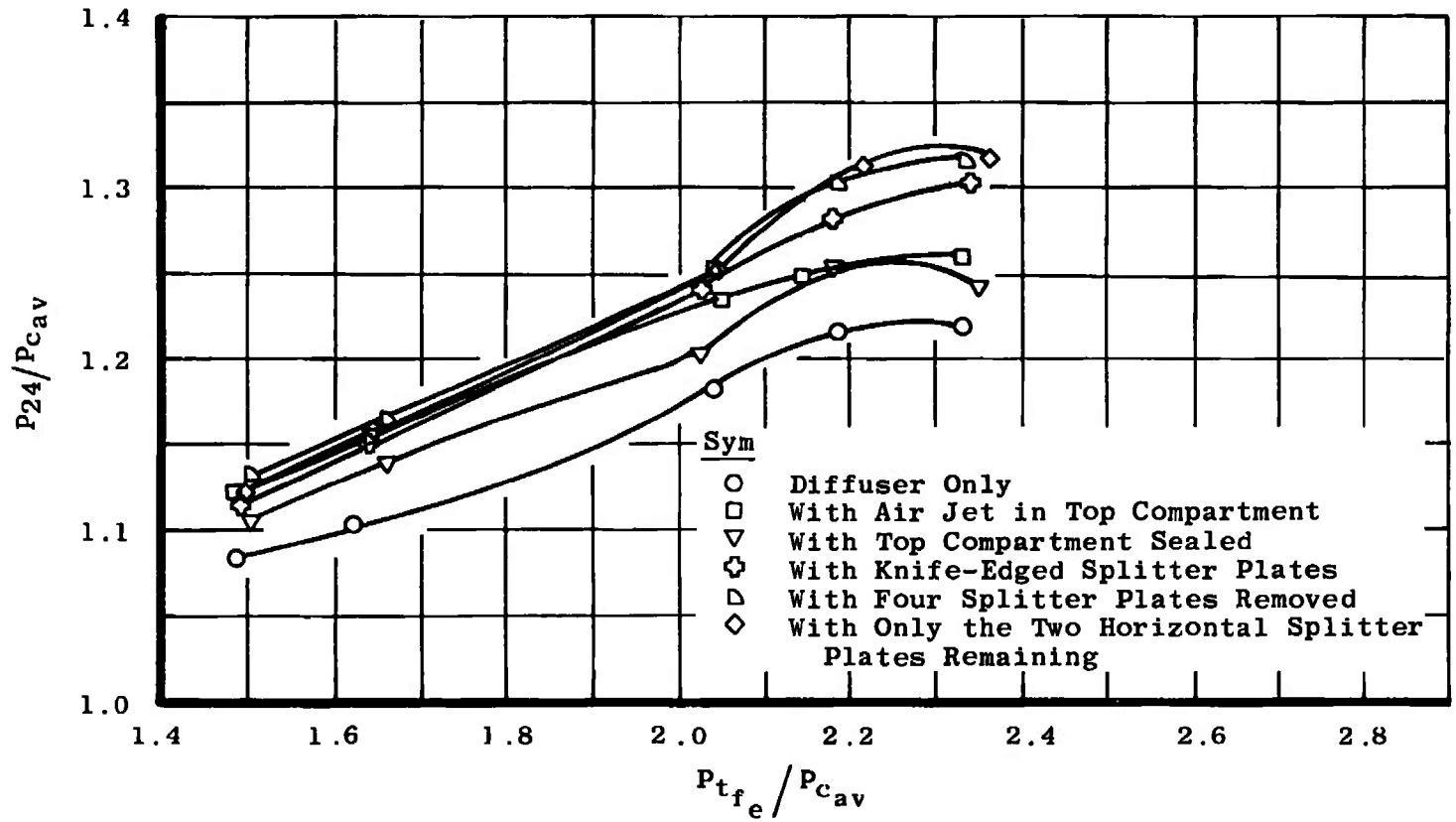

Fig. 27 Collector-Segmented Diffuser Performance

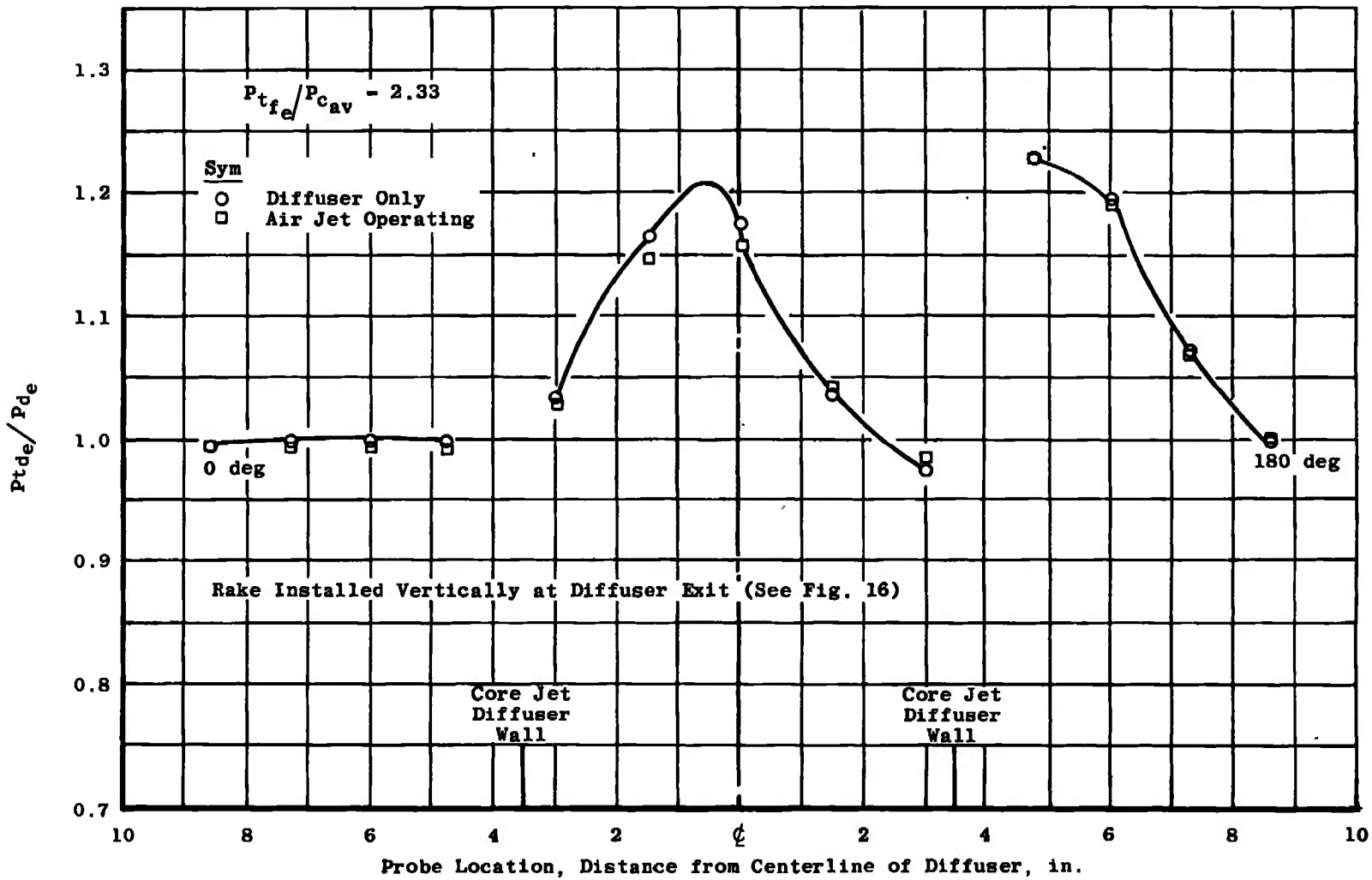

a. For $P_{t_{f_e}}/P_{c_{av}}$ Ratio of 2.33

Fig. 28 Total Pressure Profile at Segmented Diffuser Exit

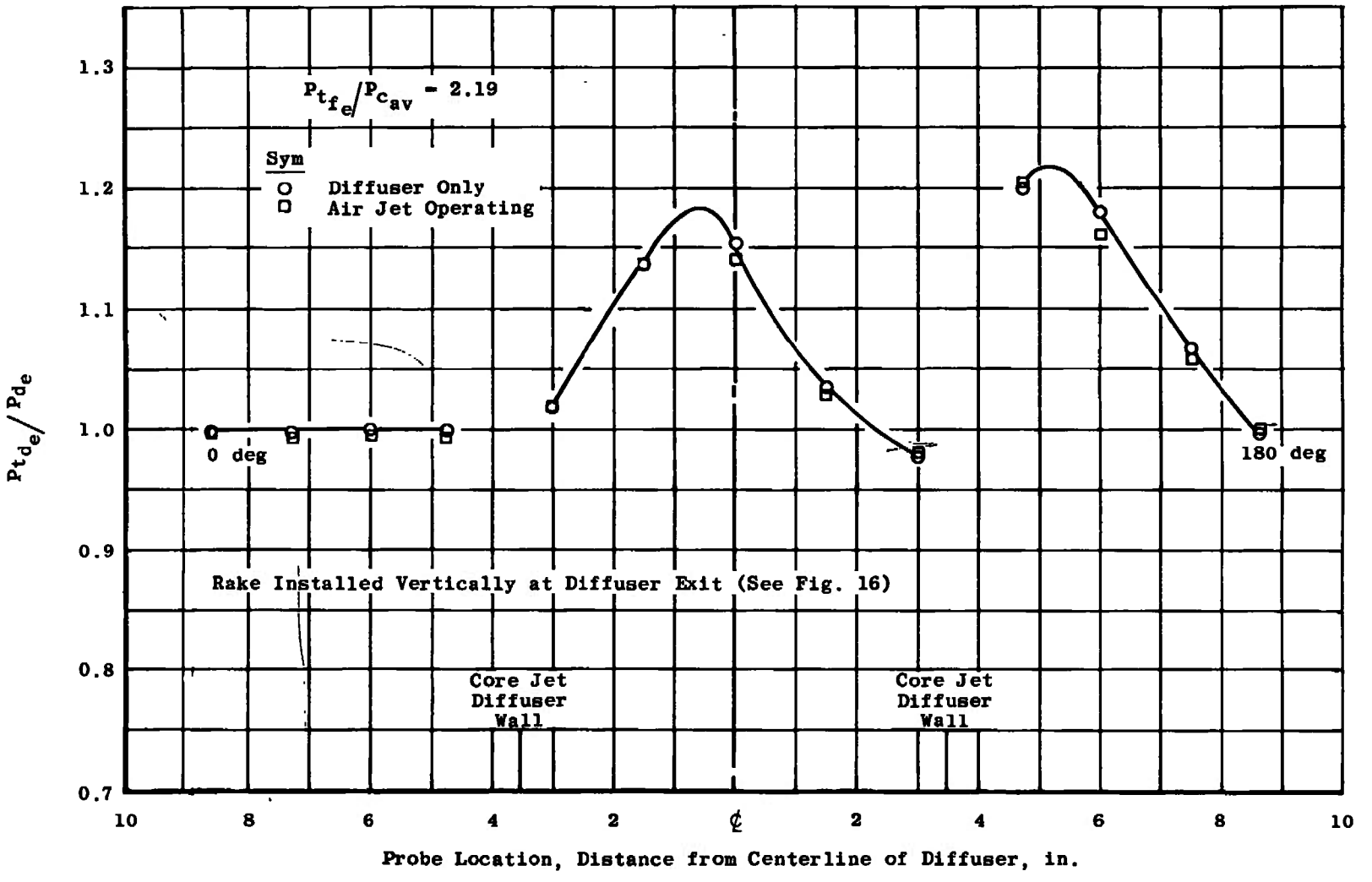

b. For $P_{t_{f_e}}/P_{c_{av}}$ Ratio of 2.19

Fig. 28 Continued

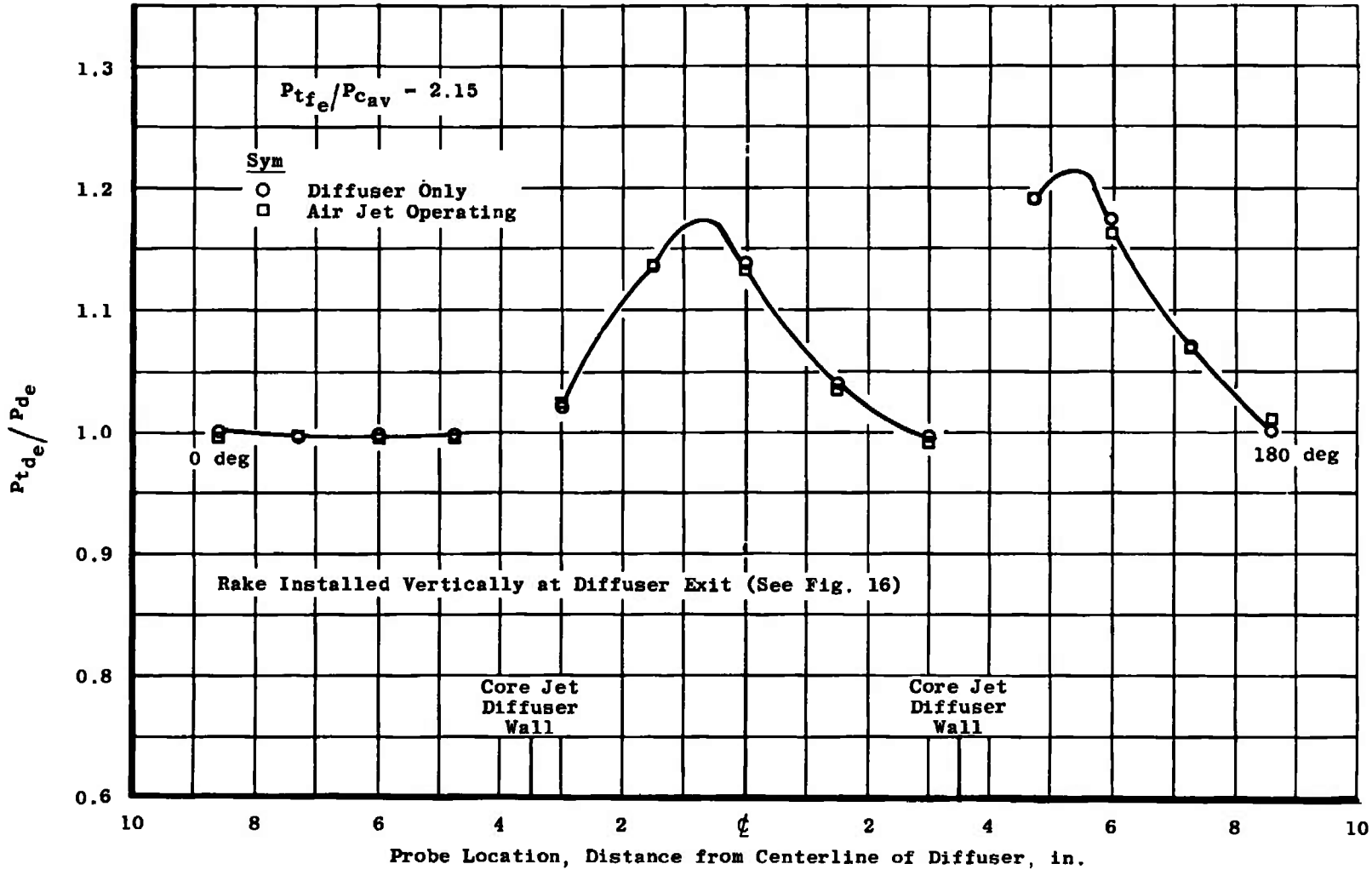

c. For $P_{t_{f_e}}/P_{c_{av}}$ Ratio of 2.15

Fig. 28 Continued

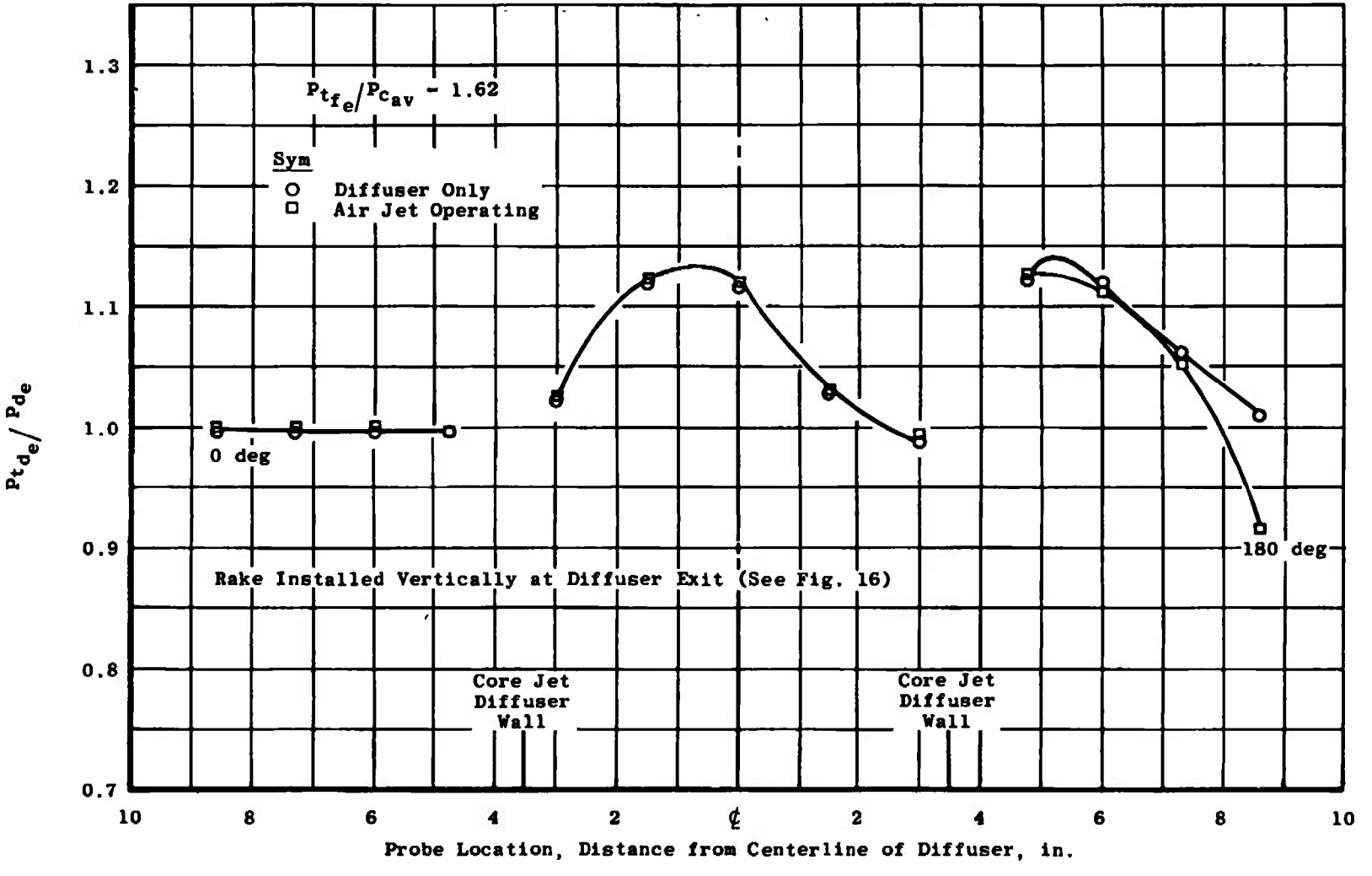

d. For $P_{t_{f_e}}/P_{c_{av}}$ Ratio of 1.62

Fig. 28 Continued

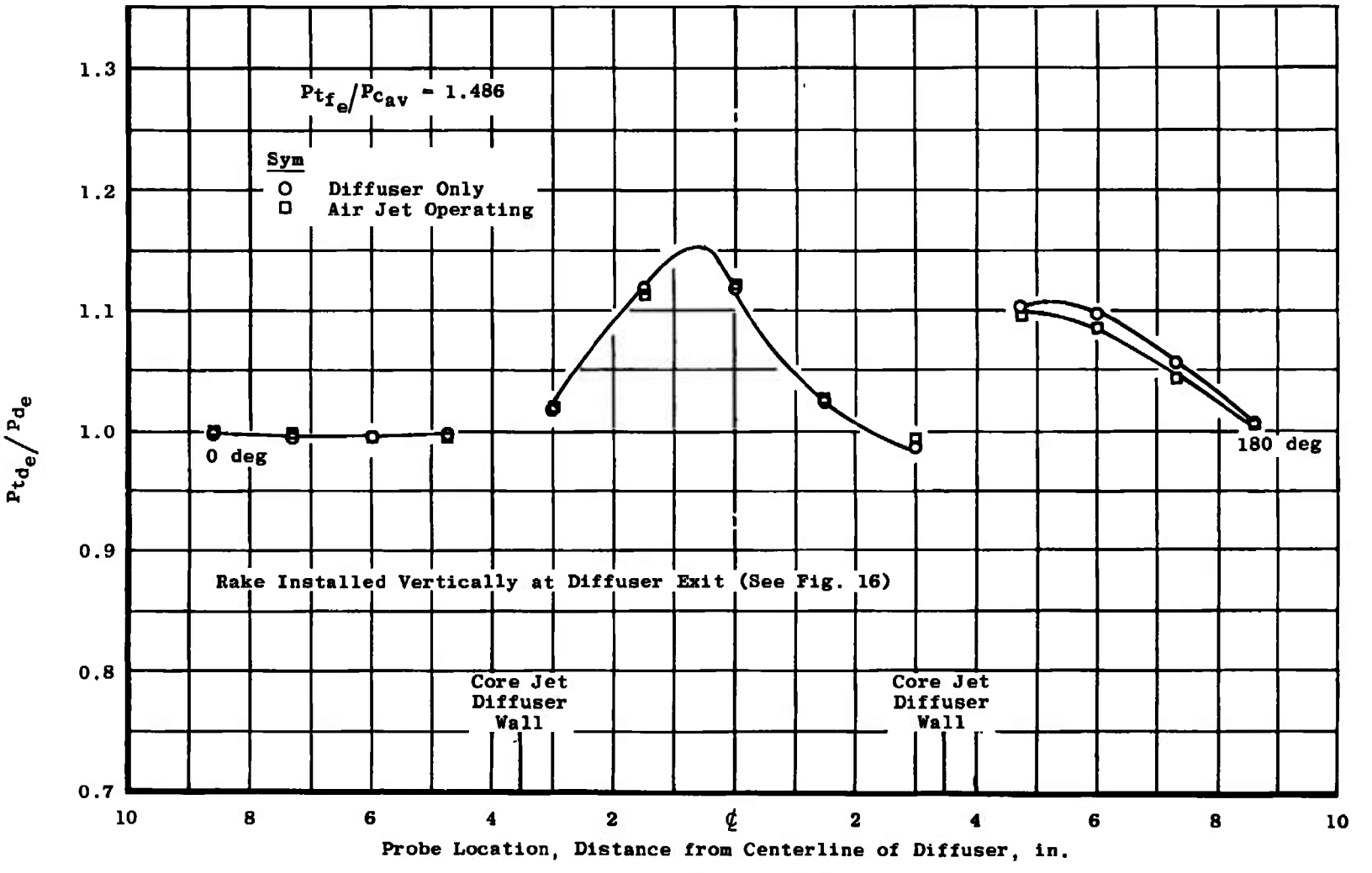

e. For $P_{t_{f_e}}/P_{c_{av}}$ Ratio of 1.48

Fig. 28 Concluded

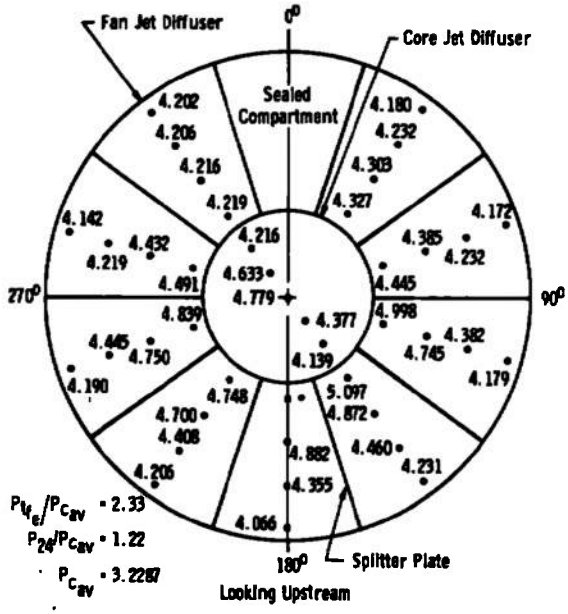

a. For $P_{t_{f_e}}/P_{c_{av}}$ Ratio of 2.33

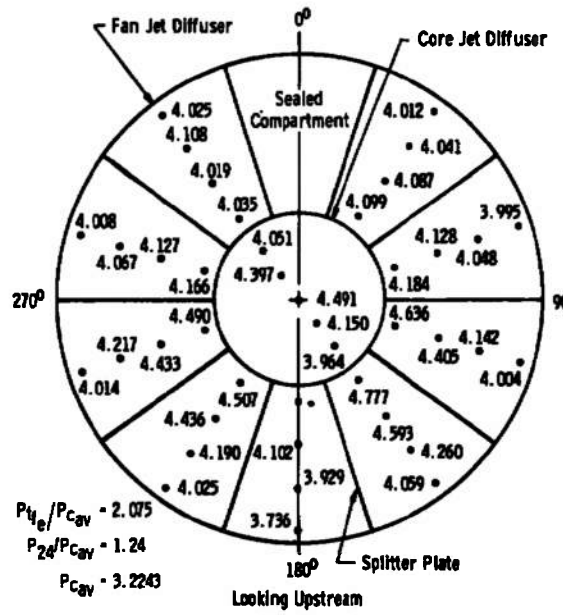

b. For $P_{t_{f_e}}/P_{c_{av}}$ Ratio of 2.07

*No Data Available

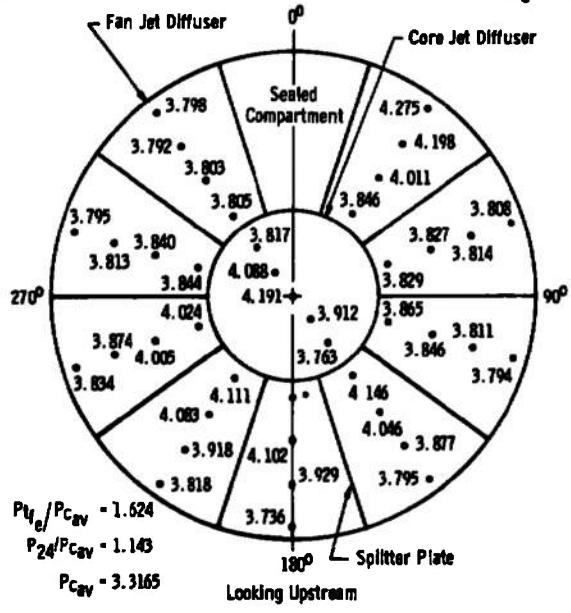

c. For $P_{t_{f_e}}/P_{c_{av}}$ Ratio of 1.62

Fig. 29 Total Pressure Survey at the Exit of the Segmented Diffuser

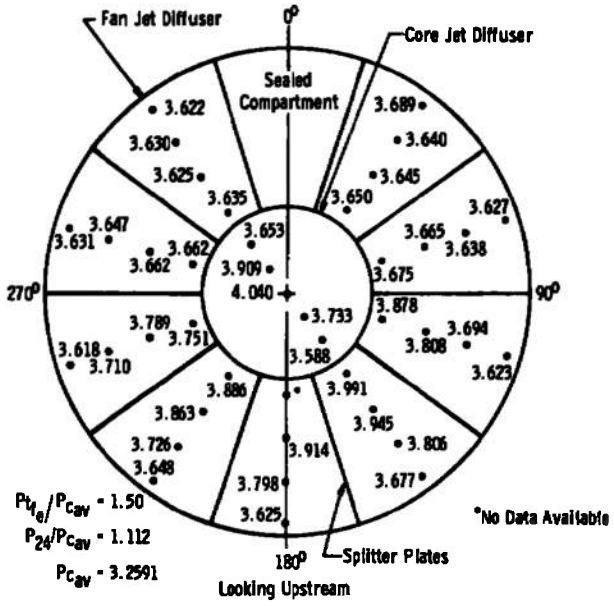

d. For $P_{t_{f_e}}/P_{c_{av}}$ Ratio of 1.50

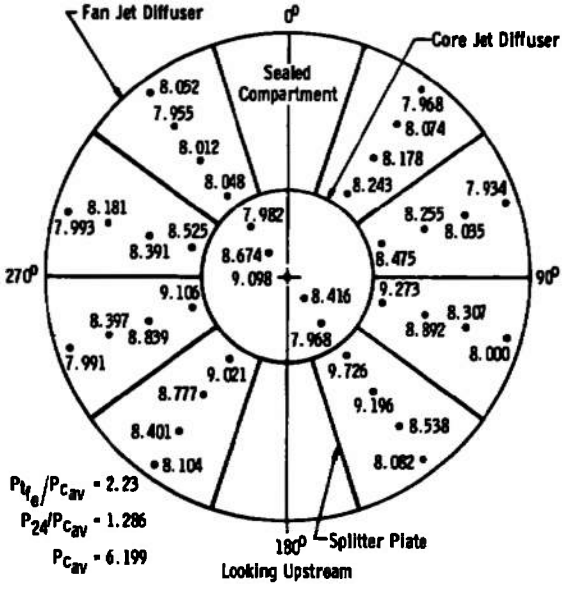

e. For $P_{t_{f_e}}/P_{c_{av}}$ Ratio of 2.20

Fig. 29 Concluded

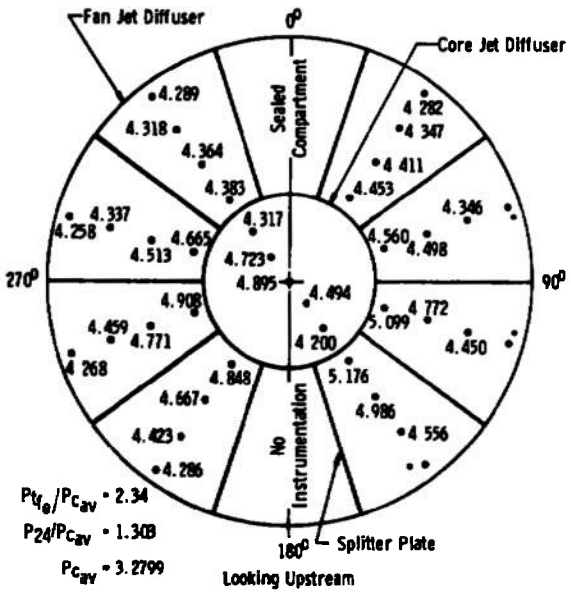

a. For $P_{t_{f_e}}/P_{c_{av}}$ Ratio of 2.34

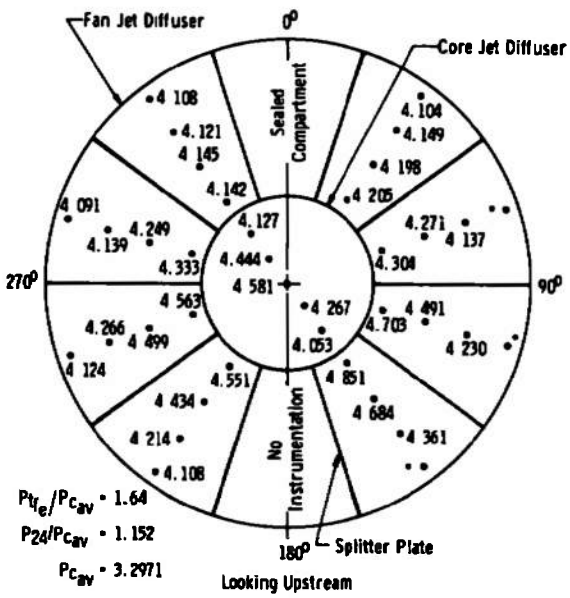

b. For $P_{t_{f_e}}/P_{c_{av}}$ Ratio of 2.02

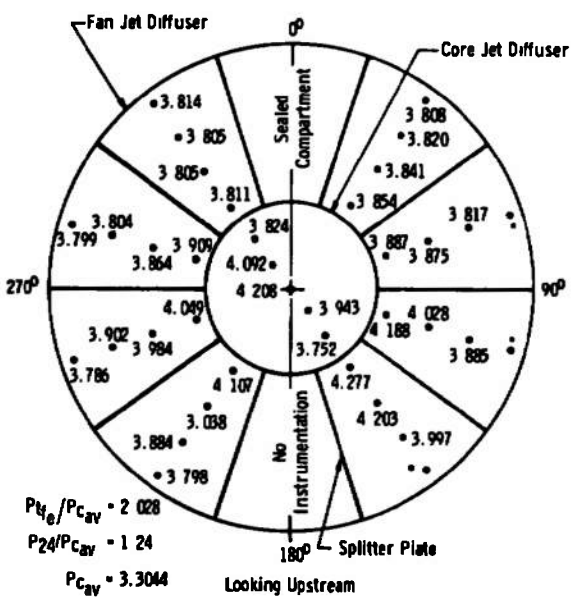

c. For $P_{t_{f_e}}/P_{c_{av}}$ Ratio of 1.64

Fig. 30 Total Pressure Survey at the Exit of the Segmented Diffuser with Sharp Leading Edge Splitter Plates

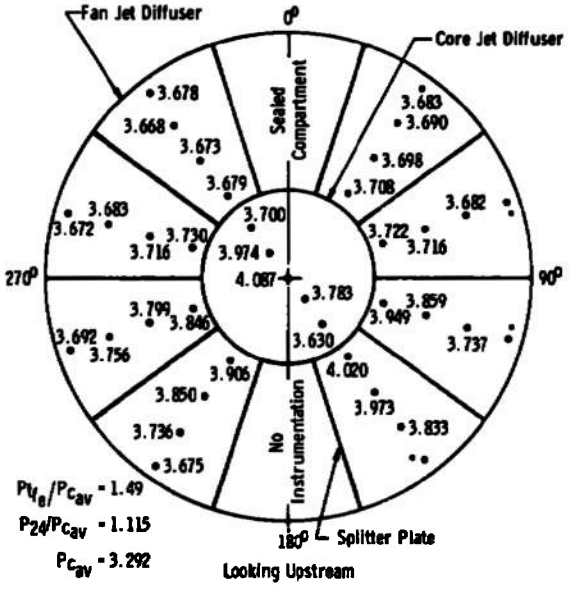

d. For $P_{t_{f_e}}/P_{c_{av}}$ Ratio of 1.50

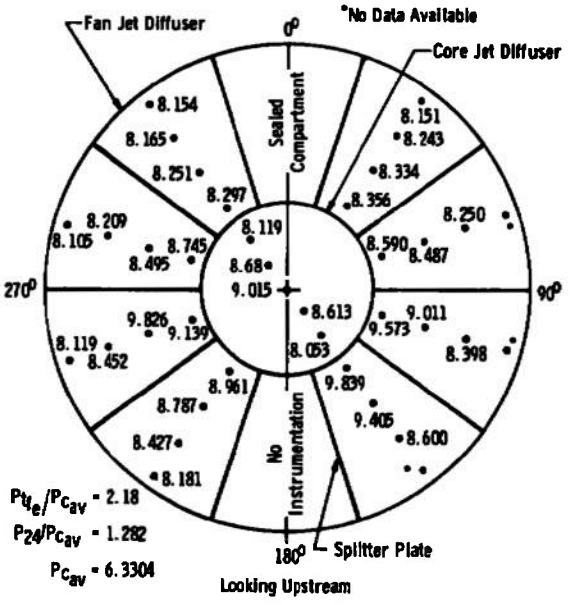

e. For $P_{t_{f_e}}/P_{c_{av}}$ Ratio of 2.20

Fig. 30 Concluded

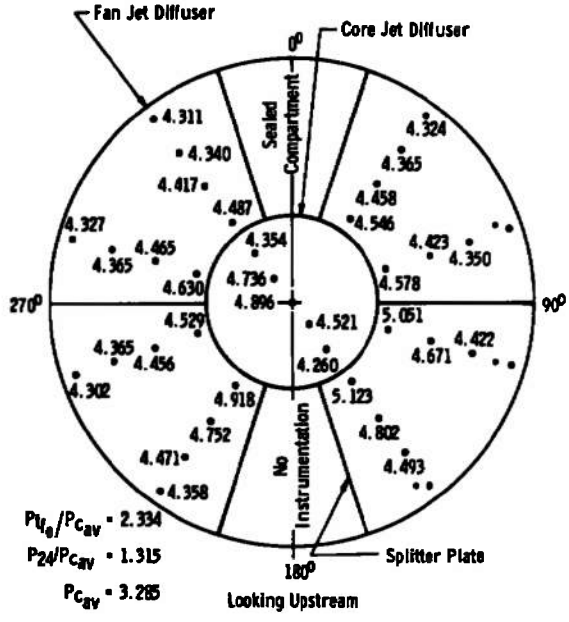

a. For $P_{t_{f_e}}/P_{c_{av}}$ Ratio of 2.33

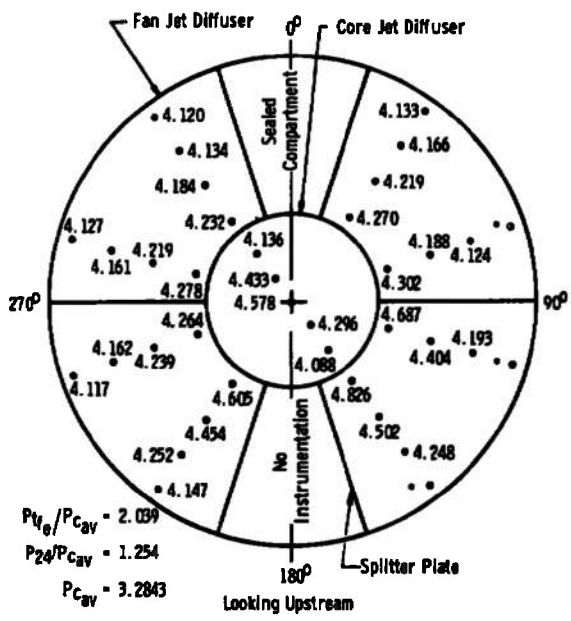

b. For $P_{t_{f_e}}/P_{c_{av}}$ Ratio of 2.04

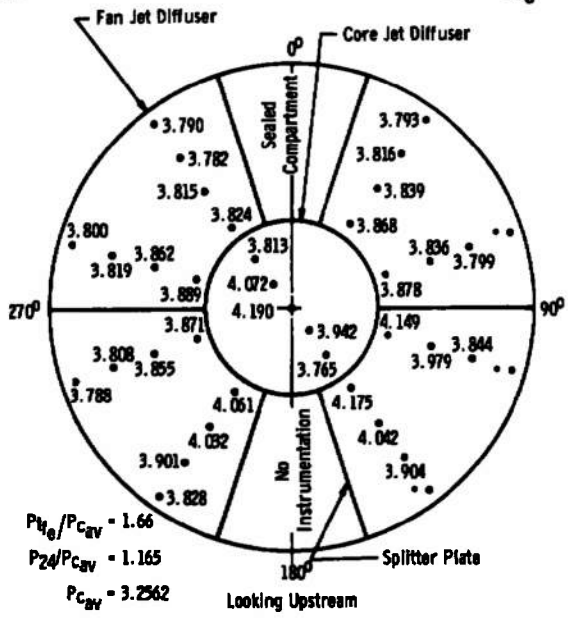

*No Data Available

c. For $P_{t_{f_e}}/P_{c_{av}}$ Ratio of 1.66

Fig. 31 Total Pressure Survey at the Exit of the Segmented Diffuser with Four Splitter Plates Removed

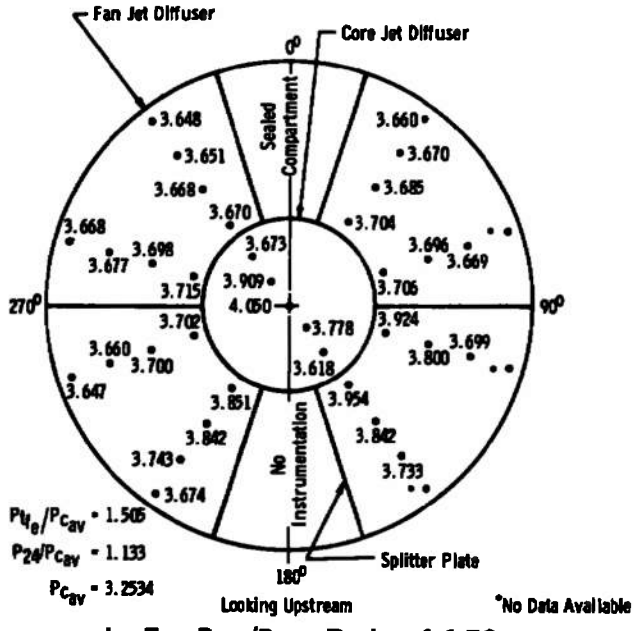

d. For $P_{t_{f_e}}/P_{c_{av}}$ Ratio of 1.50

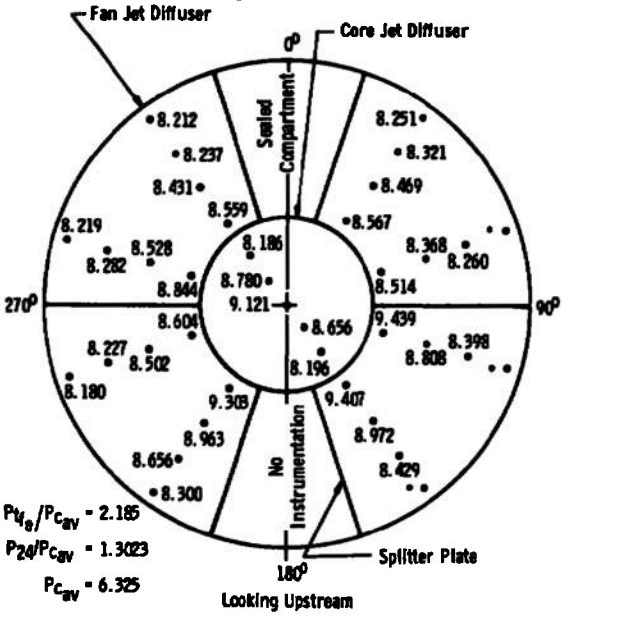

e. For $P_{t_{f_e}}/P_{c_{av}}$ Ratio of 2.20

Fig. 31 Concluded

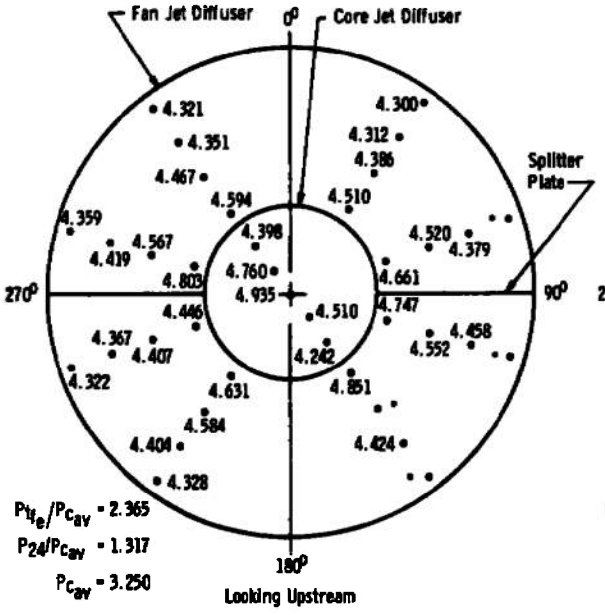

a. For $P_{t_{f_e}}/P_{c_{av}}$ Ratio of 2.36

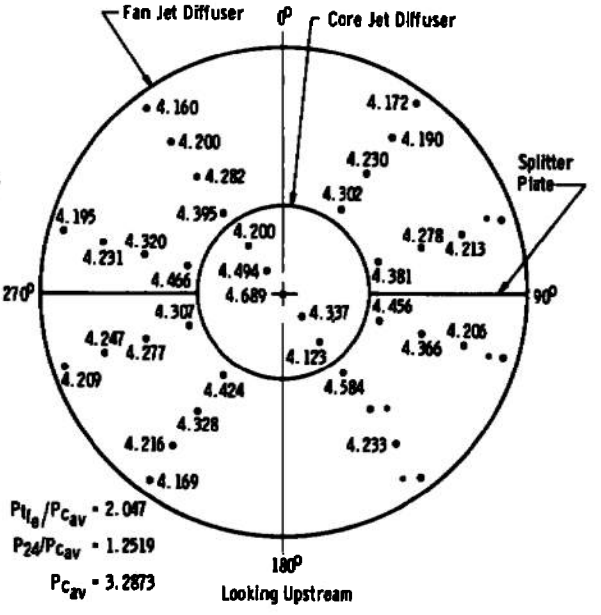

b. For $P_{t_{f_e}}/P_{c_{av}}$ Ratio of 2.05

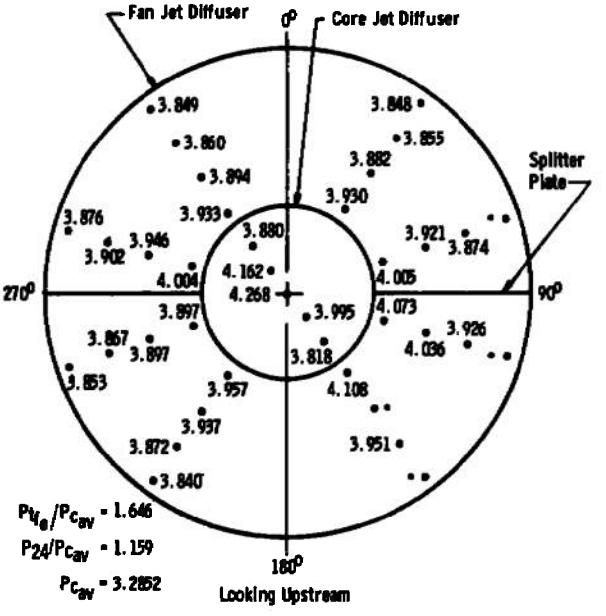

*No Data Available

c. For $P_{t_{f_e}}/P_{c_{av}}$ Ratio of 1.65

Fig. 32 Total Pressure Survey at the Exit of the Segmented Diffuser with Only the Horizontal Splitter Plates

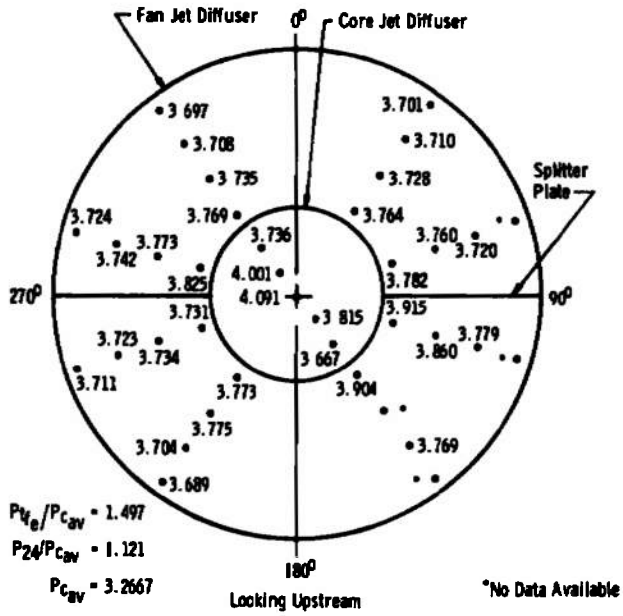

d. For $P_{t_{f_e}}/P_{c_{av}}$ Ratio of 1.50

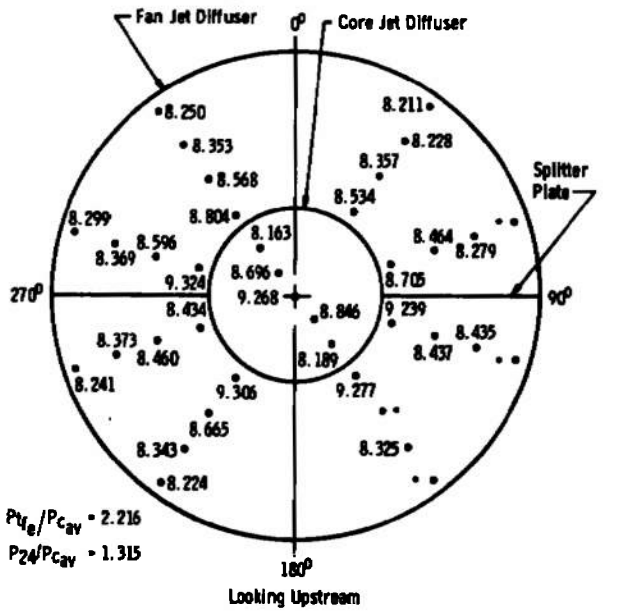

e. For $P_{t_{f_e}}/P_{c_{av}}$ Ratio of 2.20

Fig. 32 Concluded

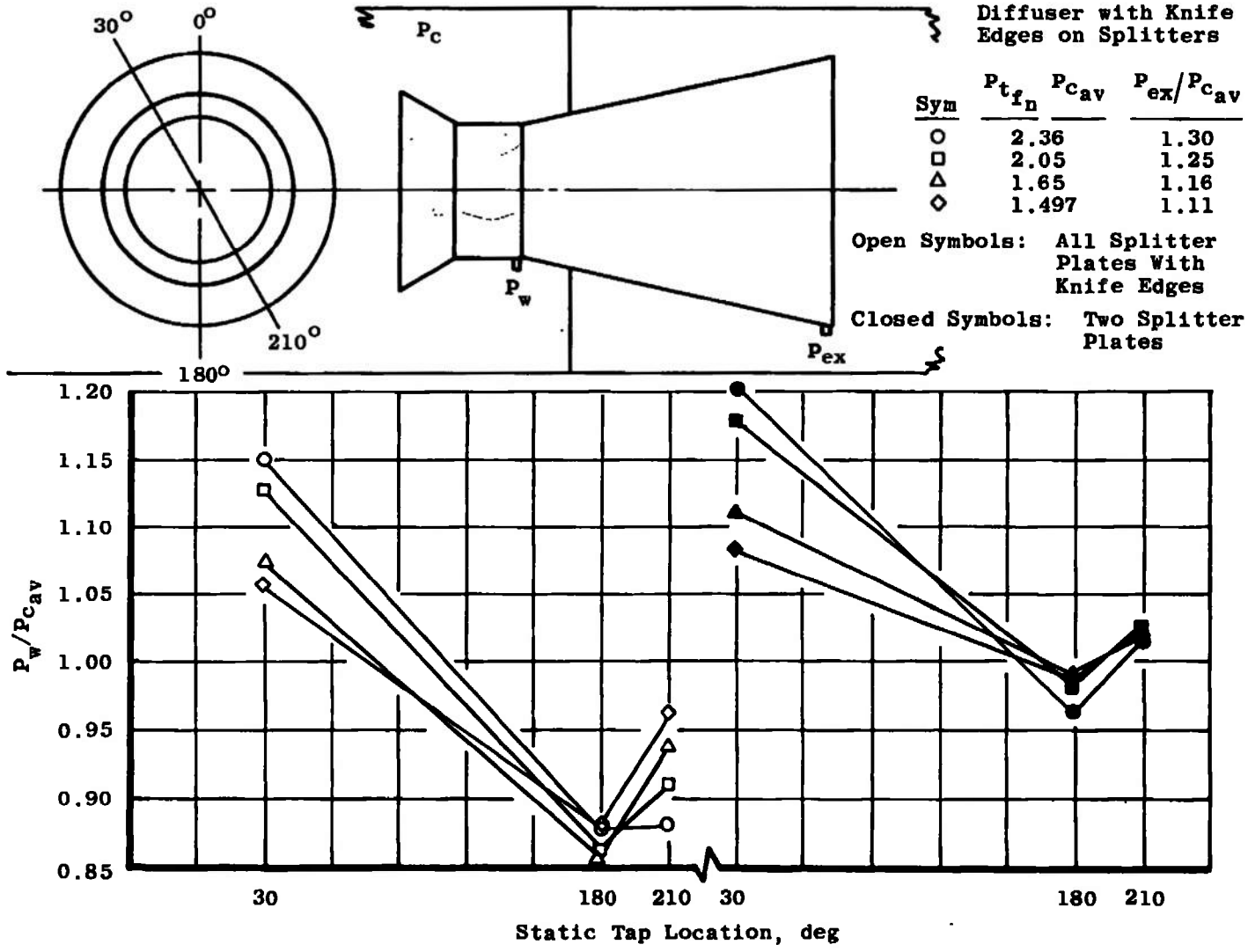

Fig. 33 Diffuser Inlet Duct Wall Pressure

TABLE I
TEST CELL PRESSURE COMPARISON PER FAN NOZZLE EXIT PRESSURE RATIO

Test Configuration	Sta	Circumferential Location, deg (Looking Downstream)								$\frac{P_{t_{f_e}}}{P_{c_{av}}}$
		0	45	90	135	180	225	270	315	
No Exhaust Hardware $P_{c_{av}}$ = 3.267	15	3.265		3.271				3.277		2.340
	16		3.263						3.259	
	17		3.249		3.240		3.263		3.255	
	18		3.252		---		3.258		---	
Model J-1 Exhaust Collector $P_{c_{av}}$ = 3.233	15	3.223		3.206		3.229		3.246		2.380
	16		3.199		3.213		3.210		3.224	
	17		3.197		3.205		3.216		3.211	
	18		3.186		---		3.163		---	
Exhaust Collector with Conventional Subsonic Diffuser $P_{c_{av}}$ = 3.299	15	3.328		3.303		3.315		3.296		2.355
	16		3.307		3.319		3.303		3.314	
	17		3.282		3.293		3.271		3.287	
	18		3.296		---		3.275		---	
Exhaust Collector with Segmented Diffuser $P_{c_{av}}$ = 3.296	15	3.308		3.315		3.319		3.287		2.332
	16		3.309		3.277		3.290		3.303	
	17		3.279		3.283		3.277		3.305	
	18		3.266		---		3.288		---	
No Exhaust Hardware $P_{c_{av}}$ = 3.376	15	3.372		3.375				3.381		1.445
	16		3.367						3.370	
	17		3.352		3.359		3.380		3.368	
	18		3.362		---		3.369		---	
Model J-1 Exhaust Collector $P_{c_{av}}$ = 3.293	16	3.289		3.296		3.294		3.284		1.474
	16		3.281		3.287		3.278		3.284	
	17		3.267		3.272		3.277		3.295	
	18		3.266		---		3.277		---	
Exhaust Collector with Conventional Subsonic Diffuser $P_{c_{av}}$ = 3.3667	15	3.369		3.389		3.386		3.401		1.488
	16		3.400		3.376		3.358		3.362	
	17		3.346		3.353		3.309		3.347	
	18		3.347		---		3.388		---	
Exhaust Collector with Segmented Diffuser $P_{c_{av}}$ = 3.3017	15	3.311		3.306		3.286		3.297		1.484
	16		3.312		3.305		3.299		3.315	
	17		3.291		3.292		3.320		3.319	
	18		3.299		---		3.302		---	
No Exhaust Hardware $P_{c_{av}}$ = 3.285	15	3.285		3.283				3.288		2.098
	18		3.289						3.276	
	17		3.268		3.258		3.287		3.269	
	18		3.273		---		3.272		---	
Model J-1 Exhaust Collector $P_{c_{av}}$ = 3.309	15	3.287		3.298		3.278		3.317		2.025
	16		3.322		3.291		3.266		3.304	
	17		3.263		3.281		3.308		3.312	
	18		3.249		---		3.306		---	

TABLE I (Concluded)

Test Configuration	Sta	Circumferential Location, deg (Looking Downstream) 10	45	90	135	180	225	270	315	$\frac{P_{t_{fe}}}{P_{c_{av}}}$
Exhaust Collector with Conventional Subsonic Diffuser $P_{c_{av}}$ = 3.297	15	3.320		3.345		3.315		3.307		2.049
	16		3.287		3.318		3.278		3.319	
	17		3.268		3.307		3.261		3.293	
	18		3.285		---		3.253		---	
Exhaust Collector with Segmented Diffuser $P_{c_{av}}$ = 3.306	15	3.291		3.306		3.316		3.316		2.040
	16		3.306		3.313		3.280		3.323	
	17		3.267		3.302		3.323		3.333	
	18		3.255		---		3.279		---	
No Exhaust Hardware $P_{c_{av}}$ = 3.303	15	3.307		3.300				3.303		1.625
	16		3.295						3.303	
	17		3.283		3.286		3.299		3.296	
	18		3.288		---		3.292		---	
Model J-1 Exhaust Collector $P_{c_{av}}$ = 3.2896	15	3.297		3.292		3.277		3.277		1.632
	16		3.281		3.270		3.264		3.290	
	17		3.256		3.270		3.280		3.280	
	18		3.278		---		3.269		---	
Exhaust Collector with Conventional Subsonic Diffuaer $P_{c_{av}}$ = 3.48035	15	3.415		3.432		3.451		3.457		1.575
	16		3.496		3.572		3.604		3.543	
	17		3.593		3.523		3.388		3.387	
	18		3.389		---		3.475		---	
Exhaust Collector with Segmented Diffuser $P_{c_{av}}$ = 3.3249	15	3.341		3.315		3.311		3.324		1.623
	16		3.332		3.318		3.314		3.335	
	17		3.322		3.321		3.335		3.332	
	18		3.328		---		3.320		---	
No Exhaust Hardware $P_{c_{av}}$ = 6.296	15	6.325		6.300				6.300		2.182
	16		6.314						6.269	
	17		6.284		6.251		6.290		6.290	
	18		6.309		---		6.308		---	
Model J-1 Exhaust Collector	15	NO DATA								
	16									
	17									
	18									
Exhaust Collector with Conventional Subsonic Diffuser $P_{c_{av}}$ = 6.295	15	6.300		6.282		6.269		6.248		2.254
	16		6.270		6.313		6.343		8.381	
	17		6.345		8.342		6.275		6.340	
	18		6.230		---		6.210		---	
Exhaust Collector with Segmented Diffuser $P_{c_{av}}$ = 6.3261	15	6.338		6.418		6.331		6.315		2.188
	16		6.308		6.317		6.288		6.378	
	17		6.287		6.363		6.258		6.312	
	18		6.290		---		6.240		---	

UNCLASSIFIED

Security Classification

DOCUMENT CONTROL DATA - R & D

(Security classification of title, body of abstract and indexing annotation must be entered when the overall report is classified)

1 ORIGINATING ACTIVITY (Corporate author)	2a. REPORT SECURITY CLASSIFICATION
Arnold Engineering Development Center Arnold Air Force Station, Tennessee 37389	UNCLASSIFIED
	2b. GROUP N/A

3 REPORT TITLE

EXPERIMENTAL STUDY OF THE EFFECT OF SUBSONIC EXHAUST GAS DIFFUSERS ON THE TEST CELL WALL AND TF39 COLD-FLOW MODEL ENGINE EXHAUST NOZZLE PLUG AND CORE ENGINE COWL SURFACE PRESSURES

4 DESCRIPTIVE NOTES (Type of report and inclusive dates)

July 1971 to July 1972--Final Report

5 AUTHOR(S) (First name, middle initial, last name)

Delbert Taylor, Marvin Simmons, and Frank T. Lee, ARO, Inc.

6 REPORT DATE	7a. TOTAL NO OF PAGES	7b. NO OF REFS
April 1973	91	5

8a. CONTRACT OR GRANT NO	9a. ORIGINATOR'S REPORT NUMBER(S)
b. PROJECT NO	AEDC-TR-73-13
c. Program Element 64719F	9b. OTHER REPORT NO(S) (Any other numbers that may be assigned this report)
d.	ARO-ETF-TR-72-130

10 DISTRIBUTION STATEMENT

Approved for public release; distribution unlimited.

11 SUPPLEMENTARY NOTES	12. SPONSORING MILITARY ACTIVITY
Available in DDC	Arnold Engineering Development Center (XON) Arnold Air Force Station, Tennessee.

13 ABSTRACT

An experimental investigation was conducted to determine the effects of exhaust gas collectors/subsonic diffusers on engine and test cell surface pressures during tests of high-bypass-ratio front-fan engines in ground test facilities. A one-tenth scale model of a TF39 turbofan engine installed in a one-tenth scale model of Propulsion Development Test Cell (J-1) was employed. Engine cowl and plug surface pressure data were recorded during model engine operation with cold air at five simulated power settings without exhaust collector, with exhaust collector, with exhaust collector equipped with a conventional subsonic diffuser, and with exhaust collector equipped with a segmented subsonic diffuser which separately diffused the fan and core engine exhaust jets. Stagnation pressure data were also recorded for the purpose of establishing the flow losses in the free-jet exhausts and in the diffusers. Data from all configurations were analyzed to determine the effect of exhaust jet collector/diffusers on engine and test cell surface pressures and to determine the efficiency of the diffusion process.

DD FORM 1 NOV 65 1473

UNCLASSIFIED

Security Classification

14 KEY WORDS	LINK A		LINK B		LINK C	
	ROLE	WT	ROLE	WT	ROLE	WT
exhaust gases						
diffusers						
cold flow						
nozzle inserts						
pressure distribution						
accumulators						
subsonic flow						
scale model						
turbofan engine						

AFSC
Arnold AFS Tenn